UNIVERSIDAD DE BURGOS

Departamento de Química

Área de Química Analítica

DEVELOPMENT OF NEW DEVICES FOR TIME-RESOLVED RAMAN SPECTROELECTROCHEMISTRY

Memoria presentada por

DAVID IBÁÑEZ MARTÍNEZ

Para optar al título de Doctor por la Universidad de Burgos

Directores:

Álvaro Colina Santamaría

Mª Aránzazu Heras Vidaurre

Burgos, mayo de 2015

DEPARTAMENTO DE QUÍMICA

FACULTAD DE CIENCIAS

UNIVERSIDAD DE BURGOS

D. Álvaro Colina Santamaría, profesor titular del Área de Química Analítica de la Universidad de Burgos

y

Dña. Mª Aránzazu Heras Vidaurre, profesora titular del Área de Química Analítica de la Universidad de Burgos

Hacen constar:

Que la presente memoria resume el trabajo titulado **“DEVELOPMENT OF NEW DEVICES FOR TIME-RESOLVED RAMAN SPECTROELECTROCHEMISTRY”** realizado por D. David Ibáñez Martínez en el Área de Química Analítica y bajo nuestra dirección para optar al grado de Doctor por la Universidad de Burgos.

Manifestamos nuestra conformidad con el contenido de la memoria y autorizamos su presentación para ser defendida como Tesis Doctoral.

Burgos, 26 de febrero de 2015.

Fdo: Álvaro Colina Santamaría

Fdo: Mª Aránzazu Heras Vidaurre

A mis padres

Agradecimientos

Llega el momento de echar la vista atrás y aunque con un poco de vértigo pensando en todo lo que he vivido durante estos años, quiero dar las gracias a todas aquellas personas que han sido partícipes de esta tesis doctoral.

En primer lugar, agradezco a mis directores de tesis, la Dra. Mª Aránzazu Heras Vidaurre y al Dr. Álvaro Colina Santamaría, así como al Prof. Jesús López Palacios por su ayuda en el desarrollo de este trabajo y por su confianza en mí a lo largo de estos años. Pero sobretodo, gracias a Álvaro y a Arancha por todos los valores que me han transmitido fuera del laboratorio, más allá de lo puramente científico y los cuales me han permitido crecer como persona. Un auténtico placer haber compartido estos años con vosotros.

Un factor clave durante estos años ha sido trabajar cómodo y a gusto. Por ello, gracias a los que no son únicamente mis compañeros del laboratorio 192, sino que son grandes amigos fuera de él: Dani, Nola y Jesús. Poco o nada me queda por decir de Dani y Nola, empezamos juntos este camino allá en el año 2004 en el aula 12 y, tras miles de anécdotas y de temporadas buenas y alguna no tan buena, lo terminamos juntos como doctores. Gracias por estar siempre a mi lado a lo largo de estos años. Gracias también a Jesús, por ser una de esas personas que hacen fácil el trabajo y de las que si hubiera más en el mundo todo funcionaría mejor.

Importante también ha sido el momento del café, tan necesario algunos días para desconectar. Por ello, gracias a los analíticos Ana, Lorena, Wil, Bego y Julia por las risas que nos hemos echado durante estos años.

Gracias también a todos los compañeros que he tenido tanto en el grupo de Análisis Instrumental como en el conjunto del área de Química Analítica, porque de cada uno de ellos he podido aprender algo.

Quiero agradecer especialmente al Prof. David J. Fermín la oportunidad de realizar una estancia en el grupo de Electroquímica de la Universidad de Bristol y vivir una de mis mejores experiencias tanto a nivel profesional como personal durante estos años. Gracias a él, a Daniela, a Vero y al resto del grupo por todo lo que aprendí con ellos durante esos meses y, sobre todo, por hacerme sentir como en casa desde el primer hasta el último día de estancia.

I would like to thank Dr. Martin Kalbáč for giving me the opportunity of working in the department of Low-dimensional Systems in the J. Heyrovsky Institute in Prague. Thanks him, Ana and the rest of the group for their help during these months. Quiero agradecer también al Dr. Martin Kalbáč el permitirme trabajar durante varios meses en el departamento de Low-dimensional Systems en el J. Heyrovsky Institute de Praga. Gracias a él, a Ana y al resto del grupo por su ayuda durante esos meses.

Parte importante para recorrer este camino han sido mis amigos. Gracias a mis químicos Leti, Miriam, Nerea, Rubén (químico frustrado) y, de nuevo, Nola y Dani por tantas noches, escapadas, fines de semana y aventuras juntos durante estos años, pero sobre todo, por saber valorar lo que supone llegar hasta aquí. Por supuesto, gracias a todos mis amigos más allá del mundo de la ciencia, Sandra, Ester, Nacho, y un largo etc. que englobe a todos, por haber estado y seguir estando acompañándome a lo largo de los años.

Por último, quiero agradecer a la pieza clave que me ha permitido llegar hasta aquí: mi familia. Sobre todo gracias a mis padres, por su continuo apoyo en todos los proyectos en los que me embarco, por la estabilidad necesaria que me han dado durante estos años y por estar siempre a mi lado. Gracias también a mi hermano y a mi cuñada, por la confianza que han puesto en mí a lo largo de este tiempo, y a Irene, mi sobrina, una de las mayores alegrías de estos últimos años. Gracias a los que están y a los que no están, llegar hasta esta meta también se lo debo a ellos.

Index

1. Introduction

1. Introduction

Electrochemistry is a very useful instrumental technique that is usually employed in very different fields (analysis, energy, biochemistry, etc). However, in general, this technique exhibits a limitation due to its intrinsic lack of molecular information. Spectroscopy is another instrumental analysis technique widely used that provides important molecular information, but in most cases, this set of techniques does not provoke any change in the studied system. The combination of spectroscopic and electrochemical techniques yields very powerful techniques denoted as Spectroelectrochemistry. These hybrid techniques provide not only molecular but also kinetic information about the reactants, products, intermediate compounds or side products that are generated during an electron transfer process. Therefore, as Kaim and Fiedler wrote in 2009 [1], Spectroelectrochemistry combines the best of two worlds.

UV/Vis absorption spectroelectrochemistry is perhaps the most used technique in which better and interesting developments have been proposed. Probably, this is the main reason why the first commercial spectroelectrochemical devices and instruments have been proposed to perform these kinds of measurement.Twenty years ago, it was very difficult to perform time-resolved UV/Vis absorption spectroelectrochemistry exeriments but nowadays it has become relatively simple. The main drawbacks of UV/Vis absorption spectroelectrochemistry are related to the lack of information about the structure of the studied compounds or materials and about the way in which these compounds interact with the electrodes. Raman spectroscopy is one of the most interesting techniques to characterize and study different materials and processes in many fields. Mainly, this spectroscopic technique provides suitable information about vibrational modes which allows us to better understand at molecular level many species. Raman effect was a very important discovery and proof of this was the Nobel Prize in Physics awarded to C.V. Raman in 1930.

A number of groups around the world have combined Raman spectroscopy and electrochemistry, obtaining very interesting results linked to the power of these two instrumental techniques. However, the number of works using time-resolved Raman Spectroelectrochemistry is significantly small. Actually, it is not easy to obtain well correlated results and high quality Raman responses recorded in short integration times. This Thesis is mainly focused on the development of new devices for time-resolved Raman spectroelectrochemistry. In this work, we have not only developed spectroelectrochemical cells, but also MATLAB functions to manage the large amount of data obtained during an experiment and, even, the Raman spectrometer has been modified to synchronize the electrochemical and the spectroscopy information.

The development of the new devices and instrumental setups are described in Chapter 3 (Experimental methodology) that is actually the core of this work. It has been the most time consuming part of this Thesis, but it has also yielded the most satisfying results.

In Chapter 4 (Results and discussion), the different spectroelectrochemical cells, devices and setups, shown in Chapter 3, have been used to study different chemical systems of particular interesting for the scientific community.

In the first section of the Chapter 4 we have studied a conducting polymer performing Raman spectroelectrochemistry on a microelectrode, demonstrating the high spatial resolution of our Confocal Raman microscope. Using microelectrodes shows clear advantages for the study of some chemical systems, as is demonstrated for poly-3-ethylenedioxythiophene.

In order to demonstrate the capability of working at very low integration times with dynamic Raman spectroelectrochemistry, we have selected single walled carbon nanotubes as a proof of concept. Carbon nanotubes have been exhaustively studied in the last years, but there are very few time-resolved Raman studies of its oxidation and reduction. Understanding the electrochemical behaviour of this material is crucial for future applications.

Raman spectroscopy is not a very sensitive technique but when Surface-enhanced Raman scattering (SERS) takes place, the sensitivity of the technique is increased in several orders of magnitude. Since this effect was observed in the 70s it has been widely used in varied scientific fields. Nowadays and after a wide controversy, SERS effect has been explained by the contribution of electromagnetic and charge transference mechanism. However, it is still unclear which factors affect it and, consequently, have to be controlled for SERS applications. In this Thesis, the complex Raman signals observed during the generation of silver nanoparticles have been explained by performing complementarily UV/Vis absorption spectroelectrochemistry that helps to understand how the shape and the size of nanoparticles affects to the SERS effect.

In the fourth section of Chapter 4 a new spectroelectrochemical cell has been developed allowing us to perform Raman spectroscopy at liquid/liquid interfaces to study charge transfer processes. Electrochemistry at liquid/liquid interfaces is technically very complicated, but it provides invaluable information on a number of chemical processes of key importance in biology, medicine, energy, etc. We hope that the development of our new devices will help to shed more light on these processes. This work has been performed in collaboration with Prof. Fermín at the University of Bristol (United Kingdom). Moreover, in this section we have modified the liquid/liquid interface with carbon nanotube films which opens up a number of possibilities to facilitate both ion and electron transfer by supporting catalysers at the interface.

Finally, in the last section of Chapter 4 we have demonstrate the utility and versatility of our cells, using our devices in a completely different Raman spectrometer in collaboration with Dr. Kalbáč at the Heyrovsky Institute in Prague (Czech Republic). To illustrate the good performance of our cells we have selected the study of the SERS effect of gold nanoparticles deposited on a carbon nanotube electrode. As chemical system we have analysed the evolution of the Raman spectra of adenine and guanine during their oxidation. Understanding the oxidation of these bases is the first step necessary before studying the oxidation of DNA in the near future.

As usually this thesis is not a finished work, and for this reason we have decided to add a final chapter about the future perspectives of our work. Currently, the new devices and setups are being used during the writing of this Thesis. As always, this work is alive.

2. Theoretical fundamentals

Objetivos del capítulo

- Introducir la espectroscopía Raman al ser la técnica en la que se basa la tesis. Para ello se hace una revisión bibliográfica sobre el recorrido histórico seguido por esta técnica desde sus inicios hasta la actualidad.
- Explicar uno de los fenómenos más importantes que se observan en la espectroscopía Raman como es el denominado efecto *Surface-Enhanced Raman Scattering (SERS)*, así como los múltiples factores que influyen en él.
- Realizar una revisión de las nanopartículas metálicas en general, y de su síntesis electroquímica en particular, al ser uno de los sistemas abordados en el capítulo de resultados de esta tesis, y al ser la metodología elegida para crear sustratos SERS.
- Introducir los diferentes materiales y sistemas que se estudiarán a lo largo del capítulo 4, como son los polímeros conductores, los nanotubos de carbono, las nanopartículas metálicas, las interfases entre dos soluciones inmiscibles y las bases nitrogenadas presentes en el ADN.

Metodología

- Búsqueda y revisión crítica y selectiva de la bibliográfica directamente vinculada con los diferentes temas abordados en esta tesis, tanto en cuanto a técnicas utilizadas como a sistemas estudiados.

Resumen del capítulo

- Se han introducido los diferentes conceptos fundamentales para el seguimiento de la tesis.

- Se ha hecho especial hincapié en explicar el efecto SERS. Para ello no solo se explica el fundamento teórico sino todos los factores de los que depende, centrándonos especialmente en el sustrato necesario para tener tal efecto (tamaño, forma, método de síntesis, etc.), la longitud de onda de excitación y su relación con el sustrato, así como en las propiedades de la muestra objeto de estudio. Como puede deducirse de los resultados encontrados en bibliografía, todavía no se han aclarado completamente todos los aspectos relacionados con este efecto.

- Los polímeros conductores son materiales muy interesantes debido a sus particulares propiedades electrocrómicas, conductoras, mecánicas, etc. Este será uno de los sistemas estudiados en el capítulo de resultados, por lo que en este capítulo se realiza una revisión general de este material.

- Los nanotubos de carbono son uno de los materiales más interesantes en la actualidad debido a sus excelentes propiedades electrónicas, vibracionales, mecánicas, térmicas y químicas. En este capítulo se presenta una visión general de este nanomaterial y se analizan sus diferentes propiedades, ofreciendo una visión detallada de este material que posteriormente será estudiado y utilizado como sustrato en el capítulo de resultados.

- Aunque las nanopartículas metálicas se pueden sintetizar de muchos modos, la síntesis electroquímica presenta importantes ventajas respecto a otros métodos sobre todo en términos de obtener nanopartículas con su superficie limpia. Además, se demuestra el amplio rango de propiedades que presentan las nanopartículas, lo que las confiere gran utilidad en muy diversas aplicaciones.

- El estudio de la interfase entre dos disoluciones inmiscibles es un sistema de gran interés electroquímico debido a los diferentes procesos que pueden producirse en ella. En este capítulo se introducen este tipo de interfases, explicándose los tres tipos de transferencia que pueden tener lugar: transferencia de iones, transferencia de iones asistida y transferencia electrónica de una fase a otra. Particularmente, la transferencia iónica es de vital importancia en procesos biológicos y la transferencia electrónica presenta un futuro prometedor en la transformación de moléculas que están impedidas en medios hidrófobos o hidrófilos.

- La oxidación de las bases nitrogenadas presentes en el ADN es un proceso particularmente importante puesto que puede provocar un funcionamiento anómalo de las células e incluso la muerte. En este capítulo se presenta una visión general sobre el ADN que posteriormente será objeto de estudio en el capítulo de resultados.

2.1. Raman spectroscopy

Although Raman effect was theoretically predicted by Smekal in 1923 [2] and Kramers and Heisenberg in 1925 [3], the first evidences of Raman spectroscopy are dated in 1928 by Raman and Krishnan [4] and almost simultaneously by Landsberg and Mandelstam [5]. The *"New Type of Secondary Radiation"* referred by Raman in his paper had great importance and it was the main reason because he received the Nobel Prize in Physics in 1930. During 1930-1940s, the instrumental limitation was an important factor in the development of this technique. One example of these restrictions can be found in the light sources used in this period when the mercury lamp was the standard source. Although in 1952 the mercury spiral Toronto arc was introduced as a new source [6], the most important innovation for this technique was the laser invention in 1960 [7]. Thanks to the laser it was possible to focus the light beam on a small sample, avoiding problems with stray light, and obtaining high quality Raman spectra. Nevertheless, the breakthrough took place in 1974 when Fleischmann observed an unexpected enhancement in the Raman signal of pyridine adsorbed on a roughened silver electrode [8] (this phenomenon will be explained in more detail in Section 2.2). The technological development and the interest in this technique have advanced together, being actually Raman spectroscopy one of the most interesting techniques to characterize, analyse and study a number of materials, systems and processes in different scientific fields. This spectroscopic technique provides suitable vibrational, rotational and low frequency modes information which allows us to understand at molecular level many species.

For a better understanding of Raman spectroscopy is necessary to define the scattering phenomenon. Scattering is produced when an incident particle (neutron, electron or photon) beam hits a sample along a certain direction and due to the interaction between the incident particle and the target, the direction and even the energy of this particle beam can changed (Figure 2.1).

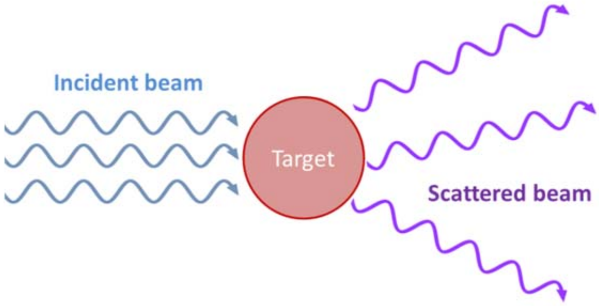

Figure 2.1. Scattering phenomenon

As a result of the interaction between the sample and the incident beam, the photons from the incident beam are absorbed by the molecules, exciting them to a virtual energy states. However, the increment of energy is not a quantized process. Therefore, depending on the frequency of the radiation source, the molecule can take the energy of any infinite value (or virtual states) between the ground state and the first electronic state.

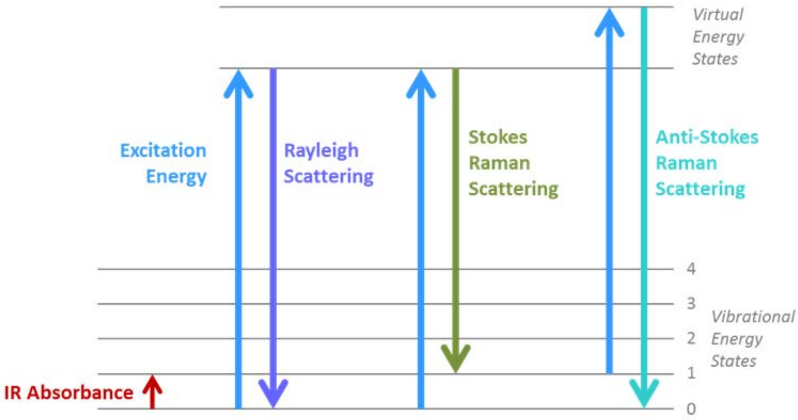

Figure 2.2. Rayleigh, Stokes and anti-Stokes Raman scattering mechanisms.

Figure 2.2 shows Rayleigh and Raman scattering mechanisms. Rayleigh dispersion is produced when the molecule is promoted from the zero vibrational state of the ground state to a virtual state and it returns to the starting state without change of energy. This kind of scattering, when the energy of the incident and the scattered beam is the same, is known as elastic scattering. However, when the energy of the incident light beam and the energy of the scattered beam are different (inelastic scattering), it is known as Stokes and anti-Stokes Raman scatterings. Stokes scattering takes place when the molecule is excited from the zero vibrational state of the ground state to a virtual state and it returns to the first vibrational state of the ground state. However, Anti-Stokes scattering is produced when the molecule is raised from the first vibrational energy of the ground state to the virtual state and after that, it backs to the zero vibrational state of the ground state. At room temperature, the fraction of molecules found in the first vibrational state of the ground state is small, so the intensity of anti-Stokes bands is always much lower than Stokes signals (I_{Stokes} / $I_{Anti-Stokes}$ > 1) (Figure 2.3). Furthermore, Raman frequency is positive or negative for anti-Stokes or Stokes scattering, respectively, being these frequencies equal in absolute value.

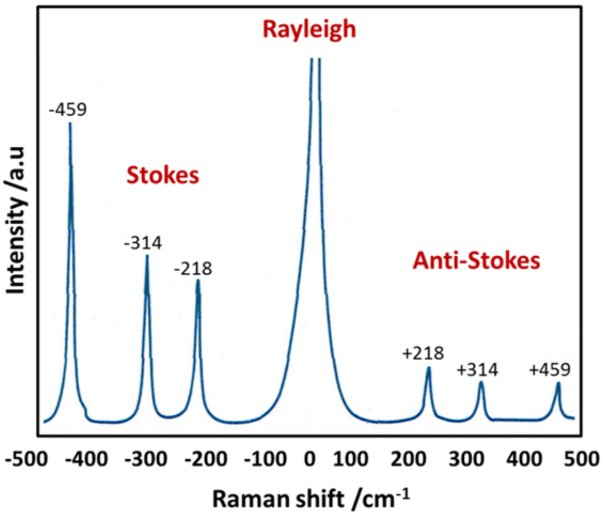

Figure 2.3. Raman spectrum of CCl_4.

2.2. Surface-enhanced Raman scattering (SERS) effect

In 1974, Fleischmann observed for the first time a huge enhancement of the Raman intensity for pyridine molecules on a roughened silver electrode [8], although this behaviour was interpreted in 1977 by Van Duyne [9]. This phenomenon was called *Surface-Enhanced Raman Scattering (SERS)* effect and its discovery opened up new horizons for Raman spectroscopy. The main difference respect to Raman spectroscopy is the presence of metal nanostructures as fundamental factor for the enhancement

(Figure 2.4). Therefore, not only the interaction sample-light has to be considered in the SERS effect but also the metal nanostructure-light interaction.

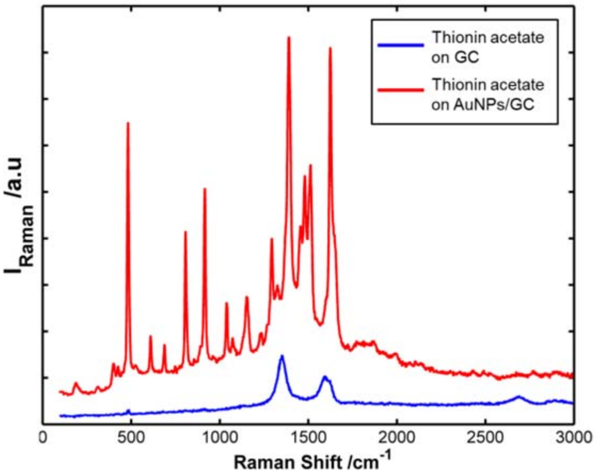

Figure 2.4. Raman spectra of thionin acetate (a) on a glassy carbon electrode and (b) on gold nanoparticles/glassy carbon electrode as SERS substrate.

SERS effect is explained by the contribution of two mechanisms, electromagnetic and chemical (also denoted as charge transference) enhancements [10–12]:

- ELECTROMAGNETIC MECHANISM is a physical effect in which the enhancement of the local electromagnetic fields is due to electromagnetic resonances owing to the collective excitation of conduction electron oscillations (plasmon resonance) in the metallic structure. For practical applications, when the electromagnetic field of the incident light beam produces the excitation of the plasmon resonance, it generates a nanometrical volume on the metal surface in which the molecules are detected, so, it is not necessary the direct contact between the analyte and the metallic surface to have a Raman signal.

- CHEMICAL MECHANISM is associated with the particular electronic properties of the molecule. It is produced by the electronic interaction between the molecule and the metal surface, resulting in an enhancement of the polarizability of the molecule. The chemical mechanism produces the perturbation of the electronic structure of the molecule adsorbed and, consequently, the modification in its optical properties. In this way, the interaction between the molecular orbitals of the molecule and the electronic band of the metal surface makes enable the electron transfer between them. Furthermore, this kind of interaction requires the direct contact, so this mechanism is a short range effect, limited to the first layer of molecules adsorbed.

The electromagnetic contribution to the enhancement factor is higher than the chemical one. In orders of magnitude, the enhancement due to the electromagnetic mechanism is between 10^3-10^{10} instead of 10-10^3 in the chemical case [11].

After a wide controversy, especially in the 1990s when the charge transfer was considered as unique contribution to SERS effect [13–15], nowadays is accepted that both mechanisms are responsible of this extraordinary effect [10–12,16–18].

2.2.1. SERS factors

In this Section, we review different factors that we consider important to remark due to their influence in the SERS effect. As we will see below, these factors are many and varied but they can be classified in 3 categories: metal nanostructures as SERS substrates, the laser used due to its specific excitation wavelength and the properties of the sample which will be studied.

A. Metal nanostructures

One of the most important factors in SERS effect, or maybe the most important one, is the metal nanostructure. According to Natan [19] and to our experience, the ideal SERS substrate should have:

- High SERS activity.
- Uniformity or ordered structure.
- Stability and reproducibility.
- Surface purity.

In our opinion, although the major contribution is the high SERS activity, we do not forget the other properties that make a substrate appropriated to SERS studies. However, it is complicated to obtain nanostructures with all these properties, and in general the substrate used (with specific properties) has to be chosen according to the final application. Nevertheless, the characteristics of these substrates are obtained by the control of different parameters such as type of metal particles, size, shape, thickness or interparticle spacing.

Noble metal Au, Ag and Cu roughened surfaces were the first SERS substrates used because they were considered the unique that could provide an enhancement. Nowadays other transition elements (Pt, Pd, Co, Fe, Ni and Rh) have showed these properties [20–28], increasing SERS applications.

If we compare the enhancement produced by the different metals, in general, Au, Ag and Cu show the highest enhancement (averaged surface enhancement up to 10^6 [29]). The reason why Pt, Pd, Co, Fe, Ni or Rh are not as useful as Au, Ag and Cu is mainly due to their dielectric properties [30]. An exact classification of the metals as a function of the enhancement order factor is not possible because it depends on several factors explained below (as nanoparticles properties, synthesis procedure or excitation wavelength). In point of fact, nanoparticles of one specific metal can show the best SERS response for a specific analyte but do not show the highest enhancement factor when the experimental conditions or the analyte studied change.

A careful control of the physical properties of a SERS substrate is necessary to obtain the desired result. Next, some of the most significant parameters are depicted:

- SIZE. Many studies have been focused on the influence of the diameter [31–38], the thickness of the layer formed [34,39] and the interparticle spacing [40]. For example, Li suggested a diameter of 50 nm as the optimal size of spherical gold nanoparticles (AuNPs) for SERS spectroscopy under different conditions [32] (**¡Error! No se encuentra el origen de la referencia.**.a). This conclusion was extracted from the analysis of the Raman intensity of 4-aminothiophenol and 4-nitrothiophenol, in which the highest SERS effect for these two compounds was observed at the same AuNPs diameter (**¡Error! No se encuentra el origen de la referencia.**.a). In this work, authors suggest that their conclusions might also be applicable to other adsorbates. However, in a similar work, Tian studied the optimal size of AuNPs to obtain the best SERS intensity of pyridine [38], and they concluded that for this system the optimal diameter was about 135 nm (**¡Error! No se encuentra el origen de la referencia.**.b).

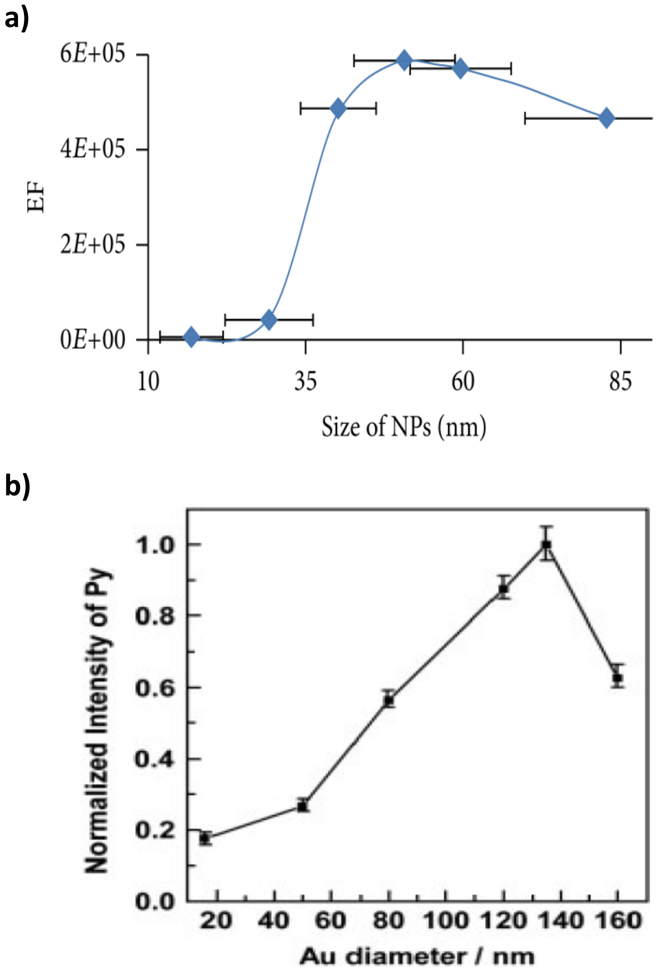

Figure 2.5. Optimal diameter of AuNPs for the study of (a) 4-nitrothiophenol [32] and (b) pyridine [38].

Something similar happens with silver nanoparticles (AgNPs). Scaiano determined 50nm as the optimal size of spherical AgNPs analysing rhodamine 6G spectra [35]. This result is not in agreement with the study of Graham, who obtained the highest enhancement factor studying malachite green oxalate, rhodamine 6G and thiophenol using AgNPs of 65 nm [41]. Li also analysed rhodamine 6G spectra, suggesting the optimal size range of AgNPs between 35-55 nm [42].

From these examples we can infer that there is not a consensus about the optimal diameter to obtain the highest SERS intensity. As we commented above, the optimal conditions highly depend on the studied system and the experimental conditions (substrate, analyte, excitation wavelength, …).

- SHAPE. It is really challenging to obtain nanoparticles (NPs) with exactly the same shape, for that reason, comparison of experiments is very problematic. However, many authors have studied the influence of the NPs shape in the SERS response [36,43–45]. The NP shapes used in those works are really varied and fascinating as is shown in **¡Error! No se encuentra el origen de la referencia.** [45]. This case evidences that is impossible to define a universal geometry which shows the best SERS response because many factors, as for example the excitation wavelength, influences in the SERS intensity obtained for the same NPs.

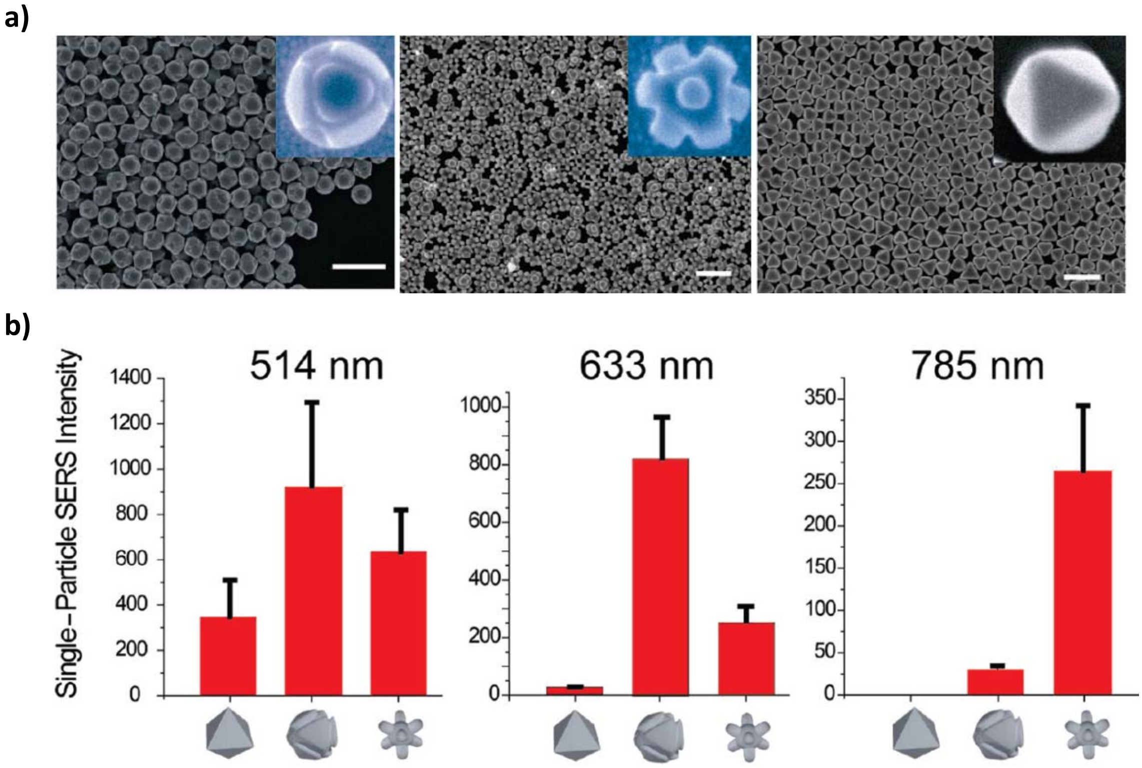

Figure 2.6. SEM images of (a) octahedral AgNPs with the edges and corners selectively etched leaving. (b) SERS intensity of benzenethiol using these AgNPs and different lasers [45].

- NPs COMPOSITION. During last years the combination of metals is being widely used to obtain SERS substrates with different properties. Examples are core@shell NPs whose core and shell are formed by different metals. Although the use of Au core is frequent, (Au/Pd [46,47], Au/Ag [48,49], Au/Pt [50], Au/Rh [51], Au/Cu [52], Au/Co [53]) other materials have been also tested, such as silver, iron, copper or titanium oxide (Ag/Pt [54], Ag/Cu [55], TiO_2/Au [56], Ag/Fe_3O_4 [57], Fe_2O_3/Ag [58], FePt/Ag [59], Fe_2O_3/Au [60], Ni/Au [61], Cu/Ni [62], etc). In some cases it has been also proposed three layers structures, Au/Pd/Pt [63], Au/Pt/Au [64] (Figure 2.7), Ag/C/Ag [65].

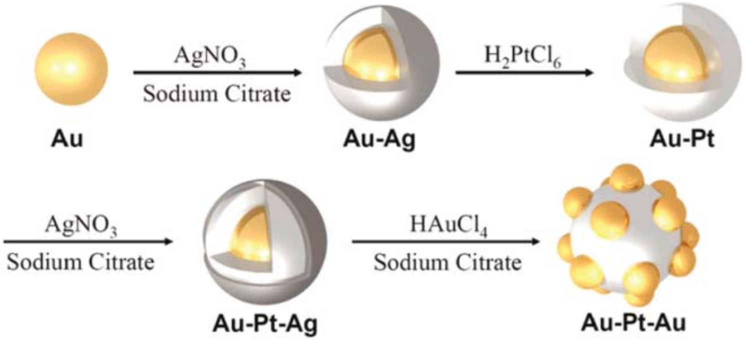

Figure 2.7. Chemical synthesis of Au/Pt/Au [64].

However, one of the most promising and interesting SERS substrate structure was proposed by Tian in 2010 [29]. This substrate consists of metal nanoparticles isolated with a very thin and optically transparent shell of SiO_2 or Al_2O_3 (Figure 2.8), known as SHINERS (Shell-isolated nanoparticles enhanced Raman spectroscopy).

SHINERS properties are due to the strong electromagnetic field of the Au core, which is transferred to improve the chemical signal associated with the vibrational bands of the sample. The shell allows controlling the distance from the core to the sample surface and furthermore, using an inert shell assures that there is not contact between them.

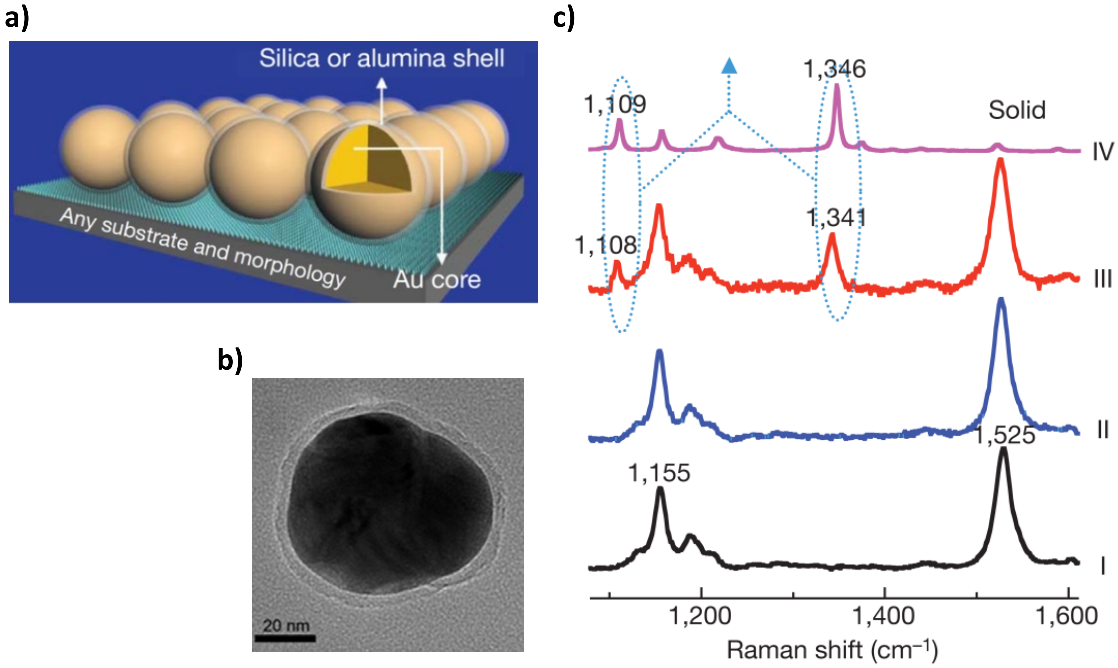

Figure 2.8. SHINERS (a) structure and (b) SEM image. (c) Pesticide (pericarps) detection: I sample without pesticide, II sample with pesticide, II sample with pesticide and SHINERS, IV pesticide solid [29].

Although initially SHINERS were made with Au core, Tian *et al.* also proposed their synthesis with Ag core [66]. They compared by three-dimensional finite-difference time-domain (3D-FDTD) calculations the enhancement factor of Ag/SiO_2 and Au/SiO_2 on smooth Au and Ag in specific conditions (core diameter 200 nm and 532 nm excitation wavelength), and they concluded that Ag is more SERS active than Au, more versatile respect to the excitation wavelength and, additionally, cheaper. SHINERS are not only useful for electrochemistry (electrocatalysis, electrochemical adsorption, electrochemical corrosion and electroplating [29,67]), but also for others fields such as biology (probing of biological structures) or for analysis (determination of glucose [29] or detection of drugs or pesticides on food [68]).

Moreover, the advances and developments in new materials, as carbon nanotubes [69,70], graphene [71–73] or polymers [74,75], make possible the fabrication of different composites with metal nanostructures. As we will see in Section 4.5, we electrodeposit AuNPs on a press-transfer single-walled carbon nanotubes electrode, obtaining a SERS substrate to study, in our case, the oxidation of purine bases of DNA.

- SYNTHESIS METHOD. These nanostructures with specific SERS substrates properties can be created in a number of ways, being chemical reaction [76–78], electrodeposition [70,79,80], electrochemical surface roughening [81–84], sputtering coating [85,86], laser ablation [87–89], lithography [90–92] and evaporation deposition [93,94] the methods which show the highest enhancements. Figure 2.9 shows an example that the enhancement depend on the synthesis route [86].

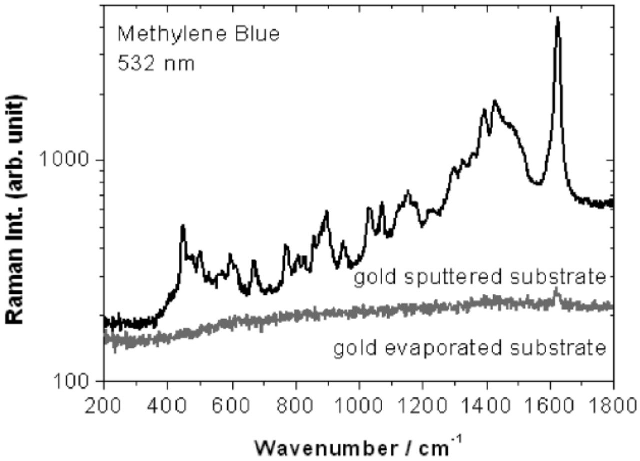

Figure 2.9. SERS spectra of methylene blue using gold substrates synthesized by different methods [86].

It is noteworthy that nowadays there is not a universal substrate to obtain the highest SERS enhancement for whatever system because there are too many factors to take into account. Hence, analyst has to look for a substrate which shows good SERS performance for specific experimental conditions. As will be seen along Chapter 4, we use a different SERS substrate for each chemical system studied and we change it depending on, for example, the laser excitation wavelength.

B. Excitation wavelength dependence

Another important factor to be considered for the SERS enhancement is the dependence of this effect on the excitation wavelength; or rather the interaction between the excitation wavelength and the metallic nanostructures plasmon band. The plasmon band is associated with the collective oscillation of the electron gas at the surface of the NPs (electrons of the conduction band) that is correlated with the electromagnetic field of the incident light. This plasmon band is characteristic of each kind of nanoparticles and it depends on their size and shape (**¡Error! No se encuentra el origen de la referencia.**).

According to the electromagnetic mechanism, the highest SERS enhancement is observed when the excitation wavelength matches with the plasmon absorption band of the substrate [86,96,97].

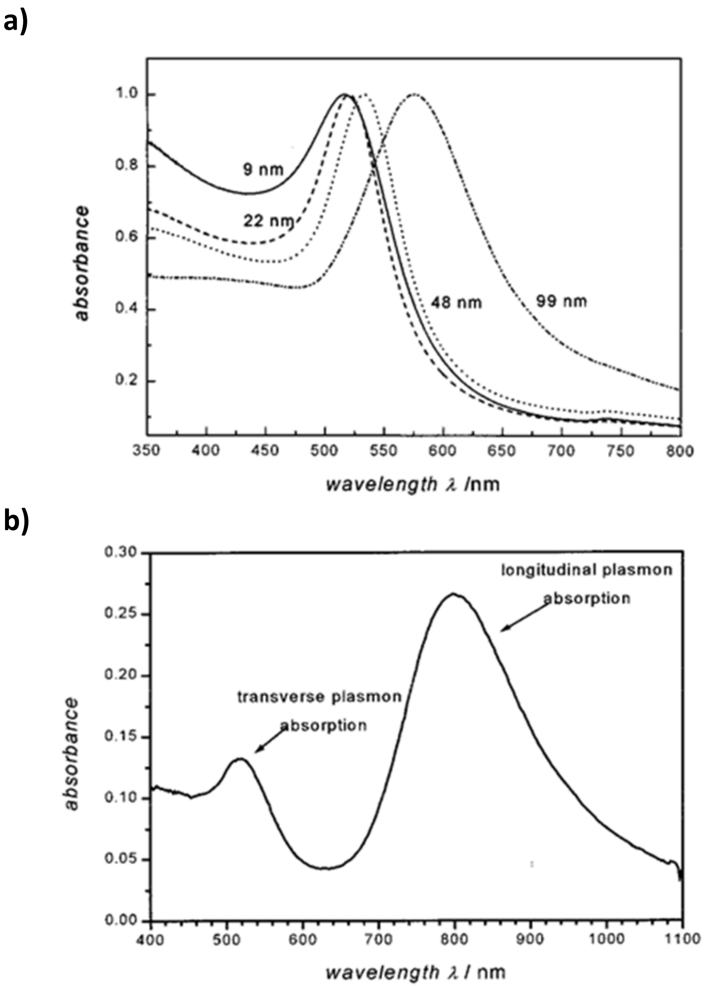

Figure 2.10. Plasmon band of (a) spherical AuNPs of different size. (b) Transversal and longitudinal components of the plasmon band of AuNPs with different shapes [95].

The enhancement factor (EF) can be calculated, if the intensities are normalized for the laser power and for the integration time, by [97,98]:

$$EF = \frac{I_{SERS}/C_{SERS}}{I_{NR}/C_{NR}} \qquad \text{(eq. 1.1)}$$

where I_{SERS} and I_{NR} are the SERS and normal Raman intensities and C_{SERS} and C_{NR} are the concentration of the sample analysed in SERS and normal Raman measurements, respectively.

As we have explained above, the classical SERS substrates are formed by Au, Ag and Cu, but Au and Ag are the most used substrates because Cu is less inert. Plasmon band of these metals is centred in the visible and near infrared wavelength (Figure 2.11), and considering that Raman scattering is produced in this range of wavelengths the use of Au and Ag as SERS substrate is widespread.

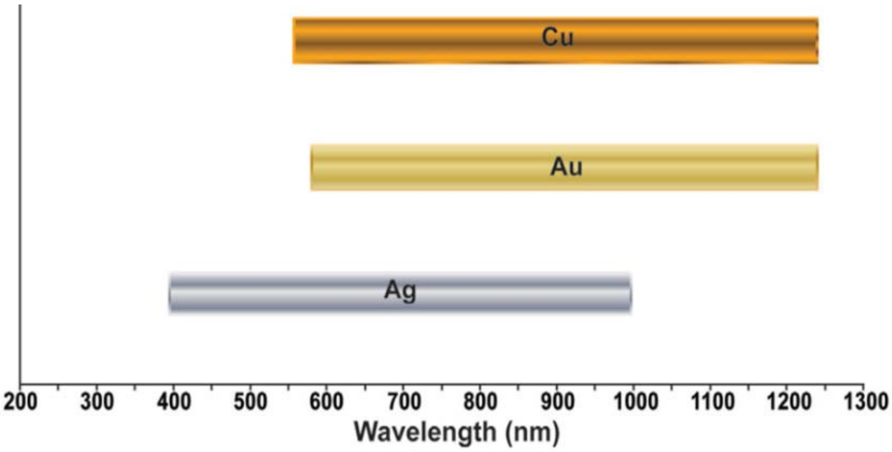

Figure 2.11. Approximate wavelength ranges where Ag, Au, and Cu have been well-characterized as SERS substrates [99].

Although some oxides and nitrides of different metals (Ti, V and Al) have been also proposed as SERS substrates due to their similar optical properties to the classical metals [100], the use of Au and Ag is still preferred.

There are a number of works which analyse the influence of the laser wavelength on the same substrates [98,101–104]. Results indicate that not only SERS intensity changes with the laser, but also the vibration modes that can be observed depend on the excitation wavelength. Figure 2.12 shows SERS bands of p-aminothiophenol on AgNPs with different excitation lasers (514.5 and 1064 nm). In both cases, the spectra shows the bands which correspond to the symmetric a_1 vibration modes, but only using the 514.5 nm excitation line is possible to observe the bands associated with other vibration mode (b_2).

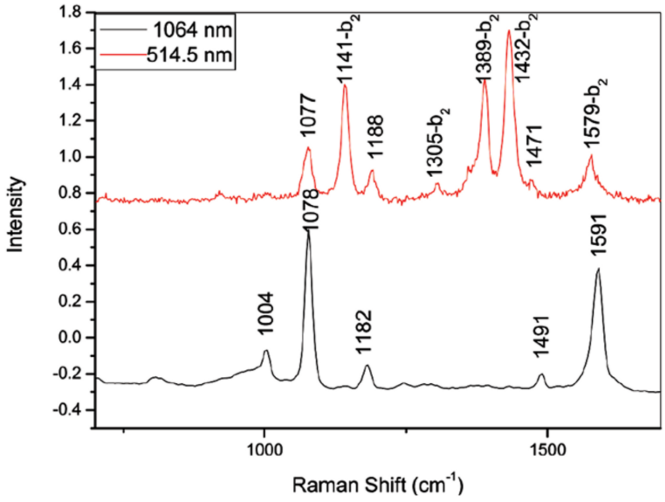

Figure 2.12. p-aminothiophenol SERS spectra using excitation lines of 514.5 and 1064 nm [103].

In our case, AgNPs SERS substrates provide a good SERS enhancement using a 532 nm laser. On the other hand, and as Figure 2.11 shows [99], the use of AuNPs requires an excitation wavelength higher than 550 nm. For that reason, the study of the oxidation mechanism of purines bases of DNA on AuNPs/carbon nanotube electrode (Section 4.5) was performed using a 633 nm laser instead of 532 nm laser.

C. Sample

After describing the properties of SERS substrates and the dependence between the excitation wavelength with the plasmon band, the characteristics of the sample to be studied have to be also described. Not all species are able to be detected by SERS scattering and only certain properties make the system able to show SERS response.

Besides the interaction between the incident light and the metal nanostructure there is also another interaction, which must be considered, the interaction between the sample and the excitation light. **¡Error! No se encuentra el origen de la referencia.** shows the SERS spectra of five oligonucleotides (R6G, FAM, ROX, Cy5.5 and Bodipy) using two excitation wavelengths, 514 and 633 nm [104]. **¡Error! No se encuentra el origen de la referencia.**.a shows that only three of these oligonucleotides (R6G, FAM and ROX) provide an intense SERS response because they are in resonance with the 514 nm excitation wavelength. **¡Error! No se encuentra el origen de la referencia.**.b shows the spectra of the same five oligonucleotides but in this case with and excitation laser of 633 nm. Now, only three oligonucleotides have an intense signal (ROX, Cy5.5 and Bodipy) because they are in resonance with the new excitation wavelength, but these spectra are significantly different from those of **¡Error! No se encuentra el origen de la referencia.**.a. Only one nucleotide is detected with both lasers because ROX shows two absorption bands that are in resonance with 514 and 633 nm excitation wavelengths.

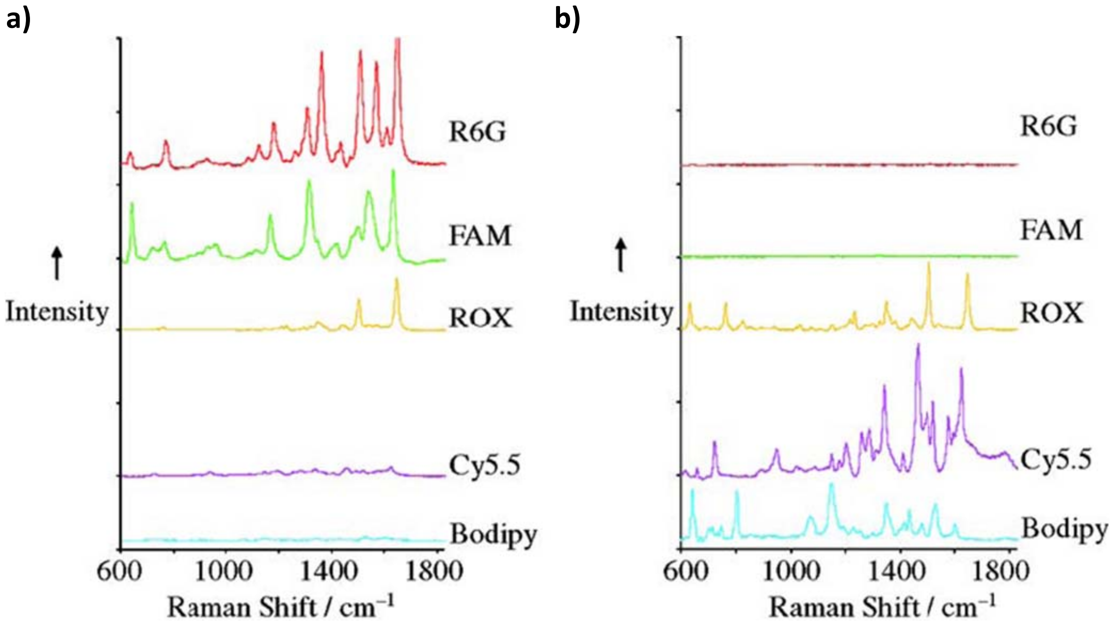

Figure 2.13. SERS spectra of five synthetic oligonucleotide with excitation wavelength of a) 514 nm and b) 632 nm [104].

The intensity of the SERS bands depends also on the concentration of the analyte, being both values linear dependent (Figure 2.14) [105–107]. Moreover, it is not possible to increase the concentration of the analyte to substitute the SERS effect, that is to say, the intensity of the Raman scattering with high analyte concentration will not be by far as intense as using a SERS substrate.

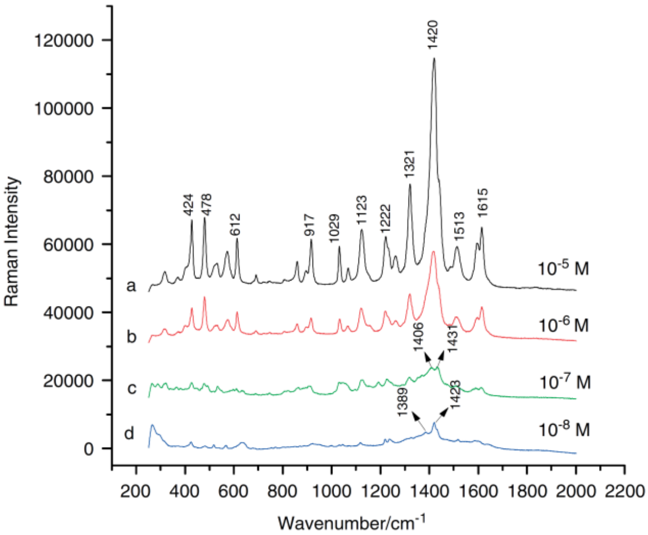

Figure 2.14. SERS spectra of thionine at concentrations of (a) 10^{-5} M, (b) 10^{-6} M, (c) 10^{-7} M and (d) 10^{-8} M using AuNPs as a substrate [107].

Other factors to take into account are the experimental conditions in which the measurements are performed because they can change the SERS activity of a substrate For example, Figure 2.15 shows the effect of the temperature in the SERS enhancement [108].

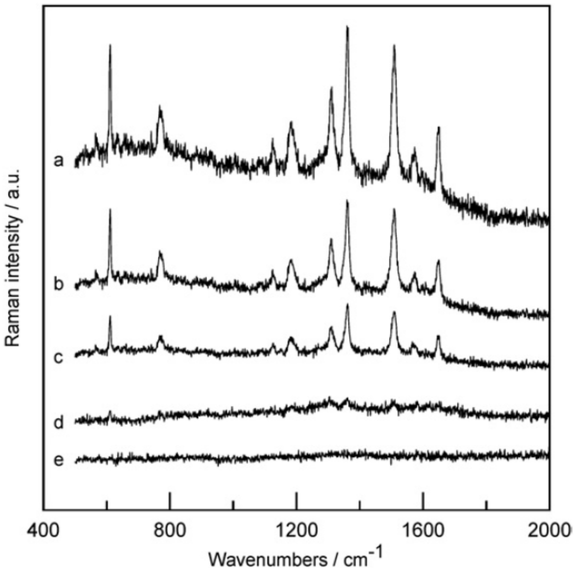

Figure 2.15. SERS spectra of rhodamine 6G adsorbed on a roughened Ag substrate at different temperatures: (a) 25 °C, (b) 50 °C, (c) 100 °C, (d) 125 °C and (e) 150 °C [108].

Distance between analyte and metal surface is another important factor that affects to the electromagnetic mechanism [97]. The electromagnetic field of the incident beam produces the excitation of the plasmon resonance, generating a volume (of few nanometres) on the surface in which the molecules are detected (Figure 2.16). Hence, it is not required that analyte and surface must be in direct contact. Although this idea is not in agreement with the chemical mechanism, which considers that the analyte must be directly adsorbed on the surface, it is accepted that distance is an important SERS factor.

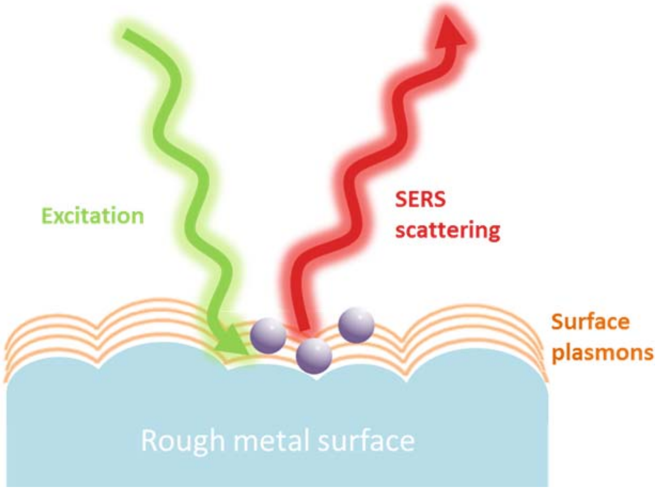

Figure 2.16. Electromagnetic mechanism contribution to the distance between the analyte and the metal surface.

However, it is necessary not only to think in terms of distance, but also in the orientation that the molecule acquires respect to the surface because it determines the interaction between this molecule and the metal structure. Changes in the intensity and position of the SERS bands can be observed due to the modification in the orientation of the molecules. Once the molecules are absorbed on the surface, it can break the symmetry and some bands that were initially forbidden can be allowed to be enhanced [18]. A clear example will be discussed in Section 4.5, in which we analyse the orientation of the adenine and guanine oxidation intermediates respect to the AuNPs deposited on a SWCNT electrode.

2.2.2. Applications

SERS has been widely used in many fields. Although there are countless examples, some of these applications could be classified in:

- SPECTROELECTROCHEMISTRY AND CATALYSIS: The combination of SERS scattering with different electrochemical techniques allows monitoring multitude of processes as for example oxygen reduction [109], carbon monoxide stripping [83,110], platinum catalysed reactions [64,111], electron transfer between proteins [112], cyanide adsorption [70,80,113], benzyl chloride reduction [114], formic acid oxidation [83], metal electrodeposition [114,115], etc.
- DETECTION OF SINGLE MOLECULES AND TRACES: SERS scattering has been demonstrated as one of the most useful techniques for the detection of different species as dyes [86,117,118], drugs [119], food additives [29,120] or explosives [121].
- BIOLOGICAL AND MEDICAL APPLICATIONS: this is one of the fields in which this spectroscopic technique has become more important due to the capacity to detect carcinogenic cells [122,123], DNA components [124–126], therapeutic agents [127], glucose [128–130], etc.
- CHARACTERIZATION OF MATERIALS: numerous and varied materials have been characterized by this technique, examples of that are carbon nanotubes [131–134], graphene [135–138], graphite [139–141], fullerenes [142,143], polymers [144,145], nanocomposites [146,147] among many others.
- ART CONSERVATION: identification of pigments, oil and pastels in paintings [148–151], textiles [151,152], wood sculptures [153] and even in archaeological samples [154] have been successfully analysed (**¡Error! No se encuentra el origen de la referencia.**).

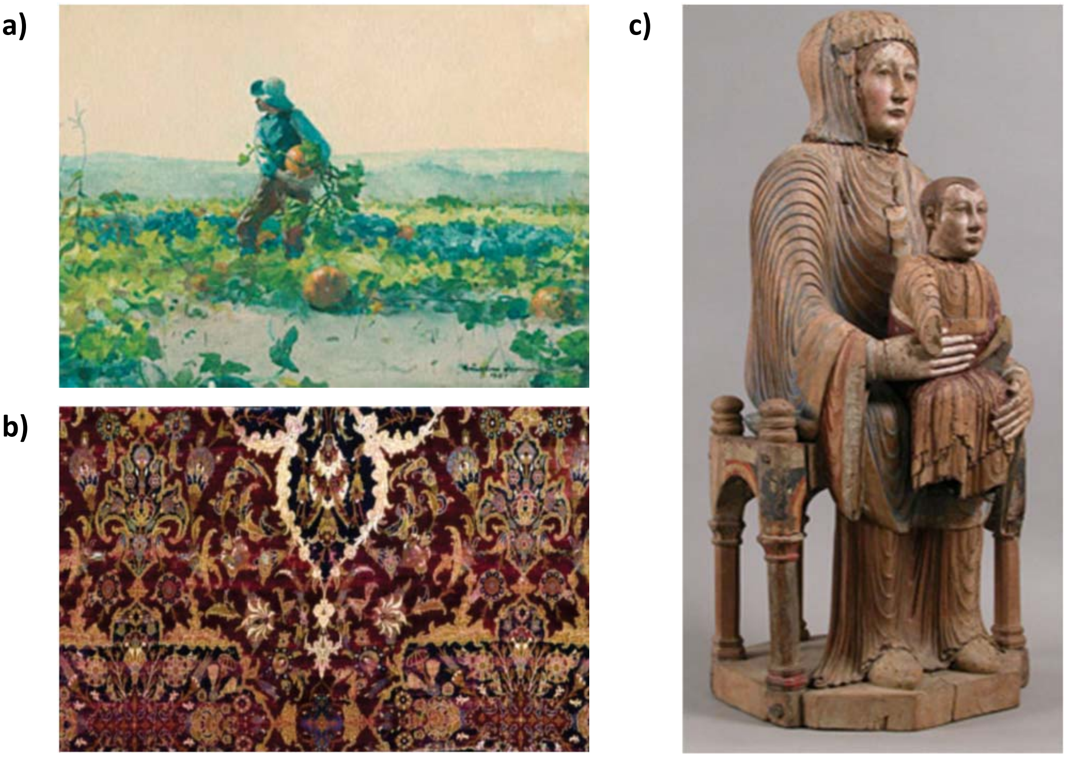

Figure 2.17. Art samples which have been analysed by SERS: (a) 'For to Be a Farmer's Boy' (Winslow Homer, 1887) [148], (b) portion of a carpet from Bursa/Turkey/Istanbul (late 16th/early 17th century) [150], (c) The Morgan Madonna, Virgin and Child in Majesty (France, 1150-1200) [153].

2.3. Conducting polymers

Although the oxidative polymerimerization of aniline was described by Letheby in 1862 [155], it was not until more than 100 years later, in the 1970s, when the research on conducting polymers intensified. Contributions of Heeger and MacDiarmid obtaining polyacetylene with high conductivity using halogens in the synthesis [156] or the improvement in the polyheterocyclic chemistry when Diaz obtained polypyrrole films with high conductivity [157] allowed an important progress in the conducting polymers chemistry.

Polymers are known to have good insulating properties. However, it is now recognized that there are some polymers which have conducting properties. These polymers that conduct the electrical current are called conducting polymers (also conductive or conjugated polymers). According to its conductivity these polymers can be classified in two categories:

- INTRINSIC CONDUCTING POLYMERS (ICPs) are those in which the electrical conductivity arises from the electron π extended conjugation along the polymer chain. This extended π-conjugated system of the conducting polymers have single and double bonds alternating along the polymer chain. Examples of ICPs are polypyrrole, polyaniline, polyacetylene and polythiophene (Figure 2.18).

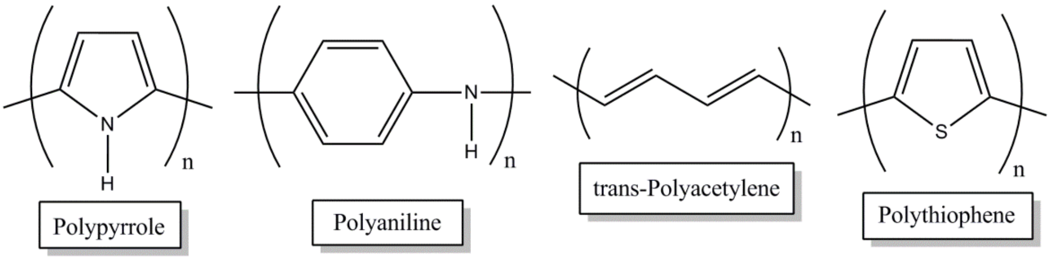

Figure 2.18. Examples of ICPs: polypyrrole, polyaniline, trans-polyacetylene and polythiophene.

- EXTRINSIC CONDUCTING POLYMERS (ECPs) are those in which the conductivity is due to the inclusion of conductive materials such as metals, graphite or charge transfer complex in the polymer matrix.

The conductivity values of conducting polymers are varied, as is shown in Figure 2.19, because different parameters can affect the conductivity of a polymer such as the current density, the concentration of monomer, the substituents on the monomer, the kind and concentration of the contraions, the solvent, the temperature or the working electrode used in the electrochemical synthesis [158].

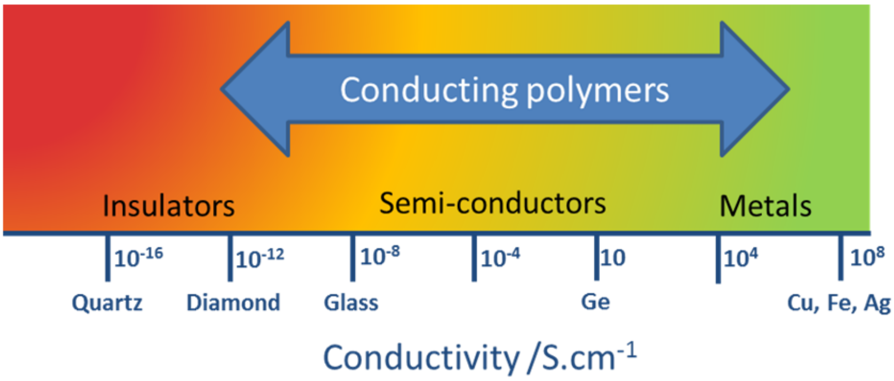

Figure 2.19. Conductivity of conducting polymers.

Charge transport and hence, the conductivity of this kind of polymers has been explained by different models:

- CHARGE DELOCALIZATION MODEL. This model considers that the π-bonding orbitals are overlapped producing the valence band. Above this band is located the conduction band, which is empty and is formed by the π-antibonding orbitals. The difference between the energy of the valence band and the conduction band is known as band gap. Band gap of neutral polymers is higher than 1.5 eV (for a semiconductor this value is around 1 eV), which makes them an insulator material. Initially, the conversion to a conducting or semiconducting material was attributed to the incorporation of an electron in the conduction band or by the removal of an electron from the valence band. However, this model was considered incorrect when solitons, unpaired electrons that can be removed to form a carbocation or paired with another electron to form a carbanion centre, were discovered in the neutral polyacetylene. Using semiconductors terminology, electron removing/adding in conducting polymers is called doping. It is named as p-doping when the polymer is oxidized and as n-doping if the polymer is reduced. In orbital terms, the electrons of the solitons are in intermediate energetic levels between the valence and the conduction bands. Thus, the conductivity in p-doping can be considered as electronic “holes” because electrons of the valence band can go to the orbital of the soliton which is empty, producing vacant positions in the valence gap (Figure 2.20.a). On the other hand, the conductivity in n-doping is explained as a soliton that has two electrons and one of them can promote to the conduction band (Figure 2.20.b). Solitons cannot be considered as radical centres because they are delocalized along the chain and reticular reactions are energetically unfavourable. However, as the concentration of solitons along the polymeric chain is not enough to explain the high increase in the conductivity of these polymers another model was proposed.

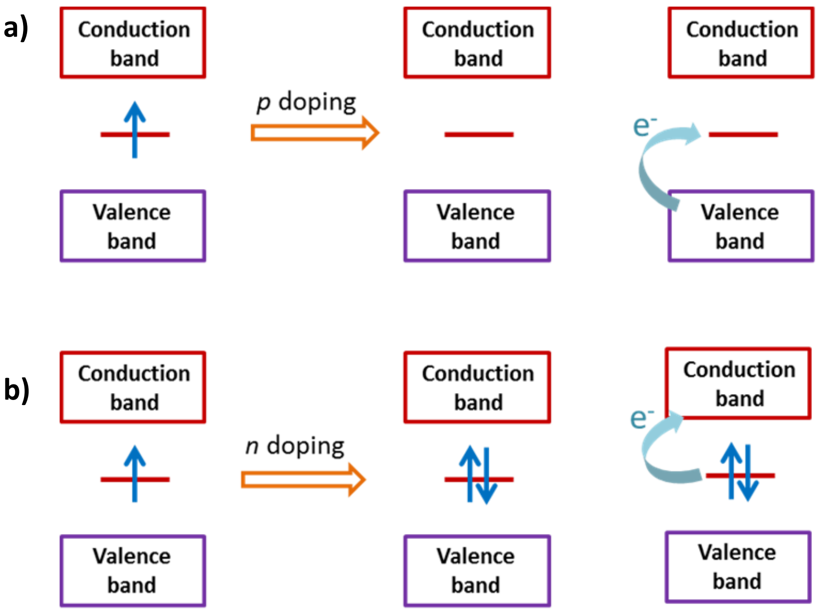

Figure 2.20. Molecular orbitals of a neutral soliton, (a) positive charged (p-doping) and (b) negative charged (n-doping).

- LOCALIZED CHARGE MODEL. This model considers that the charge is localized in the polymeric chain forming an ionic pair with the counterion [159]. The resonance energy lost with the localization of the charge is recovered by distortions in the chain. In this case, the oxidation produces the extraction of an electron of a double bond [160]. Then, a structural relaxation takes place producing a local distortion near the charge and the structure of this fragment is transformed in a quinoid structure in which simple bonds are shorter and they acquire a double bond character. The radical (anion or cation) obtained is known as polaron (Figure 2.21).

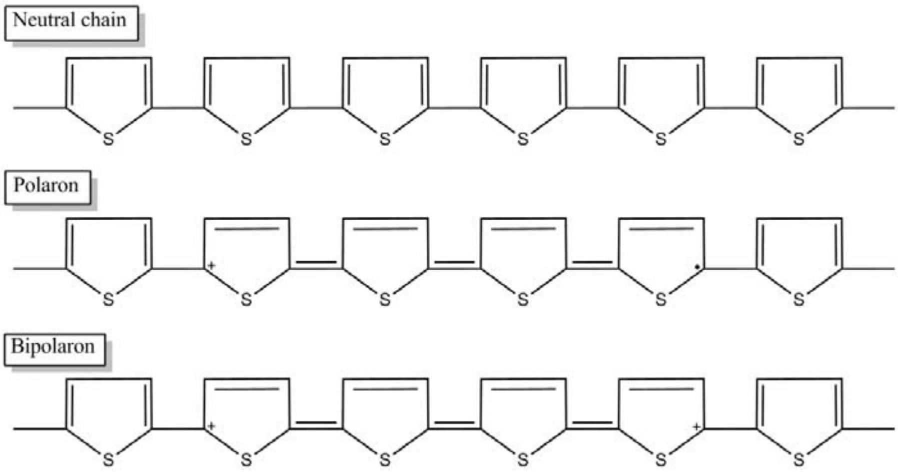

Figure 2.21. Structure of the chain of a neutral polymer, polaron and bipolaron.

If a second electron is extracted, there would be two possibilities: the electron is removed in other position forming another polaron, or the adjacent radical to the positive charge is removed producing a bipolaron (Figure 2.21).

In orbital terms, when the distortion of the chain is produced by the energy input (△E), it causes an energetic increase (+△E) of the HOMO orbital and an energetic decrease (-△E) of the LUMO orbital (Figure 2.22). Hence, the electron removing/adding in the π orbital leads to the formation of two electronic states between the valence and the conduction bands in the polaron. After the extraction of a second electron, another polaron or a bipolaron can be formed. The energy of distortion with two positive charges is higher than with one positive charge and consequently, the energetic states of the bipolaron are more separated of HOMO and LUMO than in the polaron (Figure 2.22).

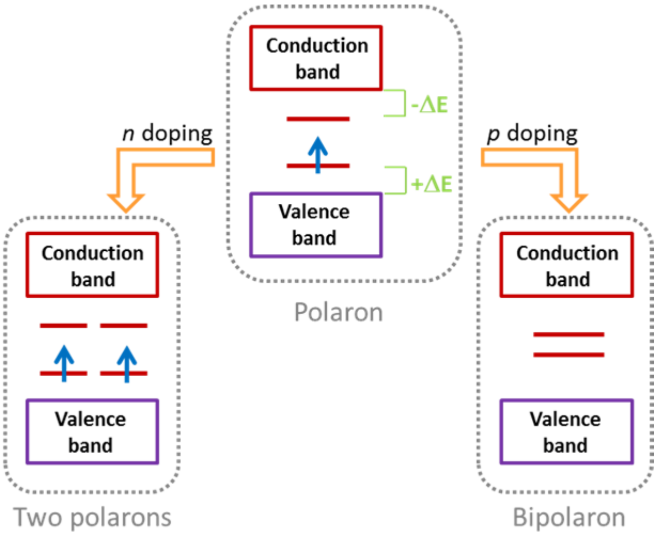

Figure 2.22. Molecular orbitals of a polaron, two polarons (n-doping) and a bipolaron (p-doping).

Therefore, the high conductivity is obtained when the polymer is highly doped due to the formation of large number of bipolarons in the polymeric chain. It leads to two bipolanoric bands between the valence and the conduction bands (Figure 2.23) [161]. Moreover, the small energetic difference between these bands can produce the partial overlapping of the lowest energetic band with the valence band and the highest energetic with the conduction band.

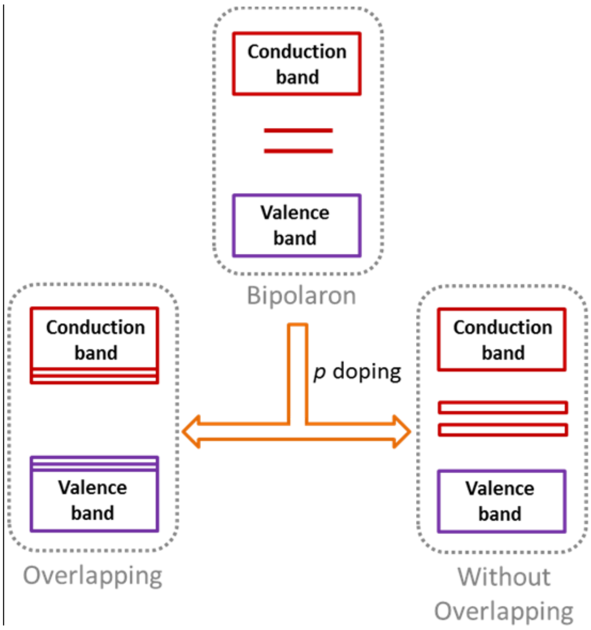

Figure 2.23. Energy levels of a bipolaron highly p-doped overlapping and without overlapping with conduction and valence bands

2.3.1. Applications

Due to their exceptional properties, conducting polymers have been widely used in many fields:

- Batteries [162–164].
- Light emitting diodes (LEDs) [165–167].
- Photovoltaic devices [168–170].
- Sensors [171–173].
- Optical devices [174–176].
- Electronic devices [177–179].
- Electrochromic devices [180–182].
- Mechanical and electromechemical devices [183,184].
- Corrosion protection [185,186].
- Catalysis [187,188].
- Drug and chemical delivery [189,190].
- Membranes [191,192].

2.3.2. Poly(3,4-ethylenedioxythiophene), PEDOT

- Many times, polythiophenes have been taken as models for studying the processes of charge transport in conducting polymers. The modification of their structure with different substituents causes changes in many properties of the polymer. Mainly, two factors should take into account: ELECTRONIC EFFECTS are related to the ability of the substituents to act as electron-acceptors or electron-donors. Electron-acceptor groups can increase the oxidation potential to incompatible values with the stability of the solvents, making difficult the polymerization. This inability to polymerize the monomers comes from the high reactivity of their radicals, which can react with the solvent or with anions in fast reactions to form soluble products instead of the polymers. On the other hand, although electron-donor groups favour the polymerization process because they reduce the oxidation potential that must be applied to oxidize the monomers, these groups can also stabilize the radical cations, making lower the reactivity.
- STERIC EFFECTS. Although steric factors not affect significantly to the oxidation of the monomer, this effect has a strongly influence in the morphology and therefore in the properties of final polymer.

In general, poly(3,4-ethylenedioxythiophene) (PEDOT, Figure 2.24.) is one of the most promising conducting polymers due to its exceptional properties.

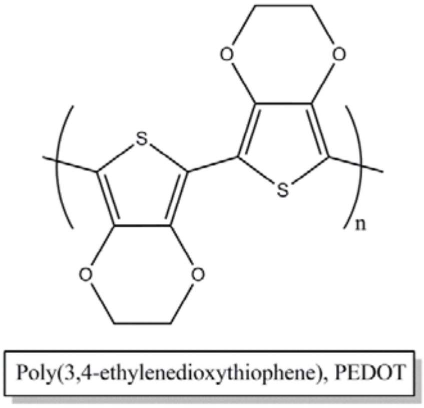

Figure 2.24. Structure of poly(3,4-ethylenedioxythiophene).

PEDOT shows a relatively high conductivity in the doped state (≈ 300 $S.cm^{-1}$) and electrochromic properties, being transparent in the doped state and coloured in the neutral state, being characterized by a relative low band-gap value [193]. Moreover, the high insolubility of PEDOT in almost all common solvents is remarkable. In many cases, once synthesized, PEDOT is used in a solvent medium different from that in which it has been formed [193].

2.4. Nanomaterials

Over the last decades, nanomaterials have been one of the most interesting systems employed in different fields due to their mechanical, thermal, electric, electronic, magnetic and optical properties. Although, nowadays there is not a universal definition, nanoscale materials are defined as a set of substances where at least one dimension is less than approximately 100 nm.

There are different classifications for this kind of materials, for example, nanomaterials can be classified on the basis of the number of dimensions which are not confined to the nanoscale range (<100 nm):

- Zero-dimensional (0-D): Materials where in all the dimensions are measured within the nanoscale (nanoparticles, quantum dots).
- One-dimensional (1-D): One dimension that is outside the nanoscale (nanotubes, nanowires, nanorods).
- Two-dimensional (2-D): Two of the dimensions are not confined to the nanoscale (nanofilms, nanolayers, nanocoatings).

As we will see below, different 0-D (gold nanoparticles and silver nanoparticles) and 1-D materials (single walled carbon nanotubes) were used in some studies performed in this Thesis.

2.4.1. Carbon nanotubes

In the carbon family there are many allotropes, such as diamond, graphite, graphene, nanotubes and fullerenes. A carbon nanotube (CNT) is a 1-D nanomaterial, where a graphene sheet is curled into a cylindrical shape. Depending on the number of graphene sheets rolled there are different kinds of carbon nanotubes. Thus, single-walled carbon nanotubes (SWCNT, **¡Error! No se encuentra el origen de la referencia.**.a) are produced when a unique graphene sheet is rolled, double-walled carbon nanotubes (DWCNT, **¡Error! No se encuentra el origen de la referencia.**.b) are obtained when two graphene sheets are curled, and, in general, multi-walled carbon nanotubes (MWCNT, **¡Error! No se encuentra el origen de la referencia.**.c) are constituted when more than one graphene sheets are rolled leading to a different number of concentric nanotubes. MWCNT were the earliest carbon nanotubes discovered by Iijima [194] in 1991, while the first SWCNT were referenced in 1993 [195,196].

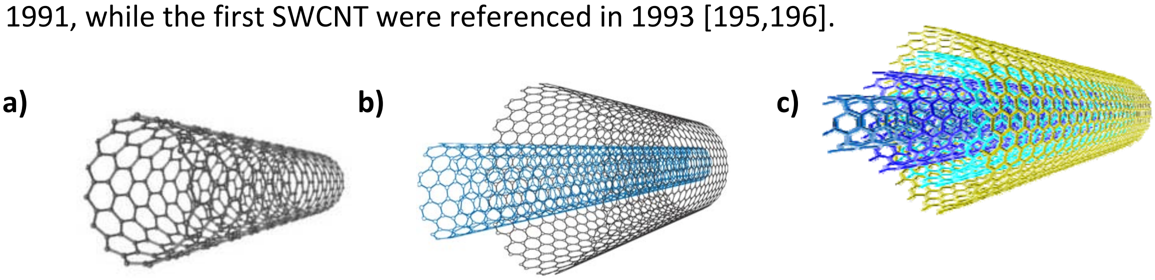

Figure 2.25. (a) SWCNT (image from http://www.carbonallotropes.com/carbon-nanotubes/39-single-wall-carbon-nanotubes.html), (b) DWCNT [197] and (c) MWCNT (image from http://medicalnanotec.com/cancer-therapy/multi-walled-carbon-nanotubes-cancer-treatment).

Depending on the final properties (orientation, alignment, nanotube length, diameter, purity and density), CNT can be produced using different methods [198,199] as discharge methods, laser ablation, pyrolysis, sonochemical/hydrothermal, high-pressure carbon monoxide conversion (HiPCO) or chemical vapour deposition (CVD).

A. *Structure of CNT*

CNT can be classified depending on how the graphene sheet is wrapped into a tube. CNT structure is described by the chirality vector:

$$C_h = na_1 + ma_2 \qquad \text{(eq. 1.2)}$$

where *n* and *m* are integer numbers and a_1 and a_2 are the unit vectors (Figure 2.26).

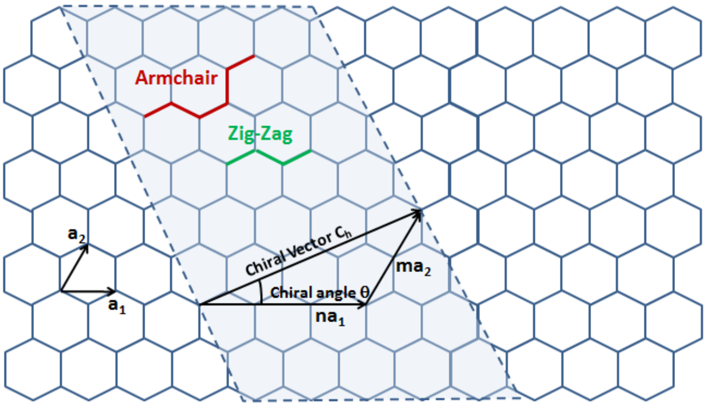

Figure 2.26. Scheme of CNT structure.

According to the chirality angle, it varies between 0 and 30 degrees, there are three possible geometries (**¡Error! No se encuentra el origen de la referencia.**):

- ARMCHAIR: the chiral angle is 30 degrees and the hexagons are lined up parallel to the axis of the nanotube. They show metallic properties.
- ZIG-ZAG: the chiral angle is 0 degrees and the hexagons are oriented in a circle around the nanotube. They only conduct an electric current when extra energy in the form of light or an electric field is applied, i.e, they have semi metallic character.
- CHIRAL NANOTUBES: the value of the chiral angle is between zero and 30 degrees and the hexagons do not form a line in the direction of the axes of the CNT.

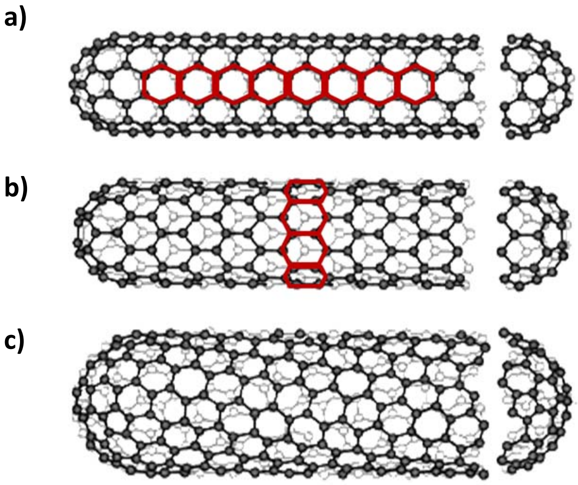

Figure 2.27. CNT (a) armchair (b) zig-zag and (c) chiral.

B. Properties of CNT

ELECTRONIC PROPERTIES

The properties of CNT are closely related to their electronic structure, which can be explained considering the electronic structure similar to a graphite sheet. Each carbon atom forms 3 covalently σ-bonds with the 3 neighbouring carbons via the orbitals sp^2. The fourth electron of each carbon atom extends over the basal plane in the p_z orbital and forms delocalized π-bonds.

Metallic and semiconducting character of CNT only depends on the chirality vector (n,m). In this way, slight structural modifications produce important changes in their electronic properties. So, only if (n - m) is a multiple of 3, the nanotubes exhibit a metallic behaviour, otherwise they show semiconducting properties. Figure 2.28 represents the electronic structure in terms of density of states (DOS), in which the energy scale is referred against the half-filling energy (ε_{hf}) that is the energy where all bonding orbitals (π) are filled and all antibonding orbitals (π^*) are empty, producing one π-orbital per carbon atom occupied. Figure 2.28 shows an example of metallic and semi-metallic CNT in resonance with the excitation laser energy (ε_{laser}), allowing several electronic transitions (E_{11} to the metallic and E_{11} and E_{22} to semiconducting CNT). This theoretical electronic transition diagram is defined by the electronic transition energy as well as the diameter (chirality parameters) of CNT.

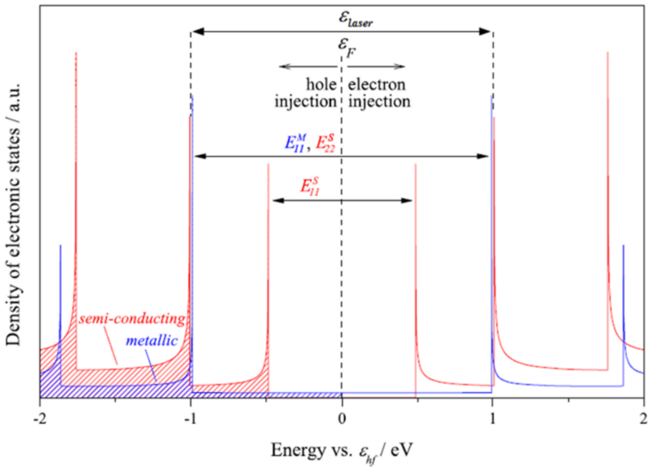

Figure 2.28. Theoretical electronic density of states (DOS) for metallic (blue) and semi-conducting (red) SWCNT where the occupied states are represented by shaded regions under the DOS and S and M denote whether this spacing belongs to a metallic or a semiconducting SWCNT [200].

- VIBRATIONAL PROPERTIES

Atomic vibrations of CNT can be studied theoretically and experimentally. One of the most theoretical procedures used is to study the phonon dispersion by the zone folding model. Experimentally, Raman spectroscopy allows identifying the vibration frequencies.

- PHONON DISPERSION

Phonons are the quantized states of the normal mode vibrations and they affect to the mechanical, transport and thermal properties in condensed matter systems. Zone folding model [201–203] is a useful tool to calculate the dependence between symmetry and chirality with the frequency vibration modes. Using this approach for a 2D carbon system as graphene it is possible to obtain also the phonon dispersion for CNT. The first approximation for the phonon dispersion of graphene starts considering it as graphite in the basal plane [204]. Graphite phonon dispersion curves are calculated and fitted with experimental results obtained by electron energy loss spectroscopy, inelastic neutron scattering, speed of sound and other techniques [205,206]. Finally, three phonon dispersion curves are obtained. They correspond to acoustic vibration modes (Figure 2.29): an in-plane tangential (bond-bending) mode, an in-plane radial (bond-stretching) mode and an out-of-plane mode [204].

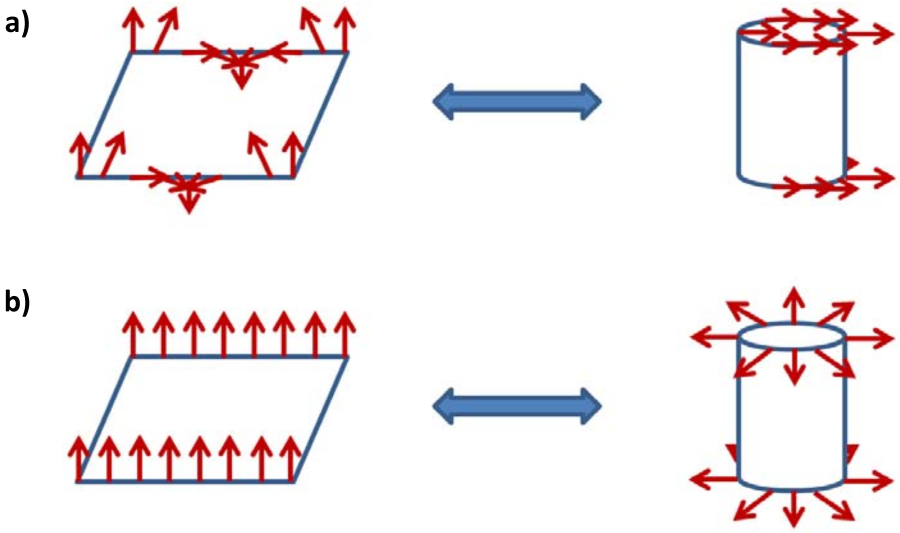

Figure 2.29. (a) An acoustic mode of a carbon nanotube, the vibration is perpendicular to the nanotube axis and it corresponds to a linear combination of both in-plane and out-of-plane graphite-derived modes. (b) Out-of-plane tangential acoustic modes in a single layer of graphite give rise to a radial breathing mode in the carbon nanotube.

These phonon dispersion relations of CNT depend on the diameter and chiral angle (n and m indices) [203]. The zone folding procedure allows obtaining the appropriate one-dimensional frequency for almost all the phonon branches of a carbon nanotube.

- RAMAN SPECTRUM

Raman spectroscopy could be considered as one of the best techniques for the characterization of carbon nanotubes [142,200,207,208]. The characteristic Raman spectrum of CNT (Figure 2.30) shows mainly four bands: the radial breathing mode (RBM), the disorder induced mode (D), the tangential displacement mode (G) and the high frequency two phonon mode (G').

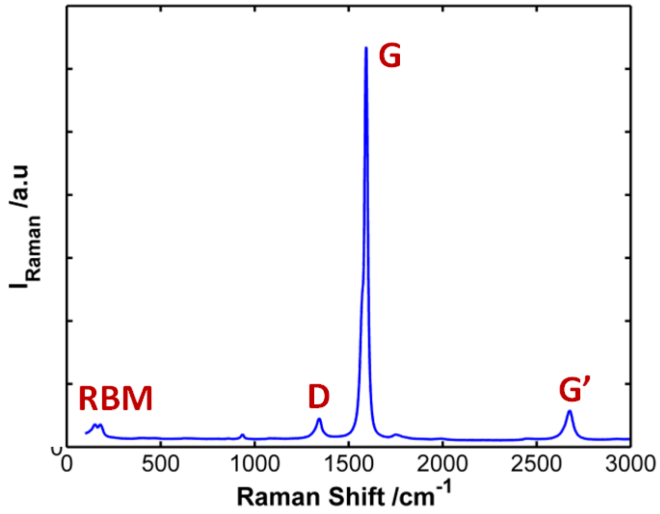

Figure 2.30. Raman spectrum of a CNT film.

RBM band appears around 150-250 cm^{-1} in the Raman spectra and provides suitable information about the diameter of the CNT (Figure 2.31.b). There are so different CNT diameters as RBM bands are distinguished in the spectrum. The relationship between the RBM frequency ω_{RBM} (cm^{-1}) and the diameter of the CNT d_t (nm) is given by the equation:

$$\omega_{RBM} = \frac{A}{d_t} + B \qquad \text{(eq. 1.3)}$$

where A (nm cm^{-1}) and B (cm^{-1}) are semiempirical parameters that take values between 220-230 nm cm^{-1} for A and 10-20 cm^{-1} for B, depending on the experimental conditions [208]. B is used to characterize the interaction of the nanotubes in a bundle and its value is 0 cm^{-1} for isolated CNT.

The most intense band, G-band, is located at 1550-1600 cm^{-1} and corresponds to the tangential vibration modes of the CNT [208] (Figure 2.31.a). G-band provides much information about the nanotubes, for example, it allows knowing the metallic or semi-metallic character of the CNT film and also it is very useful to check the charge transfer related to the doping. This band is composed of several peaks related to two effects: (1) the symmetry effect related with the CNT curvature and (2) the phonon wave vector confinement along the circumferential direction. It is composed of six active modes for chiral CNT with symmetries $2A_{1g} + 2E_{1g} + 2E_{2g}$ and of three bands for armchair and zig-zag CNT [209]. However, the intensity of the E_{1g} and E_{2g} is much lower than the symmetric A_{1g} modes, being considered only two components of the G-band, one peaked at about 1570 cm^{-1} (G^-) and other around 1590 cm^{-1} (G^+). G^- component is associated with the carbon atoms vibrations along the circumferential direction of the CNT, being highly sensitive to the metallic or semi-metallic character of the film. Its frequency depends on the diameter and the metallic or semi-metallic properties but not to the chiral angle. G^+ mode is associated with the atoms vibrations along the nanotube axis and its frequency is sensitive to the charge transfer from dopant additions (up-shifts for acceptors and down-shifts for donors) but it is independent of the chiral angle and the diameter. The dependence between the diameter and the G-band components can be only studied in isolated nanotube levels [208].

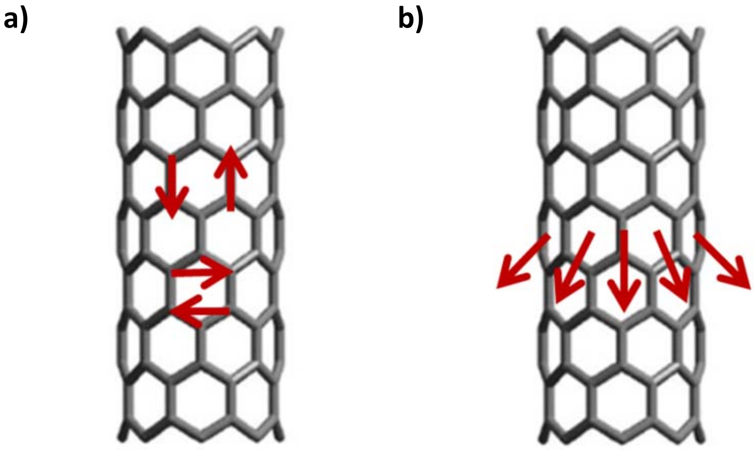

Figure 2.31. (a) Tangential vibration (G-band) and (b) RBM modes.

D-band, peaked around 1250-1450 cm^{-1}, corresponds to the presence of defects as substitutional heteroatoms, vacancies, grain boundaries or other defects and by finite size effects, all of which lower the crystalline symmetry of the quasi-infinite lattice. G’-band, centred in 2500-2800 cm^{-1} is related to the D-band, being the G’-band an overtone of the D-band and both D and G’ bands are the result of second-order Raman scattering processes. However, G’-band appears even in crystalline graphite where the D-band is absent, so G’-band is an intrinsic characteristic of the graphene lattice. In general for all kinds of sp^2 carbon materials, there is a strong dependence between the frequency of the D and G’ and the laser energy. The intensity, frequency, and width of the D and G' bands not only provide information of the electronic structure of CNT, but also these spectral properties change depending on the experimental conditions such as mechanical stress (stretching or compression) or temperature.

The frequency, intensity and width of all of these bands change during the electrochemical processes as is explained in Section 4.2. Understanding the behaviour of the CNT during their oxidation and reduction is essential to characterize them.

- *MECHANICAL PROPERTIES*

CNT show fascinating mechanical properties. The strength of the carbon bonds makes CNT one the strongest and stiffest materials known. Initially, the measurements of the elastic properties of individual nanotubes were considered impossible. However, using different theoretical studies and new experimental techniques these properties (hardness, elasticity, stiffness, elastic response, yield strength and fracture…) have been defined. For example, the hollow and closed morphology of CNT makes them very flexible in response to mechanical stress (Figure 2.32) [210].

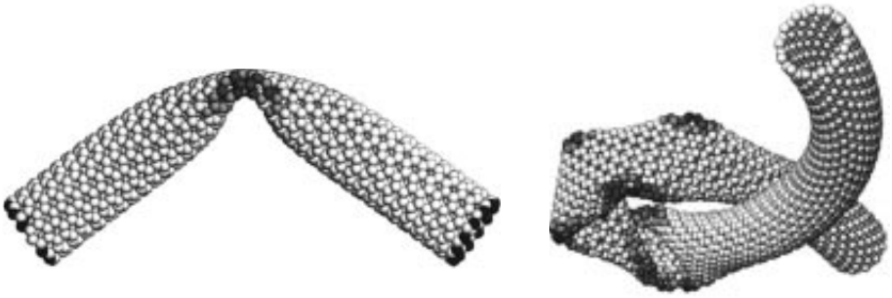

Figure 2.32. Theorical CNT response to mechanical stress [210].

Furthermore, exceptional Young’s modulus [211–213] and resistance to shock loads [212,214] have also been demonstrated. However, an important factor for the mechanical properties is the dependence on the CNT growth method and on the processing, due to the defects produced during these processes [215].

- *THERMAL PROPERTIES*

Thermal conductivity and the specific heat of CNT depend on the atomic vibrations (phonons). Different techniques have been used to study them: calorimetry [216], thermal conductivity [217], thermal relaxation [218] or pulsed photothermal reflectance technique [219]. Although the results are various, in general thermal properties of CNT are similar to graphite characteristics. Both graphite and CNT show very interesting thermal behaviour that makes them a really promising material in several fields.

- *CHEMICAL PROPERTIES*

It is complicated to obtain CNT with specific properties directly from the synthesis process. For that reason, the chemical functionalization of their walls surface is essential (**¡Error! No se encuentra el origen de la referencia.**). Although different studies have demonstrated that the ends of the CNT are positions more reactive than the cylindrical parts [220,221], the modification of the outerwall is also possible [222] (**¡Error! No se encuentra el origen de la referencia.**.b).

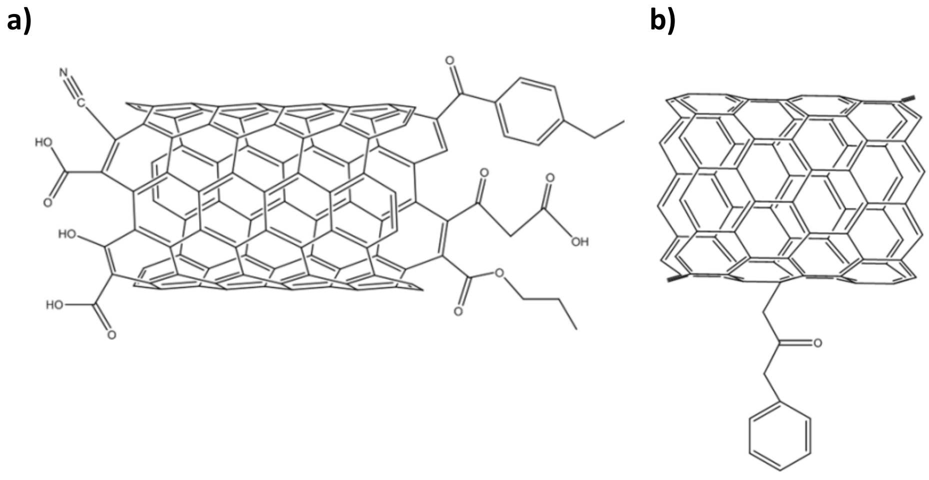

Figure 2.33. Example of CNT (a) end and (b) outerwall functionalized.

Functionalization process can be performed by different routes: oxidation at high temperature by gas reaction [221], liquid phase oxidation with different acids (HNO_3, $HClO_4$, H_2SO_4, …) [223–227], fluorination at high temperature [222], cycloadditions [228], electrochemical reactions [229], photochemical reactions [230], etc.

Furthermore, different molecules can be encapsulated inside the CNT, for example water [231–233], biomolecules [234], ion liquids [235] or drug molecules [236]. This new confinement produces modifications in the inner molecules and consequently also the CNT properties change.

2.4.2. Metal nanoparticles

Although metal nanostructures properties as SERS substrate have been explained in the Section 2.2.1.A, this Section displays a more general overview of metal nanoparticles (NPs).

NPs are defined as particles whose dimensions are in the nanometric range, between 1 and 100 nm, so they are an example of 0-D materials.

Metal NPs synthesis can be accomplished using different methods: chemical reduction [76–78], seed-mediated [237], photochemical [238], electrochemical [70,239], sonochemical [240], lithography [91,92], galvanic replacement [241], thermal evaporation [242], radiolysis [243], sol-gel [244], laser ablation [87–89], chemical vapor deposition [245], microwave assisted [246], biological (fungi, bacteria, plant) assisted [247–249]. The choice of the synthesis method, the concentration of the reagents and other specific parameters of each tecnique allow us to obtain NPs with specific size and shape. These two characteristics are specially important because they determine chemical and physical properties of NPs.

Although chemical reduction is the most used method of NPs synthesis our group is more interested in the electrochemical route due to the higher control of the synthesis and, therefore, to the generation of more reproducible NPs. In all the studies presented in Chapter 4, metal NPs are deposited by electrochemical methods.

A. Electrochemical synthesis

Electrosynthesis method allows us to control many parameters during the deposition process. Slight changes of intensity current, applied potential, electrodeposition time, electrode material, kind or concentration of supporting electrolyte or salt precursor electrolyte, etc. can produce significant modifications in the properties of NPs yielded. Another important advantage of this method is the highest surface cleaning of the NPs generated considering that a smaller amount of reactants is used leadsing to a minor contamination of the samples.

The first references of metal electrodeposition are dated in the last decades of 19th century [250–253] and first years of 20th century [254,255], when some metals as Ir, Cu, Ni and Fe were studied. Since these starting studies, this method has experimented an extraordinary evolution, enabling us now to control some of the most characteristic properties of NPs such as size and shape.

Electrosynthesis of metal NPs can yield NPs in solution or NPs deposited on the electrode surface. NPs electrosynthesis in solution is very similar to a chemical synthesis, but instead of using a chemical reducing agent, the electrons needed to reduce metal ions are provided by the electrode of an electrochemical cell, using in most cases a sacrificial anode [256]. When NPs are electrodeposited on the electrode surface as the result of applying a negative enough overpotential, a typical 3 electrode electrochemical cell is used. This last one procedure has been chosen to synthesize all NPs shown in this Thesis.

During the electrodeposition process two stages are observed. The initial stage or nucleation step corresponds to the generation of the first metal nuclei on the electrode surface, while the second or growth step relates to the growth of these. There are described two kinds of nucleation named as (Figure 2.34):

- INSTANTANEOUS NUCLEATION, in which the number of nuclei is constant during all the experiment, and they grow on their former positions on the substrate surface but no more new nuclei are formed. In general, this type of nucleation leads to obtain larger nuclei and rougher surfaces.
- PROGRESSIVE NUCLEATION, where the number of nuclei is not constant during the synthesis. While initial nuclei starts to grow, new nuclei are formed on the electrode surface.

The second step is the growth of the nuclei being possible to differenciate two types of growth: two-dimensional (2D) and three-dimensional (3D) [257]. In 2D growth, the nuclei grow faster in the two directions parallel to the electrode surface than in the perpendicular direction. On the other hand, in the 3D growth, the nuclei grow with similar rate in both parallel and perpendicular direction respect to the electrode surface.

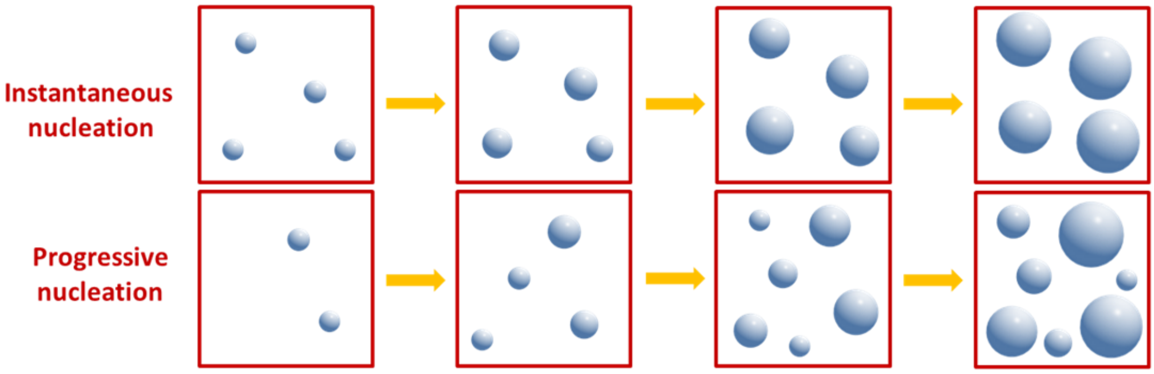

Figure 2.34. Scheme of instantaneous and progressive nucleation.

Metal NPs characterization is usually performed using a variety of techniques, such as transmission electron microscopy (TEM), scanning electron microscopy (SEM), scanning tunneling microscopy (STM), atomic force microscopy (AFM), dynamic light scattering (DLS), X-ray diffraction (XRD), X-ray photoelectron spectroscopy (XPS), UV-Vis spectroscopy, Raman spectroscopy, Fourier transform infrared spectroscopy (FTIR), nuclear magnetic resonance (NMR), matrix assisted laser desorption/ionization time-of-flight mass spectrometry (MALDI-TOF) or Rutherford backscattering spectrometry (RBS).

B. Properties and applications

Metal NPs exhibit a large range of optical, chemical, catalytic, electrical and magnetic properties due to finite size effects which make them really useful in different fields. These properties can change as function of the metal, size, shape or number of components of the NPs and are different from the bulk or their constituents because the surface of the NPs are structurally and compositionally different [258]. Metal NPs have been used in a number of applications:

- CATALYTIC APPLICATIONS. Metal NPs are used as catalyst in many reactions, such as carbon monoxide oxidation [259], oxidation of small organic molecules such as formic acid and ethanol [260], selective oxidation of cyclohexene and cyclooctene [261], degradation of rhodamine [262], nonenzymatic impedancimetric detection of glucose [263], tandem reaction of alcohols and nitrobenzenes to generate N-alkyl amines and imines [264], 4-nitrophenol and 4-aminophenol reduction [265], etc.
- BIOMEDICAL APPLICATIONS. NPs are used as contrast agents in diagnostic [266], cancer detection [267], photothermal cancer therapy [268], drug and gene delivery [269], pathogens detection [270], protein detection [271], investigation of the structure of DNA [272].
- SENSORS AND MOLECULAR RECOGNITION, such as detection of toxic ions [273], development of new biosensor [274], or in molecular recognition [275].
- ENVIRONMENTAL TREATMENTS, such as in air desifection [276], water [277], groundwater [278] and biological wastewater [279] desinfection, surfaces desinfection (antimibrobial paints [280], clinical clothing [281], paper for food preservation [282]).
- ENERGY. They have been very used in photovoltaic applications [283], batteries [284], fuel cells [285] or solar cells [286].
- ELECTRONIC, such as in memory devices [287], light emitting diodes (LEDs) [288] or photonic crystals in optical computers [289].

- MATERIALS. The use of NPs in different materials allows improving their properties as in ceramics, metal materials, NPs/CNT, NPs/graphene, NPs/C fibers and NPs/polymer composites [290,291].

2.5. Interfaces between two immiscible solutions

The interface between two immiscible electrolyte solutions (ITIES) is formed between two liquids with very low miscibility, one of these solvents is usually water and the other is a polar organic solvent, such as 1,2-dichlorobencene (DCB), nitrobenzene (NB) or 1,2-dichloroethane (DCE). Processes which take place at these interfaces have become one of the most interesting systems in electrochemistry due to its wide range of applications, as in biological membranes [292–295], pharmacokinetic characterization [296–298], catalysis [299–302], metal deposition [303–306] or electroanalysis [307–309].

The first electrochemical experiments in ITIES were performed in 1902, when Nernst and Riesenfeld observed the ion transfer through the interfaces water/phenol/water during the passage of an electrical current [310]. The first theoretical study of these interfaces was developed by Verwey and Niessen in 1939 [311]. This study was based on a similar physical model to the Gouy-Chapman electrical double layer. In 1953, Karpfen and Randles presented an important development for further studies performing an analysis of the thermodynamic equilibrium between the two phases [312]. An important moment in the development of ITIES was achieved by Gavach *et al.* in 1968, when they demonstrated that the ITIES could be polarized and the Galvani potential (potential difference between the two phases) can be used to achieve charge transfer reactions [313]. The breakthrough took place in 1977 when Samec introduced the four-electrode potentiostat with the ohmic drop compensation [314–317]. This work is fundamental because it made possible the use of new techniques to study ITIES as cyclic voltammetry [304,318–321], differential pulse voltammetry [322], alternating current voltammetry [323], chronoamperometry [324], polarography [325,326] and impedance spectroscopy [327,328]. In the last years, the development of new devices has allowed using different spectroelectrochemical techniques to study ITIES systems [329–335]. In the Section 4.4 of this work, a new cell to study the reactions which take place at the liquid/liquid (L/L) interface using time-resolved Raman spectroelectrochemistry is presented.

2.5.1. Interfacial structure

It is complicated to define the interfacial structure because the interface formed between two immiscible solutions is a molecular interface with its own dynamics, so the time scale is another parameter to define the structure. The interfacial structure has been assessed by different methods: X-ray reflectivity [336,337], neutron scattering [338], laser scattering [339], second harmonic generation (SHG) [340–342], sum frequency generation (SFG) [343–345] or molecular dynamics simulations [346–349].

The first capacitance model was a Gouy-Chapman model, which represents the interface as a double electric layer in both phases. However, this model is not able to reproduce accurately the experimental capacitance data. Verwey-Neissen model, with some modifications, propose that the interface consists in a free layer of ions (inner layer) formed by oriented solvent molecules, which separates the diffuse double-layer regions. Furthermore, it considers the penetration of ions into the inner layer (Figure 2.35).

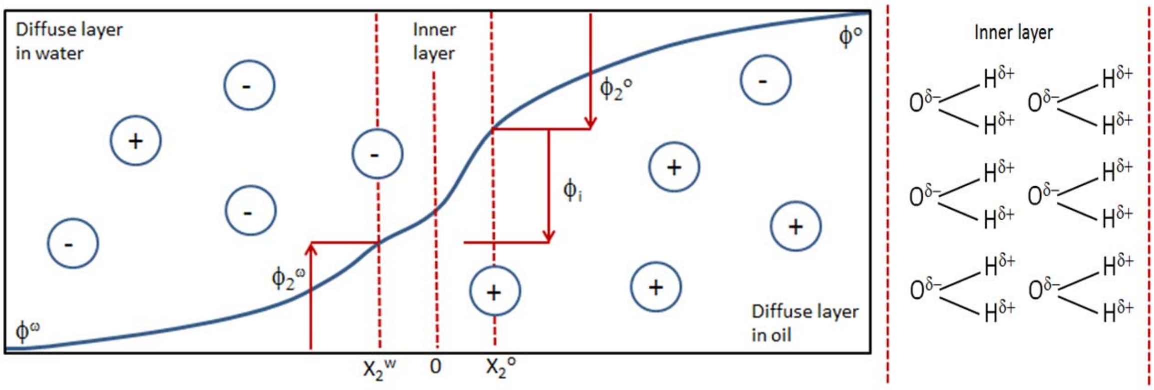

Figure 2.35. Modified Verwey-Niessen model of ITIES.

Using this model the potential difference or Galvani potential can be explains with three contributions:

$$\Delta_o^w \varphi = \varphi_2^w - \varphi_2^o + \varphi_i \qquad \text{(eq. 1.4)}$$

where φ is the Galvani potential, $\varphi_2{}^w$ and $\varphi_2{}^o$ are the potential at the boundary between the diffuse layer and the inner layer in the aqueous and organic phase respectively and φ_i is the potential at the centre of the inner layer.

2.5.2. Nernst equation

When two immiscible solutions form an interface, a distribution of charge between the two phases is produced due to the energy difference between these two phases. At constant pressure and temperature, the thermodynamic equilibrium at ITIES is expressed as:

$$\tilde{\mu}_i^o = \tilde{\mu}_i^w \qquad \text{(eq. 1.5)}$$

where $\tilde{\mu}_i^o$and $\tilde{\mu}_i^w$ are the chemical potential of the component *i* in the organic and aqueous phases, respectively. If we consider the electrical and chemical contribution the equation is expressed by:

$$\mu_i^{0,o} + RT\ln a_i^o + zF\varphi^o = \mu_i^{0,w} + RT\ln a_i^w + zF\varphi^w \qquad \text{(eq. 1.6)}$$

where $\mu_i^{0,o}$ and $\mu_i^{0,w}$ are the standard chemical potentials in aqueous and organic phases, respectively; $\varphi^o$and $\varphi^w$are the Galvani potentials in both phases; $a_i^o$and a_i^w are the activities of the *i* specie in the two phases; F is the Faraday constant and z is the charge. Using the above expression we can obtain the relationship between the Galvani potential difference ($\Delta_o^w \varphi_i^0$) and the Gibbs energy ($\Delta G_{transf,i}^0$):

$$\Delta G_{transf,i}^0 = \mu_i^{0,o} - \mu_i^{0,w} = -zF\Delta_o^w \varphi_i^0 \qquad \text{(eq. 1.7)}$$

Therefore, the relation between the Galvani potential difference and the Gibbs energy is defined by:

$$\Delta_o^w \varphi = \frac{\Delta G_{transf,i}^0}{z_i F} \qquad \text{(eq. 1.8)}$$

2.5.3. Transfer reactions

The different reactions that can take place at ITIES are classified into three main categories (Figure 2.36) [350]:

- Ion transfer
- Assisted ion transfer
- Electron transfer

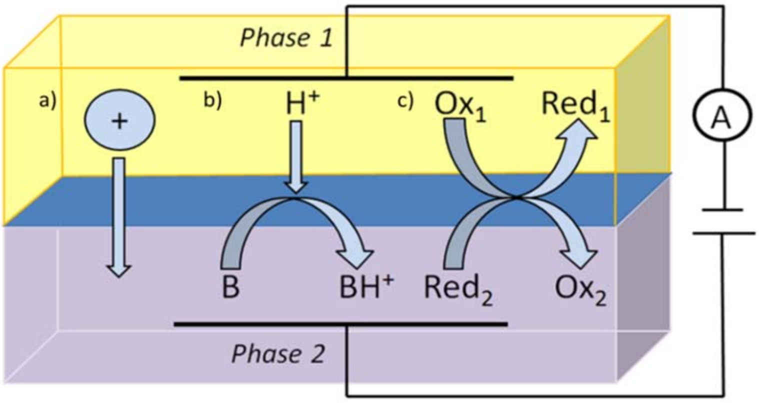

Figure 2.36. (a) Ion transfer, (b) assisted ion transfer and (c) electron transfer.

A. Ion transfer

Ion transfer reaction through ITIES has been widely studied for over last decades [314,323,351–359] and in general, it is considered that this transference occurs in 3 major steps:

- Mass transfer in one phase to the interface (mainly diffusion).
- Ion transfer reaction.
- Mass transfer in the other phase away from the interface.

In this kind of transference, it is necessary to provide the enough energy (Gibbs energy) to transfer an ion from one phase to the other.

$$X_w^{z_i} \leftrightarrows X_o^{z_i} \qquad \text{(eq. 1.9)}$$

This energy can be supplied by a suitable potential difference (Galvani potential difference) applied across the interface being defined by:

$$\Delta_o^w\varphi = \varphi^w - \varphi^o \qquad \text{(eq. 1.10)}$$

where φ is the Galvani potential at the respective phases.

At equilibrium we can consider the Nernst equation due to the equality of the ion potential located in adjacent phases:

$$\Delta_o^w\varphi = \Delta_o^w\varphi_i^0 - \frac{RT}{z_iF}\ln\left(\frac{\mathrm{a}_i^w}{\mathrm{a}_i^o}\right) \qquad \text{(eq. 1.11)}$$

where a_i is the activity, z_i is the charge of the ion (*i*) and $\Delta_o^w\varphi_i^0$ is the standard ion transfer potential which is due to the solvation difference in both phases and is defined as:

$$\Delta_o^w\varphi_i^0 = \frac{\Delta_o^w G_{transf,i}^0}{z_iF} = \frac{\mu_i^{0,o} - \mu_i^{0,w}}{z_iF} \qquad \text{(eq. 1.12)}$$

where $\Delta_o^w G_{transf,i}^0$ is the Gibbs energy of transfer of i, $\mu_i^{0,o}$ is its standard Gibbs energy of solvation and $\mu_i^{0,w}$ is its standard Gibbs energy of hydration.

B. Assisted ion transfer

This kind of reaction not only involves the transference of an ion but also neutral ligands which can be located at the interface (in either of the two phases). Depending on the concentration ratios and the distribution coefficient of the ligand, there are four possible mechanisms (Figure 2.37) [360]:

- TRANSFER BY INTERFACIAL COMPLEXATION (TIC): (1) ion H^+ is transferred to the interface, (2) the complexation with the ligand B is produced in the interface and (3) the complex BH^+ is transferred to the other phase.

- TRANSFER BY INTERFACIAL DISSOCIATION (TID): (1) the complex BH^+ is transferred to the interface, (2) it is dissociated in the interface and (3) the ion H^+ is transference the other phase.
- TRANSFER FOLLOWED BY ORGANIC PHASE COMPLEXATION (TOC): (1) the ion H^+ is transferred from one phase to the other phase, (2) where is produced the complexation BH^+ with the ligand B.
- AQUEOUS COMPLEXATION FOLLOWED BY THE TRANSFER OF THE COMPLEX (ACT): (1) the ion H^+ and the ligand B form the complex BH^+ in the aqueous phase and after that, (2) the transference of the complex to the organic phase is produced.

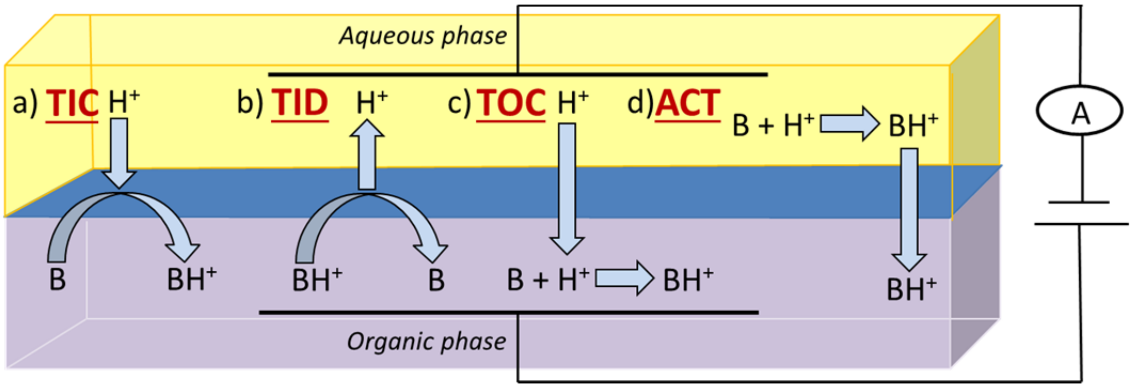

Figure 2.37. Assisted ion transfer mechanism: (a) transfer by interfacial complexation (TIC), (b) transfer by interfacial dissociation (TID), (c) transfer followed by organic phase complexation (TOC) and (d) aqueous complexation followed by the transfer of the complex (ACT).

C. Electron transfer

In the electron transfer process, there is a redox couple in one phase which will be oxidized and another couple in the other phase that will be reduced due to the passage of electrons through the interface.

$$Ox_1^w + Red_2^o \leftrightharpoons Red_1^w + Ox_2^o \qquad \text{(eq. 1.13)}$$

At equilibrium, the Galvani potential difference is defined by the Nernst equation:

$$\Delta_o^w \varphi = \Delta_o^w \varphi^0 - \frac{RT}{nF} \ln \left(\frac{a_{Ox1}^w a_{Red2}^o}{a_{Red1}^w a_{Ox2}^o} \right) \qquad \text{(eq. 1.14)}$$

where n is the number of electrons transferred and $\Delta_o^w \varphi^0$ is determined by:

$$\Delta_o^w \varphi^0 = E^{0,o}_{Ox2/Red2} - E^{0,w}_{Ox1/Red1} \qquad \text{(eq. 1.15)}$$

where $E^0_{Ox/Red}$ is the standard redox potential for the redox couples.

Electron transfer reactions can be explained in terms of elementary steps: (1) approach of the reactants to the interfacial region in both phases, (2) formation of the electron transfer precursor complex, (3) electron transfer reaction, (4) reorganization and dissociation of the successor complex and (5) products go away from the interface. However, it is not clear where the precursor formation and the electron transfer take place. Samec proposed that the electron transfer is produced across an ion-free layer composed of oriented solvent molecules [315]. On the other hand, Girault and Schiffrin assumed the electrochemical potentials are dependent on the position of the reactants at the interface in a mixed solvent region [361]. From a general point of view, the activation energy of the full process is defined by [362]:

$$\Delta G_{act} = {\left(\lambda + \Delta G^{o'} + w_p - w_r\right)^2}\Big/_{4\lambda} \qquad \text{(eq. 1.16)}$$

where λ is the energy reorganization, $\Delta G^{o'}$ is the formal Gibbs energy for the elementary electron transfer, w_r is the approaching of the reactants and w_p is the separation of the products from the interface. The dependence between the activation energy and the Galvani potential is given by these parameters ($\Delta G^{o'}$, w_r and w_p) and the Galvani potential difference can induce changes in them. Consequently, the observed potential dependence of the electron transfers can arise from two contributions: changes in the interfacial concentration of the reactants and modifications in the free energy of the elementary step [350].

2.6. DNA bases

The deoxyribonucleic acid (DNA) is a macromolecule responsible for the storage and transmission of the genetic information. The DNA chemistry started in 1868, when Miescher was studying lymphoid cells in biological material and he found a great quantity of these cells in the pus from infections. After treating the biological rests, he noticed a gelatinous precipitate with unexpected properties which did not match with those of proteins [363]. Although Miescher did most of his work in 1868, his paper was not published until 1871 [364].

However, the most famous breakthrough in the study of DNA was produced in 1953 when Watson and Crick [365] discovered the structure of the DNA. This structure is formed by a double helix of two antiparallel DNA chains which are linked by hydrogen bonds (Figure 2.38).

These chains consist of individual units, called nucleotides, which are linked to each other to form these long chains. Nucleotides are formed by a five-carbon sugar (2'-deoxyribose), a phosphate group and an organic base. The base is linked to 1'-carbon of each sugar.

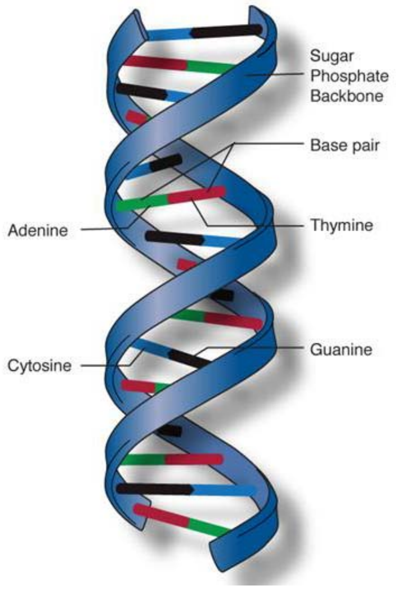

Figure 2.38. Double helix of DNA. Source: The microbiology of the Built Environment network http://microbe.net.

There are four bases: two purine bases (adenine and guanine) and two pyrimidine bases (thymine and cytosine), Figure 2.39. According to Watson and Crick rules [365] the hydrogen bonds are established only between specific pairs of bases: adenine with thymine and guanine with cytosine. But DNA bases composition is not random in a cell, the amount of adenine is the same than thymine and the quantity of guanine and cytosine is also equal.

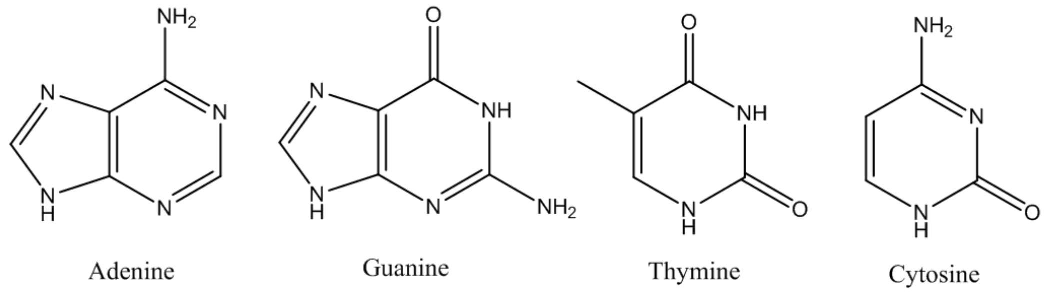
Adenine Guanine Thymine Cytosine

Figure 2.39. Bases of the DNA: adenine, guanine, thymine and cytosine.

DNA can adopt different conformations depending on the nucleotide sequence and environmental conditions. The most common structure is B-DNA, which twists in a right-handed double helix and where it is possible to differentiate a major and a minor groove. In the major groove, which is deep and wide, chemical groups which are present specify the identity of the base pair, while the minor groove, which is shallow and narrow, shows a higher negative charge density.

DNA bases can be modified producing molecular changes to the genetic machinery that leads to cell malfunction and death of it. One method to causes DNA modifications is the oxidation of the bases because during this process different oxidations products can be formed. These products are influential in mutagenesis, carcinogenesis, aging and neurodegenerative disease [366–369].

Therefore, it is important to define and characterize the oxidation mechanism in order to understand and detect possible damages in the DNA. Both purine and pyrimidine bases can be electrochemically oxidized [370–373], although adenine and guanine are oxidized at much lower positive potentials than thymine and cytosine. In the Section 4.5 of this Thesis, we propose the oxidation mechanism of adenine and guanine, analysing the oxidation products and their orientation on gold nanoparticles using Raman spectroelectrochemistry.

7. References

[1] W. Kaim, J. Fiedler, Spectroelectrochemistry: the best of two worlds, Chemical Society Reviews. 38 (2009) 3373–3382.

[2] A. Smekal, Zur Quantentheorie der Dispersion, Die Naturwissenschaften. 11 (1923) 873–875.

[3] H.A. Kramers, W. Heisenberg, Über die Streuung von Strahlung durch Atome, Zeitschrift Für Physik. 31 (1925) 681–708.

[4] C. V Raman, K.S. Krishnan, A new type of secondary radiation, Nature. 121 (1928) 501–502.

[5] G. Landsberg, L. Mandelstam, Eine neue Erscheinung bei der Lichtzerstreuung in Krystallen, Die Naturwissenschaften. 16 (1928) 557–558.

[6] H.L. Welsh, M.F. Crawford, T.R. Thomas, G.R. Love, Raman spectroscopy of low pressure gases and vapors, Canadian Journal of Physics. 30 (1952) 577–596.

[7] T.H. Maiman, Stimulated optical radiation in Ruby, Nature. 187 (1960) 493–494.

[8] M. Fleischmann, P.J. Hendra, A.J. McQuillan, Raman spectra of pyridine adsorbed at a silver electrode, Chemical Physics Letters. 26 (1974) 163–166.

[9] D.L. Jeanmaire, R.P. Van Duyne, Surface Raman electrochemistry. Part I. Heterocyclic, aromatic and aliphatic amines adsorbed on the anodised silver electrode, Journal of Electroanalytical Chemistry. 84 (1977) 1–20.

[10] K. Kneipp, H. Kneipp, I. Itzkan, R.R. Dasari, M.S. Feld, Ultrasensitive chemical analysis by Raman spectroscopy., Chemical Reviews. 99 (1999) 2957–2976.

[11] S. Schlücker, Surface-Enhanced Raman Spectroscopy: Concepts and Chemical Applications., Angewandte Chemie - International Edition. 53 (2014) 2–42.

[12] M. Moskovits, Surface-enhanced Raman spectroscopy: a brief retrospective, Journal of Raman Spectroscopy. 36 (2005) 485–496.

[13] J.F. Arenas, I. López-Tocón, J.C. Otero, J.I. Marcos, The charge transfer mechanism in the SERS of 2-methylpyrazine on silver electrode, Vibrational Spectroscopy. 19 (1999) 213–221.

[14] X. Wang, H. Wen, T. He, J. Zuo, C. Xu, F.-C. Liu, Enhancement mechanism of SERS from cyanine dyes adsorbed on Ag_2O colloids, Spectrochimica Acta Part A: Molecular and Biomolecular Spectroscopy. 53 (1997) 2495–2504.

[15] M. Osawa, N. Matsuda, K. Yoshii, I. Uchida, Charge transfer resonance Raman process in surface-enhanced Raman scattering from p-aminothiophenol adsorbed on silver: Herzberg-Teller contribution, Journal of Physical Chemistry. 98 (1994) 12702–12707.

[16] H. Ko, S. Singamaneni, V.V Tsukruk, Nanostructured surfaces and assemblies as SERS media, Small. 4 (2008) 1576–1599.

[17] R.A. Alvarez-Puebla, L.M. Liz-Marzán, SERS detection of small inorganic molecules and ions, Angewandte Chemie - International Edition. 51 (2012) 11214–11223.

[18] G. McNay, D. Eustace, W.E. Smith, K. Faulds, D. Graham, Surface-enhanced Raman scattering (SERS) and surface-enhanced resonance Raman scattering (SERRS): a review of applications., Applied Spectroscopy. 65 (2011) 825–837.

[19] M.J. Natan, Concluding Remarks: Surface enhanced Raman scattering, Faraday Discussions. 132 (2006) 321–328.

[20] F.J. Vidal-Iglesias, J. Solla-Gullón, J.M. Orts, A. Rodes, J.M. Pérez, J.M. Feliu, SERS on (111) Surface Nanofacets at Pt Nanoparticles: The Case of Acetaldehyde Oxime Reduction, Journal of Physical Chemistry C. 116 (2012) 10781–10789.

[21] M.-H. Kim, E.-S. Lee, S. Kim, Y.-U. Kwon, Low-Cost Fabrication of Pt Thin Films with Controlled Nanostructures and Their Effects on SERS, Plasmonics. 6 (2011) 715–723.

[22] S. Choi, H. Jeong, K. Choi, J.Y. Song, J. Kim, Electrodeposition of Triangular Pd Rod Nanostructures and Their Electrocatalytic and SERS Activities, ACS Applied Materials & Interfaces. 6 (2014) 3002–3007.

[23] T. Bhuvana, G.U. Kulkarni, A SERS-Active Nanocrystalline Pd Substrate and its Nanopatterning Leading to Biochip Fabrication, Small. 4 (2008) 670–676.

[24] G.F.S. Andrade, M.L.A. Temperini, Adsorption of 4-aminopyridine on Co and Ag electrodes probed by SERS, Vibrational Spectroscopy. 54 (2010) 148–154.

[25] G.F.S. Andrade, A.G. Brolo, M.L.A. Temperini, Comparison of SERS Performances of Co and Ni Ultrathin Films over Silver to Electrochemically Activated Co and Ni Electrodes, Journal of Physical Chemistry C. 112 (2008) 15348–15355.

[26] J. Du, C. Jing, Preparation of Thiol Modified Fe_3O_4@Ag Magnetic SERS Probe for PAHs Detection and Identification, Journal of Physical Chemistry C. 115 (2011) 17829–17835.

[27] Q. Gao, A. Zhao, Z. Gan, W. Tao, D. Li, M. Zhang, H. Guo, D. Wang, H. Sun, R. Mao, E. Liu, Facile fabrication and growth mechanism of 3D flower-like Fe_3O_4 nanostructures and their application as SERS substrates, CrystEngComm. 14 (2012) 4834–4842.

[28] P. Liu, P. Diao, D. Zhang, M. Xiang, Q. Zhang, F. Wang, Electrochemical deposition of Rh as an active UV-SERS substrate, Beijing Keji Daxue Xuebao/Journal of University of Science and Technology Beijing. 30 (2008) 276–280.

[29] X.-D. Lin, J.-F. Li, Y.-F. Huang, X.-D. Tian, V. Uzayisenga, S.-B. Li, B. Ren, Z.-Q. Tian, Shell-isolated nanoparticle-enhanced Raman spectroscopy: Nanoparticle synthesis, characterization and applications in electrochemistry, Journal of Electroanalytical Chemistry. 688 (2013) 5–11.

[30] G.C. Schatz, Theoretical studies of surface enhanced Raman scattering, Accounts of Chemical Research. 17 (1984) 370–376.

[31] C.S. Seney, B.M. Gutzman, R.H. Goddard, Correlation of Size and Surface-Enhanced Raman Scattering Activity of Optical and Spectroscopic Properties for Silver Nanoparticles, Journal of Physical Chemistry C. 113 (2008) 74–80.

[32] S. Hong, X. Li, Optimal size of gold nanoparticles for surface-enhanced Raman spectroscopy under different conditions, Journal of Nanomaterials. 2013 (2013) 790323.

[33] G.P. Glaspell, C. Zuo, P.W. Jagodzinski, Surface enhanced Raman spectroscopy using silver nanoparticles: The effects of particle size and halide ions on aggregation, Journal of Cluster Science. 16 (2005) 39–51.

[34] S. Cintra, M.E. Abdelsalam, P.N. Bartlett, J.J. Baumberg, T.A. Kelf, Y. Sugawara, A.E. Russell, Sculpted substrates for SERS, Faraday Discussions. 132 (2006) 191–199.

[35] K.G. Stamplecoskie, J.C. Scaiano, V.S. Tiwari, H. Anis, Optimal Size of Silver Nanoparticles for Surface-Enhanced Raman Spectroscopy, Journal of Physical Chemistry C. 115 (2011) 1403–1409.

[36] H.-W.H.-W. Cheng, Y. Li, J.-Y.J.-Y. Yang, Effects of shape and size on field enhancement of Au nanoparticles on SERS-active substrates, in: 10th IEEE International Conference on Nanotechnology, IEEE, 2010: pp. 732–735.

[37] K.H. Zheng, Y.C. Chou, Y.J. Wu, Y.T. Lee, Raman spectra of benzoic acid enhanced by the silver nanoparticles of various sizes, Journal of Raman Spectroscopy. 41 (2010) 632–635.

[38] P.-P. Fang, J.-F. Li, Z.-L. Yang, L.-M. Li, B. Ren, Z.-Q. Tian, Optimization of SERS activities of gold nanoparticles and gold-core-palladium-shell nanoparticles by controlling size and shell thickness, Journal of Raman Spectroscopy. 39 (2008) 1679–1687.

[39] K. C. Lee, S. T. Pai, Y. C. Chang, M. C. Chen, W.-H. Li, Optimum massthickness of Ag-nanoparticle film for surface enhanced Raman scattering, Materials Science and Engineering B. B52 (1998) 189–194.

[40] J. Beermann, S.M. Novikov, K. Leosson, S.I. Bozhevolnyi, Surface enhanced Raman microscopy with metal nanoparticle arrays, Journal of Optics A: Pure and Applied Optics. 11 (2009) 075004.

[41] R.N. Cassar, D. Graham, I. Larmour, A.W. Wark, K. Faulds, Synthesis of size tunable monodispersed silver nanoparticles and the effect of size on SERS enhancement, Vibrational Spectroscopy. 71 (2014) 41–46.

[42] Y.Q. Wang, S. Ma, Q.Q. Yang, X.J. Li, Size-dependent SERS detection of R6G by silver nanoparticles immersion-plated on silicon nanoporous pillar array, Applied Surface Science. 258 (2012) 5881–5885.

[43] A. Sabur, M. Havel, Y. Gogotsi, SERS intensity optimization by controlling the size and shape of faceted gold nanoparticles, Journal of Raman Spectroscopy. 39 (2008) 61–67.

[44] J. Zhang, X. Li, X. Sun, Y. Li, Surface Enhanced Raman Scattering Effects of Silver Colloids with Different Shapes, Journal of Physical Chemistry B. 109 (2005) 12544–12548.

[45] M.J. Mulvihill, X.Y. Ling, J. Henzie, P. Yang, S. Di V, L. Berkeley, Anisotropic Etching of Silver Nanoparticles for Plasmonic Structures Capable of Single-Particle SERS, Journal of American Chemical Society. 132 (2010) 895–901.

[46] L.-F. Zhang, S.-L. Zhong, A.-W. Xu, Highly branched concave Au/Pd bimetallic nanocrystals with superior electrocatalytic activity and highly efficient SERS enhancement, Angewandte Chemie - International Edition. 52 (2013) 645–649.

[47] P.-P. Fang, J.-F. Li, X.-D. Lin, J.R. Anema, D.-Y. Wu, B. Ren, Z.-Q. Tian, A SERS study of thiocyanate adsorption on Au-core Pd-shell nanoparticle film electrodes, Journal of Electroanalytical Chemistry. 665 (2012) 70–75.

[48] S. Pande, S.K. Ghosh, S. Praharaj, S. Panigrahi, S. Basu, S. Jana, A. Pal, T. Tsukuda, T. Pal, Synthesis of Normal and Inverted Gold−Silver Core−Shell Architectures in β-Cyclodextrin and Their Applications in SERS, Journal of Physical Chemistry C. 111 (2007) 10806–10813.

[49] L. Wu, Z. Wang, S. Zong, Z. Huang, P. Zhang, Y. Cui, A SERS-based immunoassay with highly increased sensitivity using gold/silver core-shell nanorods, Biosensors and Bioelectronics. 38 (2012) 94–99.

[50] L. Lu, G. Sun, H. Zhang, H. Wang, S. Xi, J. Hu, Z.-Q. Tian, R. Chen, Fabrication of core-shell Au-Pt nanoparticle film and its potential application as catalysis and SERS substrate, Journal of Materials Chemistry. 14 (2004) 1005–1009.

[51] J.-F. Li, J.R. Anema, Y.-C. Yu, Z.-L. Yang, Y.-F. Huang, X.-S. Zhou, B. Ren, Z.-Q. Tian, Core-shell nanoparticle based SERS from hydrogen adsorbed on a rhodium(111) electrode, Chemical Communications. 47 (2011) 2023–2025.

[52] L. Cao, P. Diao, L. Tong, T. Zhu, Z. Liu, Surface-Enhanced Raman Scattering of p-Aminothiophenol on a Au(core)/Cu(shell) Nanoparticle Assembly, ChemPhysChem. 6 (2005) 913–918.

[53] F. Bao, J.-F. Li, B. Ren, R.-A. Gu, Z.-Q. Tian, Synthesis and Characterization of Au@Co and Au@Ni Core−Shell Nanoparticles and Their Applications in Surface-Enhanced Raman Spectroscopy, Journal of Physical Chemistry C. 112 (2007) 345–350.

[54] S. Wojtysiak, M.S. Walczyński, A. Kudelski, Silver–platinum core–shell nanoparticles for surface-enhanced Raman spectroscopy, Vibrational Spectroscopy. 57 (2011) 261–269.

[55] L.Y. Chen, L. Zhang, T. Fujita, M.W. Chen, Surface-Enhanced Raman Scattering of Silver@Nanoporous Copper Core−Shell Composites Synthesized by an In Situ Sacrificial Template Approach, Journal of Physical Chemistry C. 113 (2009) 14195–14199.

[56] W. Li, Y. Guo, P. Zhang, General Strategy to Prepare TiO_2-Core Gold-Shell Nanoparticles as SERS-Tags, Journal of Physical Chemistry C. 114 (2009) 7263–7268.

[57] L. Sun, J. He, S. An, J. Zhang, D. Ren, Facile one-step synthesis of Ag@Fe_3O_4 core–shell nanospheres for reproducible SERS substrates, Journal of Molecular Structure. 1046 (2013) 74–81.

[58] C. Wang, S. Wang, Z. Zhou, R. Tian, Y. Li, X. Dai, S. Tian, Preparation of α-Fe_2O_3/Ag core/shell nanocomposites and SERS properties, Huagong Xuebao/CIESC Journal. 62 (2011) 276–280.

[59] N.T. Trang, T. Thuy, K. Higashimine, D. Mott, S. Maenosono, Magnetic–Plasmonic FePt@Ag Core–Shell Nanoparticles and Their Magnetic and SERS Properties, Plasmonics. 8 (2013) 1177–1184.

[60] F. Bao, J.-L. Yao, R.-A. Gu, Synthesis of Magnetic Fe_2O_3/Au Core/Shell Nanoparticles for Bioseparation and Immunoassay Based on Surface-Enhanced Raman Spectroscopy, Langmuir. 25 (2009) 10782–10787.

[61] Q. Ding, Y. Ma, Y. Ye, L. Yang, J. Liu, A simple method to prepare the magnetic Ni@Au core-shell nanostructure for the cycle surface enhanced Raman scattering substrates, Journal of Raman Spectroscopy. 44 (2013) 987–993.

[62] S.-S. Ma, Y.-J. Zhang, X.-Y. Hu, L. Cheng, H.-H. Zhou, Y.-T. Tian, X.-J. Li, J. Zhu, Surface-enhanced Raman spectrum and preparation of one-dimensional copper(core)-nickel(shell) nanostructure, Wuli Huaxue Xuebao/ Acta Physico - Chimica Sinica. 25 (2009) 1337–1341.

[63] P.-P. Fang, S. Duan, X.-D. Lin, J.R. Anema, J.-F. Li, O. Buriez, Y. Ding, F.-R. Fan, D.Y. Wu, B. Ren, Z.-L. Wang, C. Amatore, Z.-Q. Tian, Tailoring Au-core Pd-shell Pt-cluster nanoparticles for enhanced electrocatalytic activity, Chemical Science. 2 (2011) 531–539.

[64] W. Xie, C. Herrmann, K. Kömpe, M. Haase, S. Schlücker, Synthesis of bifunctional Au/Pt/Au core/shell nanoraspberries for in situ SERS monitoring of platinum-catalyzed reactions, Journal of the American Chemical Society. 133 (2011) 19302–19305.

[65] Y. Zhang, C. Xing, D. Jiang, M. Chen, Facile synthesis of core-shell-satellite Ag/C/Ag nanocomposites using carbon nanodots as reductant and their SERS properties, CrystEngComm. 15 (2013) 6305–6310.

[66] V. Uzayisenga, X.-D. Lin, L.-M. Li, J.R. Anema, Z.-L. Yang, Y.-F. Huang, H.-X. Lin, S.-B. Li, J.-F. Li, Z.-Q. Tian, Synthesis, characterization, and 3D-FDTD simulation of Ag@SiO_2 nanoparticles for shell-isolated nanoparticle-enhanced Raman spectroscopy, Langmuir. 28 (2012) 9140–9146.

[67] Y.-F. Jiang, B. Jiang, L.-K. Yang, M. Zhang, L.-B. Zhao, F.-Z. Yang, W.-B. Cai, D.-Y. Wu, Z.-Y. Zhou, Z-.Q Tian, Determination of adsorbed species of hypophosphite electrooxidation on Ni electrode by in situ infrared with shell-isolated nanoparticle-enhanced Raman spectroscopy, Electrochemistry Communications. 48 (2014) 5–9.

[68] T.T.B. Quyen, W.-N. Su, K.-J. Chen, C.-J. Pan, J. Rick, C.-C. Chang, B.-J Hwang, Au@SiO_2 core/shell nanoparticle assemblage used for highly sensitive SERS-based determination of glucose and uric acid, Journal of Raman Spectroscopy. 44 (2013) 1671–1677.

[69] Y.-C. Chen, R.J. Young, J. V Macpherson, N.R. Wilson, Single-Walled Carbon Nanotube Networks Decorated with Silver Nanoparticles: A Novel Graded SERS Substrate, Journal of Physical Chemistry C. 111 (2007) 16167–16173.

[70] D. Ibañez, C. Fernandez-Blanco, A. Heras, A. Colina, Time-Resolved Study of the Surface-Enhanced Raman Scattering Effect of Silver Nanoparticles Generated in Voltammetry Experiments., Journal of Physical Chemistry C. 118 (2014) 23426–23433.

[71] J. Huang, L. Zhang, B. Chen, N. Ji, F. Chen, Y. Zhang, Z. Zhang, Nanocomposites of size-controlled gold nanoparticles and graphene oxide: Formation and applications in SERS and catalysis, Nanoscale. 2 (2010) 2733–2738.

[72] Y. Zhang, S. Liu, L. Wang, X. Qin, J. Tian, W. Lu, G. Chang, X. Sun, One-pot green synthesis of Ag nanoparticles-graphene nanocomposites and their applications in SERS, H_2O_2, and glucose sensing, RSC Advances. 2 (2012) 538–545.

[73] W. Ren, Y. Fang, E. Wang, A Binary Functional Substrate for Enrichment and Ultrasensitive SERS Spectroscopic Detection of Folic Acid Using Graphene Oxide/Ag Nanoparticle Hybrids, ACS Nano. 5 (2011) 6425–6433.

[74] D.-G. Yu, W.-C. Lin, C.-H. Lin, L.-M. Chang, M.-C. Yang, An in situ reduction method for preparing silver/poly(vinyl alcohol) nanocomposite as surface-enhanced Raman scattering (SERS)-active substrates, Materials Chemistry and Physics. 101 (2007) 93–98.

[75] O. Dammer, B. Vlckova, M. Prochazka, J. Sedlacek, J. Vohlidal, J. Pfleger, Morphology and optical responses of SERS active pi-conjugated poly(N-ethyl-2-

ethynylpyridinium iodide)/Ag nanocomposite systems, Physical Chemistry Chemical Physics. 11 (2009) 5455–5461.

[76] A. Sánchez-Iglesias, P. Aldeanueva-Potel, W. Ni, J. Pérez-Juste, I. Pastoriza-Santos, R.A. Alvarez-Puebla, B. N. Mbenkum, L. M Liz-Marzán, SERS substrates, Nano Today. 5 (2010) 21–27.

[77] N.R. Jana, Silver coated gold nanoparticles as new surface enhanced Raman substrate at low analyte concentration, The Analyst. 128 (2003) 954–956.

[78] X.-D. Tian, B.-J. Liu, J.-F. Li, Z.-L. Yang, B. Ren, Z.-Q. Tian, SHINERS and plasmonic properties of Au Core SiO2 shell nanoparticles with optimal core size and shell thickness, Journal of Raman Spectroscopy. 44 (2013) 994–998.

[79] B. Reents, G. Lacconi, W. Plieth, Raman spectroscopy of silver plating from a cyanide electrolyte, Journal of Electroanalytical Chemistry. 325 (1992) 207–217.

[80] B. Bozzini, V. Romanello, C. Mele, A SERS investigation of the electrodeposition of Au in a phosphate solution, Surface and Coatings Technology. 201 (2007) 6267–6272.

[81] Z.Z.-Q. Tian, B. Ren, D. Wu, Surface-enhanced Raman scattering: From noble to transition metals and from rough surfaces to ordered nanostructures, Journal of Physical Chemistry B. 106 (2002) 9463–9483.

[82] Q.J. Huang, X.Q. Li, J.L. Yao, B. Ren, W.B. Cai, J.S. Gao, B. W. Mao, Z.Q. Tian, Extending surface Raman spectroscopic studies to transition metals for practical applications III . Effects of surface roughening procedure on surface-enhanced Raman spectroscopy from nickel and platinum electrodes, Surface Science. 427-428 (1999) 162–166.

[83] G.L. Beltramo, T.E. Shubina, M.T.M. Koper, Oxidation of formic acid and carbon monoxide on gold electrodes studied by surface-enhanced Raman spectroscopy and DFT., ChemPhysChem. 6 (2005) 2597–2606.

[84] W.B. Cai, B. Ren, X.Q. Li, C.X. She, F.M. Liu, X.W. Cai, Z.Q Tian, Investigation of surface-enhanced Raman scattering from platinum electrodes using a confocal Raman microscope: dependence of surface roughening pretreatment, Surface Science. 406 (1998) 9–22.

[85] A. Merlen, V. Gadenne, J. Romann, V. Chevallier, L. Patrone, J.C. Valmalette, Surface enhanced Raman spectroscopy of organic molecules deposited on gold sputtered substrates., Nanotechnology. 20 (2009) 215705.

[86] E. Harte, Surface-Enhanced Raman and Fluorescence Spectroscopy of Dye Molecules Deposited on Nanostructured Gold Surfaces, Journal of Physical Chemistry C. 114 (2010) 12878–12884.

[87] C. Domingo, V. Resta, S. Sanchez-Cortes, J. V García-Ramos, J. Gonzalo, Pulsed laser deposited au nanoparticles as substrates for surface-enhanced vibrational spectroscopy, Journal of Physical Chemistry C. 111 (2007) 8149–8152.

[88] Q.-Y. Wang, S.-L. Bai, Y.-H. Zhao, Z.-D. Liu, Effect of mechanical polishing on corrosion behavior of Hastelloy C22 coating prepared by high power diode laser cladding, Applied Surface Science. 303 (2014) 312–318.

[89] G. Krishna Podagatlapalli, S. Hamad, M. Ahamad Mohiddon, S. Venugopal Rao, Effect of oblique incidence on silver nanomaterials fabricated in water via ultrafast laser ablation for photonics and explosives detection, Applied Surface Science. 303 (2014) 217–232.

[90] C.L. Haynes, R.P. Van Duyne, Nanosphere Lithography: A Versatile Nanofabrication Tool for Studies of Size-Dependent Nanoparticle Optics, Journal of Physical Chemistry B. 105 (2001) 5599–5611.

[91] M. Green, F.M. Liu, SERS Substrates Fabricated by Island Lithography: The Silver/Pyridine System, Journal of Physical Chemistry B. 107 (2003) 13015–13021.

[92] N.A. Abu Hatab, J.M. Oran, M.J. Sepaniak, Surface-Enhanced Raman Spectroscopy Substrates Created via Electron Beam Lithography and Nanotransfer Printing, ACS Nano. 2 (2008) 377–385.

[93] J.D. Driskell, S. Shanmukh, Y. Liu, S.B. Chaney, X.-J. Tang, Y.-P. Zhao, R. A. Dluhy, The use of aligned silver nanorod arrays prepared by oblique angle deposition as surface enhanced Raman scattering substrates, Journal of Physical Chemistry C. 112 (2008) 895–901.

[94] J. Lin, H. Lan, W. Zheng, Y. Qu, F. Lai, Silver nanoparticles films deposited on AAO templates by thermal evaporation for surface-enhanced Raman scattering of R6G, Nano. 7 (2012) 1250048.

[95] S. Link, M.A. El-Sayed, Spectral Properties and Relaxation Dynamics of Surface Plasmon Electronic Oscillations in Gold and Silver Nanodots and Nanorods, Journal of Physical Chemistry B. 103 (1999) 8410–8426.

[96] G.V.P. Kumar, Surface-enhanced Raman scattering studies of carbon nanotubes using Ag-core Au-shell nanoparticles, Journal of Raman Spectroscopy. 40 (2009) 2069–2073.

[97] K.M. Kosuda, J.M. Bingham, K.L. Wustholz, R.P. Van Duyne, Nanostructures and Surface-Enhanced Raman Spectroscopy. In Comprehensive Nanoscience and Technology, Oxford, 2011.

[98] F.S. Ameer, Y. Zhou, S. Zou, D. Zhang, Wavelength-dependent correlations between ultraviolet-visible intensities and surface enhanced Raman spectroscopic enhancement factors of aggregated gold and silver nanoparticles, Journal of Physical Chemistry C. 118 (2014) 22234–22242.

[99] B. Sharma, R.R. Frontiera, A.-I. Henry, E. Ringe, R.P. Van Duyne, SERS: Materials, applications, and the future, Materials Today. 15 (2012) 16–25.

[100] A. Boltasseva, H.A. Atwater, Low-loss plasmonic metamaterials., Science. 331 (2011) 290–291.

[101] L. Kang, P. Xu, B. Zhang, H. Tsai, X. Han, H.-L. Wang, Laser wavelength- and power-dependent plasmon-driven chemical reactions monitored using single particle surface enhanced Raman spectroscopy, Chemical Communications. 49 (2013) 3389–3391.

[102] J.K. Lim, S.-W. Joo, Excitation-wavelength-dependent charge transfer resonance of bipyridines on silver nanoparticles: surface-enhanced Raman scattering study, Surface and Interface Analysis. 39 (2007) 684–690.

[103] A.P. Richter, J.R. Lombardi, B. Zhao, Size and Wavelength Dependence of the Charge-Transfer Contributions to Surface-Enhanced Raman Spectroscopy in Ag/PATP/ZnO Junctions, Journal of Physical Chemistry C. 114 (2010) 1610–1614.

[104] K. Faulds, F. McKenzie, W.E. Smith, D. Graham, Quantitative simultaneous multianalyte detection of DNA by dual-wavelength surface-enhanced resonance Raman scattering, Angewandte Chemie - International Edition. 46 (2007) 1829–1831.

[105] E.-O. Ganbold, J.-H. Park, U. Dembereldorj, K.-S. Ock, S.-W. Joo, Charge-dependent adsorption of rhodamine 6G on gold nanoparticle surfaces: fluorescence and Raman study, Journal of Raman Spectroscopy. 42 (2011) 1614–1619.

[106] A. M. Gabudean, D. Biro, S. Astilean, Localized surface plasmon resonance (LSPR) and surface-enhanced Raman scattering (SERS) studies of 4-aminothiophenol adsorption on gold nanorods, Journal of Molecular Structure. 993 (2011) 420–424.

[107] C. Ruan, W. Wang, B. Gu, Single-molecule detection of thionine on aggregated gold nanoparticles by surface enhanced Raman scattering, Journal of Raman Spectroscopy. 38 (2007) 568–573.

[108] K.-H. Yang, Y.-C. Liu, C.-C. Yu, Enhancements in intensity and stability of surface-enhanced Raman scattering on optimally electrochemically roughened silver substrates, Journal of Materials Chemistry. 18 (2008) 4849–4855.

[109] X. Li, A.A. Gewirth, Oxygen electroreduction through a superoxide intermediate on Bi-modified Au surfaces, Journal of the American Chemical Society. 127 (2005) 5252–5260.

[110] M.R. Mahoney, M.W. Howard, R.P. Cooney, Raman spectra of carbon monoxide adsorbed on silver electrodes, Journal of Electroanalytical Chemistry and Interfacial Electrochemistry. 161 (1984) 163–167.

[111] J. Solla-Gullón, R. Gómez, a. Aldaz, J.M.M. Pérez, A combination of SERS and electrochemistry in Pt nanoparticle electrocatalysis: Promotion of formic acid oxidation by ethylidyne, Electrochemistry Communications. 10 (2008) 319–322.

[112] J.A. Dieringer, R.B. Lettan II, K.A. Scheidt, R.P. Van Duyne, A frequency domain existence proof of single-molecule surface-enhanced Raman spectroscopy, Journal of the American Chemical Society. 129 (2007) 16249–16256.

[113] B. Ren, D. Wu, B. Mao, Z. Tian, Surface-Enhanced Raman Study of Cyanide Adsorption at the Platinum Surface, Journal of Physical Chemistry B. 107 (2003) 2752–2758.

[114] A. Wang, Y.-F. Huang, U.K. Sur, D.-Y. Wu, B. Ren, S. Rondinini, C. Amatore, Z.-Q. Tian, In situ identification of intermediates of benzyl chloride reduction at a silver electrode by SERS coupled with DFT calculations, Journal of the American Chemical Society. 132 (2010) 9534–9536.

[115] B. Reents, G. Lacconi, W. Plieth, Nucleation in the electrocrystallization process studied by surface-enhanced Raman spectroscopy, Journal of Electroanalytical Chemistry. 376 (1994) 185–188.

[116] Y.W. Alsmeyer, R.L. McCreery, Surface-enhanced Raman spectroscopy of carbon electrode surfaces following silver electrodeposition, Analytical Chemistry. 63 (1991) 1289–1295.

[117] N. Horimoto, N. Ishikawa, A. Nakajima, Preparation of a SERS substrate using vacuum-synthesized silver nanoparticles, Chemical Physics Letters. 413 (2005) 78–83.

[118] C. Lee, D. Meisel, Adsorption and Surface-Enhanced Raman of Dyes on Silver and Gold Sols', Journal of Physical Chemistry. 86 (1982) 3391–3395.

[119] K. Faulds, W.E. Smith, D. Graham, R.J. Lacey, Assessment of silver and gold substrates for the detection of amphetamine sulfate by surface enhanced Raman scattering (SERS), Analyst. 127 (2002) 282–286.

[120] M. Lin, L. He, J. Awika, L. Yang, D.R. Ledoux, H. Li, A. Mustapha, Detection of melamine in gluten, chicken feed, and processed foods using surface enhanced Raman spectroscopy and HPLC, Journal of Food Science. 73 (2008) T129–T134.

[121] M. Liu, W. Chen, Graphene nanosheets-supported Ag nanoparticles for ultrasensitive detection of TNT by surface-enhanced Raman spectroscopy, Biosensors and Bioelectronics. 46 (2013) 68–73.

[122] C.T. Nguyen, J.T. Nguyen, S. Rutledge, J. Zhang, C. Wang, G.C. Walker, Detection of chronic lymphocytic leukemia cell surface markers using surface enhanced Raman scattering gold nanoparticles., Cancer Letters. 292 (2010) 91–97.

[123] P.K. Sekhar, N.S. Ramgir, S. Bhansali, Metal-Decorated Silica Nanowires: An Active Surface-Enhanced Raman Substrate for Cancer Biomarker Detection, Journal of Physical Chemistry C. 112 (2008) 1729–1734.

[124] J. Li, Y. Fang, An investigation of the surface enhanced Raman scattering (SERS) from a new substrate of silver-modified silver electrode by magnetron sputtering., Spectrochimica Acta Part A: Molecular and Biomolecular Spectroscopy. 66 (2007) 994–1000.

[125] J. Kundu, O. Neumann, B.G. Janesko, D. Zhang, S. Lal, A. Barhoumi, Adenine and Adenosine Monophosphate (AMP) - Gold Binding Interactions Studied by Surface-Enhanced Raman and Infrared Spectroscopies, Journal of Physical Chemistry C. 113 (2009) 14390–14397.

[126] K. Kneipp, H. Kneipp, V. Bhaskaran Kartha, R. Manoharan, G. Deinum, I. Itzkan, R. R. Dasari, M.S. Feld, Detection and identification of a single DNA base molecule using surface-enhanced Raman scattering (SERS), Physical Review E - Statistical Physics, Plasmas, Fluids, and Related Interdisciplinary Topics. 57 (1998) 6281–6284.

[127] R.J. Stokes, E. McBride, C.G. Wilson, J.M. Girkin, W.E. Smith, D. Graham, Surface-enhanced Raman scattering spectroscopy as a sensitive and selective technique for the detection of folic acid in water and human serum, Applied Spectroscopy. 62 (2008) 371–376.

[128] K.E. Shafer-Peltier, C.L. Haynes, M.R. Glucksberg, R.P. Van Duyne, Toward a glucose biosensor based on surface-enhanced Raman scattering, Journal of the American Chemical Society. 125 (2003) 588–593.

[129] D.A. Stuart, J.M. Yuen, N. Shah, O. Lyandres, C.R. Yonzon, M.R. Glucksberg, J. T. Walsh, R.P. Van Duyne, In vivo glucose measurement by surface-enhanced Raman spectroscopy, Analytical Chemistry. 78 (2006) 7211–7215.

[130] X. Sun, S. Stagon, H. Huang, J. Chen, Y. Lei, Functionalized aligned silver nanorod arrays for glucose sensing through surface enhanced Raman scattering, RSC Advances. 4 (2014) 23382–23388.

[131] M. Zukalová, J. Tarábek, M. Kalbáč, L. Kavan, L. Dunsch, In situ optical spectroelectrochemistry of single-walled carbon nanotube thin films, Journal of Solid State Electrochemistry. 12 (2008) 1279–1284.

[132] L. Kavan, L. Dunsch, Spectroelectrochemistry of carbon nanotubes., Chemphyschem : A European Journal of Chemical Physics and Physical Chemistry. 12 (2011) 47–55.

[133] D. Ibañez, E.C. Romero, A. Heras, A. Colina, Dynamic Raman spectroelectrochemistry of single walled carbon nanotubes modified electrodes using a Langmuir-Schaefer method, Electrochimica Acta. 129 (2014) 171–176.

[134] A. Colina, V. Ruiz, A. Heras, E. Ochoteco, E. Kauppinen, J. López-Palacios, Low resolution Raman spectroelectrochemistry of single walled carbon nanotube electrodes, Electrochimica Acta. 56 (2011) 1294–1299.

[135] M. Kalbac, H. Farhat, J. Kong, P. Janda, L. Kavan, M.S. Dresselhaus, Raman spectroscopy and in situ Raman spectroelectrochemistry of bilayer 12C/ 13C graphene, Nano Letters. 11 (2011) 1957–1963.

[136] M.H. Kalbacova, M. Verdanova, A. Broz, A. Vetushka, A. Fejfar, M. Kalbac, Modulated surface of single-layer graphene controls cell behavior, Carbon. 72 (2014) 207–214.

[137] X. Li, B.K. Tay, J. Li, D. Tan, C.W. Tan, K. Liang, Mildly reduced graphene oxide-Ag nanoparticle hybrid films for surface-enhanced Raman scattering., Nanoscale Research Letters. 7 (2012) 205.

[138] Z. Komínková, M. Kalbáč, Raman spectroscopy of strongly doped CVD-graphene, Physica Status Solidi (B) Basic Research. 250 (2013) 2659–2661.

[139] F.J. García-Rodríguez, J.F. Pérez-Robles, J. González-Hernández, Y. Vorobiev, S. Jiménez-Sandoval, A. Manzano-Ramírez, Surface Enhanced Raman Scattering of graphite on metals, Solid State Communications. 105 (1998) 85–87.

[140] A.C. Ferrari, Raman spectroscopy of graphene and graphite: Disorder, electron-phonon coupling, doping and nonadiabatic effects, Solid State Communications. 143 (2007) 47–57.

[141] K.N. Kudin, B. Ozbas, H.C. Schniepp, R.K. Prud'homme, I.A. Aksay, R. Car, Raman spectra of graphite oxide and functionalized graphene sheets, Nano Letters. 8 (2008) 36–41.

[142] L. Kavan, L. Dunsch, Spectroelectrochemistry of carbon nanostructures., ChemPhysChem. 8 (2007) 974–998.

[143] M.G. Mitch, J.S. Lannin, Raman scattering in K_4C_{60} and Rb_4C_{60} fullerenes, Physical Review B. 51 (1995) 6784–6787.

[144] M. Trchová, Z. Morávková, J. Dybal, J. Stejskal, Detection of Aniline Oligomers on Polyaniline–Gold Interface using Resonance Raman Scattering, ACS Applied Materials & Interfaces. 6 (2013) 942–950.

[145] G. Kister, G. Cassanas, M. Vert, Effects of morphology, conformation and configuration on the IR and Raman spectra of various poly(lactic acid)s, Polymer. 39 (1998) 267–273.

[146] G.S. Petreska, J. Blazevska-Gilev, R. Fajgar, R. Tomovska, Surface-Enhanced Raman Scattering activity of Ag/graphene/polymer nanocomposite films synthesized by laser ablation, Thin Solid Films. 564 (2014) 115–120.

[147] T. Halamus, P. Wojciechowski, Synthesis of the (hydroxypropyl) cellulose - titania hybrid nanocomposite as seen by Raman spectroscopy, Polymers for Advanced Technologies. 18 (2007) 411–417.

[148] C.L. Brosseau, F. Casadio, R.P. Van Duyne, Revealing the invisible: Using surface-enhanced Raman spectroscopy to identify minute remnants of color in Winslow Homer's colorless skies, Journal of Raman Spectroscopy. 42 (2011) 1305–1310.

[149] C.L. Brosseau, K.S. Rayner, F. Casadio, C.M. Grzywacz, R.P. Van Duyne, Surface-Enhanced Raman Spectroscopy: A Direct Method to Identify Colorants in Various Artist Media, Analytical Chemistry. 81 (2009) 7443–7447.

[150] C.L. Brosseau, A. Gambardella, F. Casadio, C.M. Grzywacz, J. Wouters, R.P. Van Duyne, Ad-hoc Surface-Enhanced Raman Spectroscopy Methodologies for the Detection of Artist Dyestuffs: Thin Layer Chromatography-Surface Enhanced Raman Spectroscopy and in Situ On the Fiber Analysis, Analytical Chemistry. 81 (2009) 3056–3062.

[151] K. Chen, M. Leona, T. Vo-Dinh, Surface-enhanced Raman scattering for identification of organic pigments and dyes in works of art and cultural heritage material, Sensor Review. 27 (2007) 109–120.

[152] K.L. Wustholz, C.L. Brosseau, F. Casadio, R.P. Van Duyne, Surface-enhanced Raman spectroscopy of dyes: from single molecules to the artists' canvas, Physical Chemistry Chemical Physics. 11 (2009) 7350–7359.

[153] M. Leona, Microanalysis of organic pigments and glazes in polychrome works of art by surface-enhanced resonance Raman scattering, Proceedings of the National Academy of Sciences of the United States of America. 106 (2009) 14757–14762.

[154] E. Van Elslande, S. Lecomte, A.-S. Le Hô, Micro-Raman spectroscopy (MRS) and surface-enhanced Raman scattering (SERS) on organic colourants in archaeological pigments, Journal of Raman Spectroscopy. 39 (2008) 1001–1006.

[155] H. Letheby, On the production of a blue substance by the electrolysis of sulphate of aniline, Journal of the Chemical Society. 15 (1862) 161–163.

[156] C.K. Chiang, C.R. Fincher, Y.W. Park, A.J. Heeger, H. Shirakawa, E.J. Louis, S.C. Gau, G.C. MacDiarmid., Electrical conductivity in doped polyacetylene, Physical Review Letters. 39 (1977) 1098–1101.

[157] A.F. Diaz, K.K. Kanazawa, G.P. Gardini, Electrochemical polymerization of pyrrole, Journal of the Chemical Society, Chemical Communications. (1979) 635–636.

[158] R. John, A. Talaie, G.G. Wallace, S. Fletcher, Characterisation of conductive, electroactive polymers using resistometry, Journal of Electroanalytical Chemistry. 319 (1991) 365–371.

[159] J.L. Brédas, G.B. Street, Polarons, bipolarons, and solitons in conducting polymers, Accounts of Chemical Research. 18 (1985) 309–315.

[160] V. Ruiz, Espectroelectroquímica Bidimensional aplicada a la electrosíntesis y caracterización de poli[4,4’-bis(alquiltio)-2,2'-bitiofeno]s, University of Burgos, 2002.

[161] G. Inzel, Mechanism of Charge Transport in Polymer Modified Electrodes, in: A.J. Bard (Ed.), Electroanalytical Chemistry: A Series of Advances, Vol. 18, Marcel Dekker, New York, 1994: pp. 89–241.

[162] L. Xiao, Y. Cao, J. Xiao, B. Schwenzer, M.H. Engelhard, L. V Saraf, Z. Nie, G.J. Exarhos, J. Liu, A soft approach to encapsulate sulfur: Polyaniline nanotubes for lithium-sulfur batteries with long cycle life, Advanced Materials. 24 (2012) 1176–1181.

[163] S.W. Choi, S.M. Jo, W.S. Lee, Y.-R. Kim, An electrospun poly(vinylidene fluoride) nanofibrous membrane and its battery applications, Advanced Materials. 15 (2003) 2027–2032.

[164] M.H.T. Nguyen, E.-S. Oh, Improvement of the characteristics of poly(acrylonitrile-butylacrylate) water-dispersed binder for lithium-ion batteries by the addition of acrylic acid and polystyrene seed, Journal of Electroanalytical Chemistry. 739 (2015) 111–114.

[165] J.H. Burroughes, D.D.C. Bradley, A.R. Brown, R.N. Marks, K. Mackay, R.H. Friend, P.L Burns, A.B. Holmes, Light-emitting diodes based on conjugated polymers, Nature. 347 (1990) 539–541.

[166] N.F. Ayub, S. Hashim, N. Adrus, Development of UV LED hydrogel formulation based on polyacrylamide hydrogel, Applied Mechanics and Materials. 695 (2015) 102–105.

[167] M. Sudhakar, P.I. Djurovich, T.E. Hogen-Esch, M.E. Thompson, Phosphorescence quenching by conjugated polymers, Journal of the American Chemical Society. 125 (2003) 7796–7797.

[168] I. Riedel, V. Dyakonov, Influence of electronic transport properties of polymer-fullerene blends on the performance of bulk heterojunction photovoltaic devices, Physica Status Solidi (A) Applied Research. 201 (2004) 1332–1341.

[169] D. Chirvase, Z. Chiguvare, M. Knipper, J. Parisi, V. Dyakonov, J.C. Hummelen, Temperature dependent characteristics of poly(3 hexylthiophene)-fullerene based heterojunction organic solar cells, Journal of Applied Physics. 93 (2003) 3376–3383.

[170] C.J. Brabec, N.S. Sariciftci, J.C. Hummelen, Plastic solar cells, Advanced Funtional Materials. 11 (2001) 15–26.

[171] M.A. Rahman, N.-H. Kwon, M.-S. Won, E.S. Choe, Y.-B. Shim, Functionalized conducting polymer as an enzyme-immobilizing substrate: An amperometric glutamate microbiosensor for in vivo measurements, Analytical Chemistry. 77 (2005) 4854–4860.

[172] V. Tabard-Cossa, M. Godin, P. Grütter, I. Burgess, R.B. Lennox, Redox-induced surface stress of polypyrrole-based actuators, Journal of Physical Chemistry B. 109 (2005) 17531–17537.

[173] M. Lahav, C. Durkan, R. Gabai, E. Katz, I. Willner, M.E. Welland, Redox activation of a polyaniline-coated cantilever: An electro-driven microdevice, Angewandte Chemie - International Edition. 40 (2001) 4095–4097.

[174] N. Tessler, G.J. Denton, R.H. Friend, Lasing from conjugated-polymer microcavities, Nature. 382 (1996) 695–696.

[175] M.R. Islam, A. Ahiabu, X. Li, M.J. Serpe, Poly (N-isopropylacrylamide) microgel-based optical devices for sensing and biosensing, Sensors (Switzerland). 14 (2014) 8984–8995.

[176] A. Otomo, T. Yamada, S.-I. Inoue, Organic electro-optic polymer devices for ultra-high-speed optical communication, Journal of the National Institute of Information and Communications Technology. 60 (2013) 3–12.

[177] A. Tsumura, H. Koezuka, T. Ando, Macromolecular electronic device: Field-effect transistor with a polythiophene thin film, Applied Physics Letters. 49 (1986) 1210–1212.

[178] Y. Gao, H.-L. Yip, K.-S. Chen, K.M. O'Malley, O. Acton, Y. Sun, G. Ting, H. Chen, A.K.-J.Jen, Surface doping of conjugated polymers by graphene oxide and its application for organic electronic devices, Advanced Materials. 23 (2011) 1903–1908.

[179] P.C. Ramamurthy, A.M. Malshe, W.R. Harrell, R. V Gregory, K. McGuire, A.M. Rao, Polyaniline/single-walled carbon nanotube composite electronic devices, Solid-State Electronics. 48 (2004) 2019–2024.

[180] B. Sankaran, J.R. Reynolds, High-contrast electrochromic polymers from alkyl-derivatized poly(3,4-ethylenedioxythiophenes), Macromolecules. 30 (1997) 2582–2588.

[181] H.W. Heuer, R. Wehrmann, S. Kirchmeyer, Electrochromic window based on conducting poly(3,4-ethylenedioxythiophene)- poly(styrene sulfonate), Advanced Functional Materials. 12 (2002) 89–94.

[182] G.A. Sotzing, J.R. Reynolds, P.J. Steel, Electrochromic conducting polymers via electrochemical polymerization of bis(2-(3,4-ethylenedioxy)thienyl) monomers, Chemistry of Materials. 8 (1996) 882–889.

[183] N. Terasawa, Y. Hayashi, T. Koga, N. Higashi, K. Asaka, High-performance polymer actuators based on poly(ethylene oxide) and single-walled carbon nanotube-ionic liquid-based gels, Sensors and Actuators, B: Chemical. 202 (2014) 382–387.

[184] C. Della Pina, E. Zappa, G. Busca, A. Sironi, E. Falletta, Electromechanical properties of polyanilines prepared by two different approaches and their applicability in force measurements, Sensors and Actuators, B: Chemical. 201 (2014) 395–401.

[185] B. Wessling, Passivation of metals by coating with polyaniline: Corrosion potential shift and morphological changes, Advanced Materials. 6 (1994) 226–228.

[186] M.B. González, S.B. Saidman, Electrodeposition of bilayered polypyrrole on 316 L stainless steel for corrosion prevention, Progress in Organic Coatings. 78 (2015) 21–27.

[187] T.R. Chan, R. Hilgraf, K.B. Sharpless, V. V Fokin, Polytriazoles as copper(I)-stabilizing ligands in catalysis, Organic Letters. 6 (2004) 2853–2855.

[188] D.E. Bergbreiter, B.L. Case, Y.-S. Liu, J.W. Caraway, Poly(N-isopropylacrylamide) soluble polymer supports in catalysis and synthesis, Macromolecules. 31 (1998) 6053–6062.

[189] R. Esfand, D.A. Tomalia, Poly(amidoamine) (PAMAM) dendrimers: From biomimicry to drug delivery and biomedical applications, Drug Discovery Today. 6 (2001) 427–436.

[190] K. Knop, R. Hoogenboom, D. Fischer, U.S. Schubert, Poly(ethylene glycol) in drug delivery: Pros and cons as well as potential alternatives, Angewandte Chemie - International Edition. 49 (2010) 6288–6308.

[191] H.M. Li, Q.G. Zhang, N.N. Guo, A.M. Zhu, Q.L. Liu, Ultrafine polystyrene nanofibers and its application in nanofibrous membranes, Chemical Engineering Journal. 264 (2015) 329–335.

[192] N. Ghaemi, S.S. Madaeni, P. Daraei, H. Rajabi, S. Zinadini, A. Alizadeh, R. Heydari, M. Beygzadeh, S. Ghouzivand, Polyethersulfone membrane enhanced with iron oxide nanoparticles for copper removal from water: Application of new functionalized Fe_3O_4 nanoparticles, Chemical Engineering Journal. 263 (2015) 101–112.

[193] B. Zanfrognini, A. Colina, A. Heras, C. Zanardi, R. Seeber, J. López-Palacios, A UV–Visible/Raman spectroelectrochemical study of the stability of poly(3,4-ethylendioxythiophene) films, Polymer Degradation and Stability. 96 (2011) 2112–2119.

[194] S. Iijima, Helical microtubules of graphitic carbon, Nature. 354 (1991) 56–58.

[195] S. Iijima, T. Ichihashi, Single-shell carbon nanotubes of 1-nm diameter, Nature. 363 (1993) 603–605.

[196] D.S. Bethune, C.H. Kiang, M.S. de Vries, G. Gorman, R. Savoy, J. Vazquez, R. Beyers, Cobalt-catalysed growth of carbon nanotubes with single-atomin-layer walls, Nature. 363 (1993) 605–607.

[197] T. Pichler, Carbon ahead, Nature Materials. 6 (2007) 332–333.

[198] J. Prasek, J. Drbohlavova, J. Chomoucka, J. Hubalek, O. Jasek, V. Adam, R. Kizek, Methods for carbon nanotubes synthesis-review, Journal of Materials Chemistry. 21 (2011) 15872-15884.

[199] A. Szabó, C. Perri, A. Csató, G. Giordano, D. Vuono, J.B. Nagy, Synthesis Methods of Carbon Nanotubes and Related Materials, Materials. 3 (2010) 3092–3140.

[200] P.W. Ruch, L.J. Hardwick, M. Hahn, A. Foelske, R. Kötz, A. Wokaun, Electrochemical doping of single-walled carbon nanotubes in double layer capacitors studied by in situ Raman spectroscopy, Carbon. 47 (2009) 38–52.

[201] E. Richter, K.R. Subbaswamy, Theory of Size-Dependent Resonance Raman Scattering from Carbon Nanotubes, Physical Review Letters. 79 (1997) 2738–2741.

[202] P. Eklund, J. Holden, R.A. Jishi, Vibrational modes of carbon nanotubes; spectroscopy and theory, Carbon. 33 (1995) 959–972.

[203] M.S. Dresselhaus, P.C. Eklund, Advances in Physics Phonons in carbon nanotubes, Advances in Physics. 47 (2000) 705–814.

[204] R.A. Jishi, L. Venkataraman, M.S. Dresselhaus, G. Dresselhaus, Phonon modes in carbon nanotubules, Chemical Physics Letters. 209 (1993) 77–82.

[205] T. Aizawa, R. Souda, S. Otani, Y. Ishizawa, C. Oshima, Bond softening in monolayer graphite formed on transition-metal carbide surfaces, Physical Review B. 42 (1990) 11469–11478.

[206] C. Oshima, T. Aizawa, R. Souda, Y. Ishizawa, Y. Sumiyoshi, Surface phonon dispersion curves of graphite (0001) over the entire energy region, Solid State Communications. 65 (1988) 1601–1604.

[207] M.S. Dresselhaus, A. Jorio, M. Hofmann, G. Dresselhaus, R. Saito, Perspectives on carbon nanotubes and graphene Raman spectroscopy., Nano Letters. 10 (2010) 751–758.

[208] M.S. Dresselhaus, G. Dresselhaus, R. Saito, A. Jorio, Raman spectroscopy of carbon nanotubes, Physics Reports. 409 (2005) 47–99.

[209] M. Kalbac, Y.-P. Hsieh, H. Farhat, L. Kavan, M. Hofmann, J. Kong, M.S. Dresselhaus, Defects in individual semiconducting single wall carbon nanotubes: Raman spectroscopic and in situ Raman spectroelectrochemical study., Nano Letters. 10 (2010) 4619–4626.

[210] B.I. Yakobson, C.J. Brabec, J. Bernholc, Nanomechanics of carbon tubes: instabilities beyond linear response, Physical Review Letters. 76 (1996) 2511–2514.

[211] M.M.J. Treacy, T.W. Ebbesen, J.M. Gibson, Exceptionally high Young's modulus observed for individual carbon nanotubes, Nature. 381 (1996) 678–680.

[212] M.-F. Yu, Fundamental Mechanical Properties of Carbon Nanotubes: Current Understanding and the Related Experimental Studies, Journal of Engineering Materials and Technology. 126 (2004) 271–278.

[213] D. Qian, G.J. Wagner, W.K. Liu, M.-F. Yu, R.S. Ruoff, Mechanics of carbon nanotubes, Applied Mechanics Reviews. 55 (2002) 495–533.

[214] Y.Q. Zhu, T. Sekine, T. Kobayashi, E. Takazawa, M. Terrones, H. Terrones, Collapsing carbon nanotubes and diamond formation under shock waves, Chemical Physics Letters. 287 (1998) 689–693.

[215] P.M. Ajayan, Nanotubes from Carbon, Chemical Reviews. 99 (1999) 1787–1799.

[216] S. Sinha, A. Schwab, Off-axis thermal properties of carbon nanotubes films, Journal of Nanoparticle Research. 7 (2005) 651–657.

[217] P. Kim, L. Shi, A. Majumdar, P. McEuen, Thermal Transport Measurements of Individual Multiwalled Nanotubes, Physical Review Letters. 87 (2001) 215502.

[218] A. Mizel, L.X. Benedict, M.L. Cohen, S.G. Louie, A. Zettl, Analysis of the low-temperature specific heat of multiwalled carbon nanotubes and carbon nanotube ropes, Physical Review B. 60 (1999) 3264–3270.

[219] D. Yang, Q. Zhang, G. Chen, S. Yoon, J. Ahn, S. Wang, Q. Zhou, Q. Wang, J. Li, Thermal conductivity of multiwalled carbon nanotubes, Physical Review B. 66 (2002) 165440.

[220] S.C. Tsang, P.J.F. Harris, M.L.H. Green, Thinning and opening of carbon nanotubes by oxidation using carbon dioxide, Nature. 362 (1993) 520–522.

[221] P.M. Ajayan, T.W. Ebbesen, T. Ichihashi, S. Iijima, K. Tanigaki, H. Hiura, Opening carbon nanotubes with oxygen and implications for filling, Nature. 362 (1993) 522–525.

[222] T. Nakajima, S. Kasamatsu, Y. Matsuo, Synthesis and characterization of fluorinated carbon nanotube, European Journal of Solid State and Inorganic Chemistry. 33 (1996) 831–840.

[223] A.C. Dillon, T. Gennett, K.M. Jones, J.L. Alleman, P.A. Parilla, M.J. Heben, A Simple and Complete Purification of Single-Walled Carbon Nanotube Materials, Advanced Materials. 11 (1999) 1354–1358.

[224] E. Dujardin, T.W. Ebbesen, A. Krishnan, M.M.J. Treacy, Purification of Single-Shell Nanotubes, Advanced Materials. 10 (1998) 611–613.

[225] S. Nagasawa, M. Yudasaka, K. Hirahara, T. Ichihashi, S. Iijima, Effect of oxidation on single-wall carbon nanotubes, Chemical Physics Letters. 328 (2000) 374–380.

[226] R. Yu, L. Chen, Q. Liu, J. Lin, K.-L. Tan, S.C. Ng, H.S.O. Chan, G.-Q. Xu, T.S.A. Hor, Platinum Deposition on Carbon Nanotubes via Chemical Modification, Chemistry of Materials. 10 (1998) 718–722.

[227] H. Hiura, T.W. Ebbesen, K. Tanigaki, Opening and purification of carbon nanotubes in high yields, Advanced Materials. 7 (1995) 275–276.

[228] V. Georgakilas, K. Kordatos, M. Prato, D.M. Guldi, M. Holzinger, A. Hirsch, Organic Functionalization of Carbon Nanotubes, Journal of the American Chemical Society. 124 (2002) 760–761.

[229] S.E. Kooi, U. Schlecht, M. Burghard, K. Kern, Electrochemical Modification of Single Carbon Nanotubes, Angewandte Chemie - International Edition. 41 (2002) 1353–1355.

[230] P.M. Ajayan, M. Terrones, A. de la Guardia, V. Huc, N. Grobert, B.Q. Wei, H. Lezec, G. Ramanath, T.W. Ebbesen, Nanotubes in a flash-ignition and reconstruction., Science. 296 (2002) 705.

[231] G. Hummer, J.C. Rasaiah, J.P. Noworyta, Water conduction through the hydrophobic channel of a carbon nanotube, Nature. 414 (2001) 188–190.

[232] J.K. Holt, H.G. Park, Y. Wang, M. Stadermann, A.B. Artyukhin, C.P. Grigoropoulos, A. Noy, O. Bakajin, Fast Mass Transport Through Sub-2-Nanometer Carbon Nanotubes, Science. 312 (2006) 1034–1037.

[233] K. Koga, G.T. Gao, H. Tanaka, X.C. Zeng, Formation of ordered ice nanotubes inside carbon nanotubes, Nature. 412 (2001) 802–805.

[234] D. Tasis, N. Tagmatarchis, A. Bianco, M. Prato, Chemistry of Carbon Nanotubes, Chemical Reviews. 106 (2006) 1105–1136.

[235] S. Chen, G. Wu, M. Sha, S. Huang, Transition of Ionic Liquid [bmim][PF6] from Liquid to High-Melting-Point Crystal When Confined in Multiwalled Carbon Nanotubes, Journal of the American Chemical Society. 129 (2007) 2416–2417.

[236] Z. Su, S. Zhu, A.D. Donkor, C. Tzoganakis, J.F. Honek, Controllable Delivery of Small-Molecule Compounds to Targeted Cells Utilizing Carbon Nanotubes, Journal of the American Chemical Society. 133 (2011) 6874–6877.

[237] V. Sharma, K. Park, M. Srinivasarao, Colloidal dispersion of gold nanorods: Historical background, optical properties, seed-mediated synthesis, shape separation and self-assembly, Materials Science and Engineering R: Reports. 65 (2009) 1–38.

[238] X. Huang, X. Zhou, S. Wu, Y. Wei, X. Qi, J. Zhang, F. Boey, H. Zhang, Reduced graphene oxide-templated photochemical synthesis and in situ assembly of Au nanodots to orderly patterned Au nanodot chains, Small. 6 (2010) 513–516.

[239] C. Fernández-Blanco, A. Colina, A. Heras, V. Ruiz, J. López-Palacios, Multipulse strategies for the electrosynthesis of gold nanoparticles studied by UV/Vis spectroelectrochemistry, Electrochemistry Communications. 18 (2012) 8–11.

[240] A. Gedanken, Using sonochemistry for the fabrication of nanomaterials, Ultrasonics Sonochemistry. 11 (2004) 47–55.

[241] Y. Sun, Direct growth of dense, pristine metal nanoplates with well-controlled dimensions on semiconductor substrates, Chemistry of Materials. 19 (2007) 5845–5847.

[242] M. Frank, M. Baumer, From atoms to crystallites: Adsorption on oxide-supported metal particles, Physical Chemistry Chemical Physics. 2 (2000) 3723–3737.

[243] B.D. Du, D. V Phu, N.N. Duy, N.T.K. Lan, V.T.K. Lang, N.V.K. Thanh, N.T.P. Phong, N.Q. Hien, Preparation of colloidal silver nanoparticles in poly(N-vinylpyrrolidone) by γ-irradiation, Journal of Experimental Nanoscience. 3 (2008) 207–213.

[244] R. Narayanan, M.A. El-Sayed, Catalysis with transition metal nanoparticles in colloidal solution: Nanoparticle shape dependence and stability, Journal of Physical Chemistry B. 109 (2005) 12663–12676.

[245] A.M. Boies, J.T. Roberts, S.L. Girshick, B. Zhang, T. Nakamura, A. Mochizuki, SiO_2 coating of silver nanoparticles by photoinduced chemical vapor deposition, Nanotechnology. 20 (2009) 295604.

[246] M. Tsuji, M. Hashimoto, Y. Nishizawa, M. Kubokawa, T. Tsuji, Microwave-assisted synthesis of metallic nanostructures in solution, Chemistry - A European Journal. 11 (2005) 440–452.

[247] I.D.G. Macdonald, W.E. Smith, Orientation of cytochrome c adsorbed on a citrate-reduced silver colloid surface, Langmuir. 12 (1996) 706–713.

[248] N. Saifuddin, C.W. Wong, A.A.N. Yasumira, Rapid biosynthesis of silver nanoparticles using culture supernatant of bacteria with microwave irradiation, E-Journal of Chemistry. 6 (2009) 61–70.

[249] A.R. Vilchis-Nestor, V. Sánchez-Mendieta, M.A. Camacho-López, R.M. Gómez-Espinosa, M.A. Camacho-López, J.A. Arenas-Alatorre, Solventless synthesis and optical properties of Au and Ag nanoparticles using Camellia sinensis extract, Materials Letters. 62 (2008) 3103–3105.

[250] G. Goire, Electro-deposition of aluminium and silicium, Journal of the Franklin Institute. 57 (1854) 353–354.

[251] No author name available, Electro-deposition of iron, Journal of the Franklin Institute. 98 (1874) 299–301.

[252] W.H. Wahl, On the electro-deposition of platinum, Journal of the Franklin Institute. 130 (1890) 62–75.

[253] W.L. Dudley, The electro-deposition of iridium; a method of maintaining the uniform composition of an electroplating bath without the use of an anode., Journal of the American Chemical Society. 15 (1893) 274–276.

[254] O.W. Brown, F.C. Mathers, Electrodeposition of Copper upon Iron, Journal of Physical Chemistry. 10 (1905) 39–51.

[255] F.M. Perkin, W.E. Hughes, Studies on the electrodeposition of metals, Transactions of the Faraday Society. 6 (1910) 14–17.

[256] A. Martínez, Síntesis electroquímica y caracterización de nanopartículas metálicas mediante técnicas multirrespuesta, University of Burgos, 2011.

[257] B.J. Hwang, R. Santhanam, Y.-L. Lin, Nucleation and growth mechanism of electropolymerization of polypyrrole on gold/highly oriented pyrolytic graphite electrode, Journal of the Electrochemical Society. 147 (2000) 2252–2257.

[258] T.K. Sau, A.L. Rogach, F. Jäckel, T.A. Klar, J. Feldmann, Properties and applications of colloidal nonspherical noble metal nanoparticles, Advanced Materials. 22 (2010) 1805–1825.

[259] M.A. Sanchez-Castillo, C. Couto, W.B. Kim, J.A. Dumesic, Gold-nanotube membranes for the oxidation of CO at gas-water interfaces, Angewandte Chemie - International Edition. 43 (2004) 1140–1142.

[260] N. Tian, Z.-Y. Zhou, S.-G. Sun, Y. Ding, L.W. Zhong, Synthesis of tetrahexahedral platinum nanocrystals with high-index facets and high electro-oxidation activity, Science. 316 (2007) 732–735.

[261] M.D. Hughes, Y.-J. Xu, P. Jenkins, P. McMorn, P. Landon, D.I. Enache, A.F. Carley, G.A. Attard, G.J. Hutchings, F. King, E.H. Stitt, P. Johnston, K. Griffin, C.J. Kiely, Tunable gold catalysts for selective hydrocarbon oxidation under mild conditions, Nature. 437 (2005) 1132–1135.

[262] P. Li, Z. Wei, T. Wu, Q. Peng, Y. Li, Au-ZnO hybrid nanopyramids and their photocatalytic properties, Journal of the American Chemical Society. 133 (2011) 5660–5663.

[263] C.C. Mayorga-Martinez, M. Guix, R.E. Madrid, A. Merkoi, Bimetallic nanowires as electrocatalysts for nonenzymatic real-time impedancimetric detection of glucose, Chemical Communications. 48 (2012) 1686–1688.

[264] X. Cui, C. Zhang, F. Shi, Y. Deng, Au/Ag-Mo nano-rods catalyzed reductive coupling of nitrobenzenes and alcohols using glycerol as the hydrogen source, Chemical Communications. 48 (2012) 9391–9393.

[265] Y. Yu, K. Kant, J.G. Shapter, J. Addai-Mensah, D. Losic, Gold nanotube membranes have catalytic properties, Microporous and Mesoporous Materials. 153 (2012) 131–136.

[266] E.L. Somin, D.Y. Sasaki, T.D. Perroud, D. Yoo, K.D. Patel, L.P. Lee, Biologically functional cationic phospholipid-gold nanoplasmonic carriers of RNA, Journal of the American Chemical Society. 131 (2009) 14066–14074.

[267] C. Zheng, L. Liang, S. Xu, H. Zhang, C. Hu, L. Bi, Z. Fan, B. Han, W. Xu, The use of Au@SiO_2 shell-isolated nanoparticle-enhanced Raman spectroscopy for human breast cancer detection, Analytical and Bioanalytical Chemistry. 406 (2014) 5425–5432.

[268] J. You, R. Zhang, G. Zhang, M. Zhong, Y. Liu, C.S. Van Pelt, D. Liang, W. Wei, A.K. Sood, C. Li, Photothermal-chemotherapy with doxorubicin-loaded hollow gold nanospheres: A platform for near-infrared light-trigged drug release, Journal of Controlled Release. 158 (2012) 319–328.

[269] Y. Horiguchi, T. Niidome, S. Yamada, N. Nakashima, Y. Niidome, Expression of plasmid DNA released from DNA conjugates of gold nanorods, Chemistry Letters. 36 (2007) 952–953.

[270] R.L. Edelstein, C.R. Tamanaha, P.E. Sheehan, M.M. Miller, D.R. Baselt, L.J. Whitman, R.J. Colton, The BARC biosensor applied to the detection of biological warfare agents, Biosensors and Bioelectronics. 14 (2000) 805–813.

[271] J.-M. Nam, C.S. Thaxton, C.A. Mirkin, Nanoparticle-based bio-bar codes for the ultrasensitive detection of proteins, Science. 301 (2003) 1884–1886.

[272] T. Donnelly, W.E. Smith, K. Faulds, D. Graham, Silver and magnetic nanoparticles for sensitive DNA detection by SERS, Chemical Communications. 50 (2014) 12907–12910.

[273] C.J. Murphy, A.M. Gole, S.E. Hunyadi, J.W. Stone, P.N. Sisco, A. Alkilany, B.E. Kinard, P. Hankins, Chemical sensing and imaging with metallic nanorods, Chemical Communications. 8 (2008) 544–557.

[274] E.T. Castellana, R.C. Gamez, D.H. Russell, Label-free biosensing with lipid-functionalized gold nanorods, Journal of the American Chemical Society. 133 (2011) 4182–4185.

[275] M.-C. Daniel, J. Ruiz, S. Nlate, J.-C. Blais, D. Astruc, Nanoscopic assemblies between supramolecular redox active metallodendrons and gold nanoparticles: Synthesis, characterization, and selective recognition of $H_2PO_4^-$, HSO_4^-, and adenosine-5′-triphosphate (ATP^{2-}) anions, Journal of the American Chemical Society. 125 (2003) 2617–2628.

[276] J.H. Jung, G.B. Hwang, J.E. Lee, G.N. Bae, Preparation of airborne Ag/CNT hybrid nanoparticles using an aerosol process and their application to antimicrobial air filtration, Langmuir. 27 (2011) 10256–10264.

[277] I. Yakub, W.O. Soboyejo, Adhesion of E. coli to silver- or copper-coated porous clay ceramic surfaces, Journal of Applied Physics. 111 (2012) 124324.

[278] L. Mpenyana-Monyatsi, N.H. Mthombeni, M.S. Onyango, M.N.B. Momba, Cost-effective filter materials coated with silver nanoparticles for the removal of pathogenic bacteria in groundwater, International Journal of Environmental Research and Public Health. 9 (2012) 244–271.

[279] Z. Sheng, Y. Liu, Effects of silver nanoparticles on wastewater biofilms, Water Research. 45 (2011) 6039–6050.

[280] A. Kumar, P.K. Vemula, P.M. Ajayan, G. John, Silver-nanoparticle-embedded antimicrobial paints based on vegetable oil, Nature Materials. 7 (2008) 236–241.

[281] A.I. Freeman, L.J. Halladay, P. Cripps, The effect of silver impregnation of surgical scrub suits on surface bacterial contamination, Veterinary Journal. 192 (2012) 489–493.

[282] R. Gottesman, S. Shukla, N. Perkas, L.A. Solovyov, Y. Nitzan, A. Gedanken, Sonochemical coating of paper by microbiocidal silver nanoparticles, Langmuir. 27 (2011) 720–726.

[283] C.-H. Kim, S.-H. Cha, S.C. Kim, M. Song, J. Lee, W.S. Shin, S.-J. Moon, N.A. Kotov, S.-H. Jin, Silver nanowire embedded in P3HT:PCBM for high-efficiency hybrid photovoltaic device applications, ACS Nano. 5 (2011) 3319–3325.

[284] P. Poizot, S. Laruelle, S. Grugeon, L. Dupont, J.-M. Tarascon, Nano-sized transition-metal oxides as negative-electrode materials for lithium-ion batteries, Nature. 407 (2000) 496–499.

[285] J. Zhang, K. Sasaki, E. Sutter, R.R. Adzic, Stabilization of platinum oxygen-reduction electrocatalysts using gold clusters, Science. 315 (2007) 220–222.

[286] C.K. Hong, Y.H. Jung, H.J. Kim, K.H. Park, Electrochemical properties of TiO_2 nanoparticle/nanorod composite photoanode for dye-sensitized solar cells, Current Applied Physics. 14 (2014) 294–299.

[287] J.-S. Lee, J. Cho, C. Lee, I. Kim, J. Park, Y.-M. Kim, H. Shin, J. Lee, F. Caruso, Layer-by-layer assembled charge-trap memory devices with adjustable electronic properties, Nature Nanotechnology. 2 (2007) 790–795.

[288] E. Kolb, C. Kummerlöwe, M. Klare, Characterization of a nanoparticle-filled resin for application in scan-LED-technology, Journal of Materials Science: Materials in Medicine. 22 (2011) 2165–2173.

[289] V. Balzani, Photochemical molecular devices, Photochemical and Photobiological Sciences. 2 (2003) 459–476.

[290] Q. Guo, D. Liu, X. Zhang, L. Li, H. Hou, O. Niwa, T. You, Pd-Ni alloy nanoparticle/carbon nanofiber composites: Preparation, structure, and superior electrocatalytic properties for sugar analysis, Analytical Chemistry. 86 (2014) 5898–5905.

[291] D. Liu, Q. Guo, H. Hou, O. Niwa, T. You, Pd_xCo_Y nanoparticle/carbon nanofiber composites with enhanced electrocatalytic properties, ACS Catalysis. 4 (2014) 1825–1829.

[292] S. Amemiya, X. Yang, T.L. Wazenegger, Voltammetry of the phase transfer of polypeptide protamines across polarized liquid/liquid interfaces, Journal of the American Chemical Society. 125 (2003) 11832–11833.

[293] T. Spătaru, N. Spătaru, N. Bonciocat, C. Luca, Potentiometric investigation of the effect of the pH on the ionic transfer of some amino acids at the interface between two immiscible electrolyte solutions, Bioelectrochemistry. 62 (2004) 67–71.

[294] H.A. Santos, V. García-Morales, C.M. Pereira, Electrochemical Properties of Phospholipid Monolayers at Liquid-Liquid Interfaces, ChemPhysChem. 11 (2010) 28–41.

[295] S. O'Sullivan, D.W.M. Arrigan, Electrochemical behaviour of myoglobin at an array of microscopic liquid-liquid interfaces, Electrochimica Acta. 77 (2012) 71–76.

[296] H. Alemu, Voltammetry of drugs at the interface between two immiscible electrolyte solutions, Pure and Applied Chemistry. 76 (2004) 697–705.

[297] R. Gulaboski, M.N.D.S. Cordeiro, N. Milhazes, J. Garrido, F. Borges, M. Jorge, C.M. Pereira, I. Bogeski, A.H. Morales, B. Naumoski, A.F. Silva, Evaluation of the lipophilic properties of opioids, amphetamine-like drugs, and metabolites through electrochemical studies at the interface between two immiscible solutions, Analytical Biochemistry. 361 (2007) 236–243.

[298] V. Gobry, S. Ulmeanu, F. Reymond, G. Bouchard, P.-A. Carrupt, B. Testa, H.H. Girault, Generalization of ionic partition diagrams to lipophilic compounds and to biphasic systems with variable phase volume ratios, Journal of the American Chemical Society. 123 (2001) 10684–10690.

[299] Y. Shao, M. V Mirkin, J.F. Rusling, Liquid/liquid interface as a model system for studying electrochemical catalysis in microemulsions. Reduction of trans-1,2-dibromocyclohexane with vitamin B12, Journal of Physical Chemistry B. 101 (1997) 3202–3208.

[300] C. Forssten, J. Strutwolf, D.E. Williams, Liquid-liquid interface electrochemistry applied to study of a two-phase permanganate oxidation, Electrochemistry Communications. 3 (2001) 619–623.

[301] A. Trojánek, J. Langmaier, Z. Samec, Electrocatalysis of the oxygen reduction at a polarised interface between two immiscible electrolyte solutions by electrochemically generated Pt particles, Electrochemistry Communications. 8 (2006) 475–481.

[302] A.N.J. Rodgers, S.G. Booth, R.A.W. Dryfe, Particle deposition and catalysis at the interface between two immiscible electrolyte solutions (ITIES): A mini-review, Electrochemistry Communications. 47 (2014) 17–20.

[303] J. Guo, T. Tokimoto, R. Othman, P.R. Unwin, Formation of mesoscopic silver particles at micro- and nano-liquid/liquid interfaces, Electrochemistry Communications. 5 (2003) 1005–1010.

[304] M. Platt, R.A.W. Dryfe, E.P.L. Roberts, Structural and electrochemical characterisation of Pt and Pd nanoparticles electrodeposited at the liquid/liquid interface, Electrochimica Acta. 49 (2004) 3937–3945.

[305] A. Trojánek, J. Langmaier, Z. Samec, Random nucleation and growth of Pt nanoparticles at the polarised interface between two immiscible electrolyte solutions, Journal of Electroanalytical Chemistry. 599 (2007) 160–166.

[306] A. Uehara, T. Hashimoto, R.A.W. Dryfe, Au electrodeposition at the liquid-liquid interface: Mechanistic aspects, Electrochimica Acta. 118 (2014) 26–32.

[307] L. Basáez, P. Vanýsek, Transport studies of β-lactam antibiotics and their degradation products across electrified water/oil interface, Journal of Pharmaceutical and Biomedical Analysis. 19 (1999) 183–192.

[308] Z. Hongying, X. Xiangzhu, L. Peibiao, Application of Fourier transform to four-electrode microvoltammetric system for studies on micro-ITIES electroanalysis, Analytica Chimica Acta. 382 (1999) 137–144.

[309] B. Hundhammer, T. Solomon, T. Zerihun, M. Abegaz, A. Bekele, M. Graichen, Investigation of ion transfer across the membrane-stabilized interface of two immiscible electrolyte solutions. Part III. Facilitated ion transfer, Journal of Electroanalytical Chemistry. 371 (1994) 1–11.

[310] W. Nerst, E.H. Riesenfeld, Ueber elektrolytische Erscheinungen an der Grenzfläche zweier Lösungsmittel, Annalen Der Physik. 313 (1902) 600–608.

[311] E.J. Verwey, K.F. Niessen, First theorical study, Phylos. Mag. 28 (2014) 435–446.

[312] F.M. Karpfen, J.E.B. Randles, Ionic equilibria and phase-boundary potentials in oil-water systems, Transactions of the Faraday Society. 49 (1953) 823–831.

[313] C. Gavach, T. Mlodnicka, J.C.R. Gustalla, Galvani potential difference, Academy of Science. 266 (1968) 1196–1199.

[314] Z. Samec, V. Mareček, J. Koryta, M.W. Khalil, Investigation of ion transfer across the interface between two immiscible electrolyte solutions by cyclic voltammetry, Journal of Electroanalytical Chemistry. 83 (1977) 393–397.

[315] Z. Samec, Charge transfer between two immiscible electrolyte solutions. Part I. Basic equation for the rate of the charge transfer across the interface, Journal of Electroanalytical Chemistry. 99 (1979) 197–205.

[316] Z. Samec, V. Mareček, J. Weber, Charge transfer between two immiscible electrolyte solutions. Part IV. Electron transfer between hexacyanoferrate(III) in water and ferrocene in nitrobenzene investigated by cyclic voltammetry with four-electrode system, Journal of Electroanalytical Chemistry. 103 (1979) 11–18.

[317] Z. Samec, V. Mareček, J. Weber, Detection of an electron transfer across the interface between two immiscible electrolyte solutions by cyclic voltammetry with four-electrode system, Journal of Electroanalytical Chemistry. 96 (1979) 245–247.

[318] C. Johans, K. Kontturi, D.J. Schiffrin, Nucleation at liquid|liquid interfaces: galvanostatic study, Journal of Electroanalytical Chemistry. 526 (2002) 29–35.

[319] Y. Gründer, H.L.T. Ho, J.F.W. Mosselmans, S.L.M. Schroeder, R.A.W. Dryfe, Inhibited and enhanced nucleation of gold nanoparticles at the water|1,2-dichloroethane interface., Physical Chemistry Chemical Physics. 13 (2011) 15681–15689.

[320] S. Fantini, J. Clohessy, K. Gorgy, F. Fusalba, C. Johans, Influence of the presence of a gel in the water phase on the electrochemical transfer of ionic forms of B-blockers across a large water|1,2-dichloroethane interface, 18 (2003) 251–257.

[321] B. Sefer, R. Gulaboski, V. Mirčeski, Electrochemical deposition of gold at liquid–liquid interfaces studied by thin organic film-modified electrodes, Journal of Solid State Electrochemistry. 16 (2011) 2373–2381.

[322] V. Mareček, Z. Samec, Determination of calcium, barium and strontium ions by differential pulse stripping voltammetry at a hanging electrolyte drop electrode, Analytica Chimica Acta. 151 (1983) 265–269.

[323] B. Hundhammer, T. Solomon, H. Alemu, Investigation of the ion transfer across the water-nitrobenzene interface by ac cyclic voltammetry, Journal of Electroanalytical Chemistry. 149 (1983) 179–183.

[324] T. Kakutani, T. Osakai, M. Senda, Potential-step chronoamperometric study of ion transfer at the water/nitrobenzene interface., Bulletin of the Chemical Society of Japan. 56 (1983) 991–996.

[325] D. Homolka, V. Mareček, Charge transfer between two immiscible electrolyte solutions. Part VI. Polarographic and voltammetric study of picrate ion transfer across the water/nitrobenzene interface, Journal of Electroanalytical Chemistry. 112 (1980) 91–96.

[326] T. Osakai, T. Kakutani, M. Senda, A. C. polarographic study of ion transfer at the water/nitrobenzene interface, Bulletin of the Chemical Society of Japan. 57 (1984) 370–376.

[327] Z. Samec, V. Mareček, J. Weber, D. Homolka, Charge transfer between two immiscible electrolyte solutions. Part VII. Convolution potential sweep voltammetry of Cs^+ ion transfer and of electron transfer between ferrocene and hexacyanoferrate (III) ion across the water/nitrobenzen interface, Journal of Electroanalytical Chemistry. 126 (1981) 105–119.

[328] P.D. Beattie, A. Delay, H.H. Girault, Investigation of the kinetics of ion and assisted ion transfer by the technique of ac impedance of the micro-ities, Electrochimica Acta. 40 (1995) 2961–2969.

[329] A. Martínez, A. Colina, R.A.W. Dryfe, V. Ruiz, Spectroelectrochemistry at the liquid|liquid interface: Parallel beam UV–Vis absorption, Electrochimica Acta. 54 (2009) 5071–5076.

[330] S.E.C. Dale, P.R. Unwin, Polarised liquid/liquid micro-interfaces move during charge transfer, Electrochemistry Communications. 10 (2008) 723–726.

[331] Y. Cheng, D.J. Schifiin, D.J. Schiffrin, Electrodeposition of metallic gold clusters at the water/1,2-dichloroethane interface, Journal of the Chemical Society, Faraday Transactions. 92 (1996) 3865–3871.

[332] T. Osakai, H. Jensen, H. Nagatani, D.J. Fermin, Mechanistic aspects associated with the oxidation of L-ascorbic acid at the 1,2-dichloroethane water interface, Journal of Electroanalytical Chemistry. 510 (2001) 43–49.

[333] B. Kralj, R.A.W. Dryfe, Hydrodynamic voltammetry at the liquid|liquid interface: facilitated ion transfer and the rotating diffusion cell, Journal of Electroanalytical Chemistry. 560 (2003) 127–133.

[334] S.G. Booth, D.P. Cowcher, R. Goodacre, R.A.W. Dryfe, Electrochemical modulation of SERS at the liquid/liquid interface., Chemical Communications. 50 (2014) 4482–4484.

[335] J.M. Perera, G.W. Stevens, Spectroscopic studies of molecular interaction at the liquid-liquid interface., Analytical and Bioanalytical Chemistry. 395 (2009) 1019–1032.

[336] D.M. Mitrinovic, Z. Zhang, S.M. Williams, Z. Huang, M.L. Schlossman, X-ray reflectivity study of the water-hexane interface, Journal of Physical Chemistry B. 103 (1999) 1781–1782.

[337] A.M. Tikhonov, D.M. Mitrinovic, M. Li, Z. Huang, M.L. Schlossman, An X-ray Reflectivity Study of the Water-Docosane Interface, Journal of Physical Chemistry B. 104 (2000) 6336–6339.

[338] J. Strutwolf, A.L. Barker, M. Gonsalves, D.J. Caruana, P.R. Unwin, D.E. Williams, J.R.P Webster, Liquid interfaces using neutron reflection measurements and scanning electrochemical microscopy, Journal of Electroanalytical Chemistry. 483 (2000) 163–173.

[339] A. Trojánek, P. Krtil, Z. Samec, Quasi-elastic laser light scattering from thermally excited capillary waves on the polarised water/1,2-dichloroethane interface, Electrochemistry Communications. 3 (2001) 613–618.

[340] A.A.T. Luca, P. Hebert, P.F. Brevet, H.H. Girault, Surface second-harmonic generation at air/solvent and solvent/solvent interfaces, Journal of the Chemical Society, Faraday Transactions. 91 (1995) 1763–1768.

[341] M.J. Crawford, J.G. Frey, T.J. VanderNoot, Y. Zhao, Investigation of transport across an immiscible liquid/liquid interface. Electrochemical and second harmonic generation studies, Journal of the Chemical Society, Faraday Transactions. 92 (1996) 1369–1373.

[342] J.C. Conboy, G.L. Richmond, Examination of the electrochemical interface between two immiscible electrolyte solutions by second harmonic generation, Journal of Physical Chemistry B. 101 (1997) 983–990.

[343] Q. Du, E. Freysz, Y.R. Shen, Surface vibrational spectroscopic studies of hydrogen bonding and hydrophobicity, Science. 264 (1994) 826–828.

[344] L.F. Scatena, M.G. Brown, G.L. Richmond, Water at hydrophobic surfaces: Weak hydrogen bonding and strong orientation effects, Science. 292 (2001) 908–912.

[345] G.L. Richmond, Structure and bonding of molecules at aqueous surfaces, Annual Review of Physical Chemistry. 52 (2001) 357–389.

[346] D. Michael, I. Benjamin, Molecular dynamics computer simulations of solvation dynamics at liquid/liquid interfaces, Journal of Chemical Physics. 114 (2001) 2817–2824.

[347] K. Schweighofer, I. Benjamin, Ion pairing and dissociation at liquid/liquid interfaces: Molecular dynamics and continuum models, Journal of Chemical Physics. 112 (2000) 1474–1482.

[348] I. Benjamin, Mechanism and dynamics of ion transfer across a liquid-liquid interface, Science. 261 (1993) 1558–1560.

[349] D. Michael, I. Benjamin, Molecular dynamics simulation of the water|nitrobenzene interface, Journal of Electroanalytical Chemistry. 450 (1998) 335–345.

[350] F. Reymond, D. Fermin, H.J. Lee, H.H. Girault, Electrochemistry at liquid/liquid interfaces : methodology and potential applications, Electrochimica Acta. 45 (2000) 2647–2662.

[351] Z. Samec, A.R. Brown, L.J. Yellowlees, H.H. Girault, K. Basě, Photochemical ion transfer across the interface between two immiscible electrolyte solutions, Journal of Electroanalytical Chemistry. 259 (1989) 309–313.

[352] S.N. Faisal, C.M. Pereira, S. Rho, H.J. Lee, Amperometric proton selective sensors utilizing ion transfer reactions across a microhole liquid/gel interface., Physical Chemistry Chemical Physics. 12 (2010) 15184–15189.

[353] Y. Shao, S.N. Tan, V. Devaud, H.H. Girault, Ion transfer facilitated by the neutral carrier N,N,-dicyclohexyl-N′,N′-diisobutyl-cis-cyclohexane-1,2-dicarboxamide across the water/1,2-dichloroethane interface, Journal of the Chemical Society, Faraday Transactions. 89 (1993) 4307–4312.

[354] Z. Ding, R.G. Wellington, P.-F. Brevet, H.H. Girault, Differential cyclic voltabsorptometry and chronoabsorptometry studies of ion transfer reactions at the water, Journal of Electroanalytical Chemistry. 420 (1997) 35–41.

[355] A.V. Juárez, A.M. Baruzzi, L.M. Yudi, Ohmic drop effects in square-wave voltammetry response for an ion transfer process at a liquid–liquid interface, Journal of Electroanalytical Chemistry. 577 (2005) 281–286.

[356] A. Manzanares, D.E. Williams, Effect of self-assembled surfactant structures on ion transport across the liquid|liquid interface, 1 (1999) 139–144.

[357] J.A. Manzanares, R. Lahtinen, B. Quinn, K. Kontturi, D.J. Schiffrin, Determination of rate constants of ion transfer kinetics across immiscible electrolyte solutions, Electrochimica Acta. 44 (1998) 59–71.

[358] H.J. Lee, G. Lagger, C.M. Pereira, A.F. Silva, H.H. Girault, Amperometric tape ion sensors for cadmium(II) ion analysis., Talanta. 78 (2009) 66–70.

[359] L.M. Yudi, Voltammetric analysis of lipophilicity of benzodiazepine derivatives at the water 1,2-dichloroethane interface, 495 (2001) 146–151.

[360] Y. Shao, M.D. Osborne, H.H. Girault, Assisted ion transfer at micro-ITIES of micropipettes supported at the tip, Journal of Electroanalytical Chemistry. 318 (1992) 101–109.

[361] H.H.J. Girault, D.J. Schiffrin, Electron transfer reactions at the interface between two immiscible electrolyte solutions, Journal of Electroanalytical Chemistry. 244 (1988) 15–26.

[362] R.A. Marcus, On the Theory of Electron-Transfer Reactions. VI. Unified Treatment for Homogeneous and Electrode Reactions, Journal of Chemical Physics. 43 (1965) 679–701.

[363] R. Dahm, Friedrich Miescher and the discovery of DNA, Developmental Biology. 278 (2005) 274–288.

[364] F. Miescher, Ueber die chemische Zusammensetzung der Eiterzellen, Medizinisch-Chemische Untersuchungen. 4 (1871) 441–460.

[365] J.D. Watson, F.H.C. Crick, Molecular structure of nucleic acids: A structure for deoxyribose nucleic acid, Nature. 171 (1953) 737–738.

[366] M. Valko, M. Izakovic, M. Mazur, C.J. Rhodes, J. Telser, Role of oxygen radicals in DNA damage and cancer incidence, Molecular and Cellular Biochemistry. 266 (2004) 37–56.

[367] B.N. Ames, Endogenous oxidative DNA damage, aging, and cancer, Free Radical Research. 7 (1989) 121–128.

[368] J.-W. Park, K.C. Cundy, B.N. Ames, Detection of DNA adducts by high-performance liquid chromatography with electrochemical detection, Carcinogenesis. 10 (1989) 827–832.

[369] J. Cadet, T. Douki, D. Gasparutto, J.-L. Ravanat, Oxidative damage to DNA: Formation, measurement and biochemical features, Mutation Research - Fundamental and Molecular Mechanisms of Mutagenesis. 531 (2003) 5–23.

[370] A. Oliveira-Brett, J.A. Piedade, L. Silva, V. Diculescu, Voltammetric determination of all DNA nucleotides., Analytical Biochemistry. 332 (2004) 321–329.

[371] E. Paleček, M. Bartošík, Electrochemistry of nucleic acids., Chemical Reviews. 112 (2012) 3427–3481.

[372] G. Dryhurst, Electrochemical determination of adenine and adenosine, Talanta. 19 (1972) 768–778.

[373] G. Dryhurst, Dicarbonium Ions as Products of Electrochemical Oxidation of Biologically Important Purines at the Pyrolytic Graphite Electrode, Journal of The Electrochemical Society. 116 (1969) 1411–1412.

[374] D.L. Jeanmaire, M.R. Suchanski, R.P. Van Duyne, Resonance Raman spectroelectrochemistry. I. The tetracyanoethylene anion radical, Journal of the American Chemical Society. 97 (1975) 1699–1707.

[375] D.L. Jeanmaire, R.P. Van Duyne, Resonance Raman spectroelectrochemistry V. Intensity transients on the millisecond time scale following double potential step initiation of a diffusion controlled electrode reaction, Journal of Electroanalytical Chemistry. 66 (1975) 235–247.

[376] D.L. Jeanmaire, R.P. Van Duyne, Resonance Raman spectroelectrochemistry. II. Scattering spectroscopy accompanying excitation of the lowest2B1u excited state of the tetracyanoquinodimethane anion radical, Journal of the American Chemical Society. 98 (1976) 4029–4033.

[377] M.R. Suchanski, R.P. Van Duyne, Resonance Raman spectroelectrochemistry. IV. The oxygen decay chemistry of the tetracyanoquinodimethane dianion, Journal of the American Chemical Society. 98 (1976) 250–252.

[378] D.L. Jeanmaire, R.P. Van Duyne, Resonance Raman spectroelectrochemistry. III. Tunable dye laser excitation spectroscopy of the lowest2B1u excited state of the tetracyanoquinodimethane anion radical, Journal of the American Chemical Society. 98 (1976) 4034–4039.

[379] J.E. Pemberton, R.P. Buck, Rotating disk cell for Raman spectroelectrochemistry: investigation of an electrode surface species and an electrogenerated solution species., Applied Spectroscopy. 35 (1981) 571–576.

[380] J.E. Pemberton, R.P. Buck, Dithizone adsorption at metal electrodes. 2. Raman spectroelectrochemical investigation of effect of applied potential at a silver electrode, Journal of Physical Chemistry. 85 (1981) 248–262.

[381] J.E. Pemberton, R.P. Buck, Dithizone adsorption at metal electrodes. Part VII. Preliminary characterization of adsorption kinetics using surface Raman spectroelectrochemistry at a rotating disk silver electrode, Journal of Electroanalytical Chemistry. 136 (1982) 201–208.

[382] J.E. Pemberton, R.P. Buck, Dithizone adsorption at metal electrodes. 4. Voltammetric and surface Raman spectroelectrochemical investigation at a copper electrode, Journal of the American Chemical Society. 104 (1982) 4076–4084.

[383] J.E. Pemberton, R.P. Buck, Dithizone adsorption at metal electrodes. 5. Voltammetric and surface raman spectroelectrochemical investigation at a gold electrode, Journal of Physical Chemistry. 87 (1983) 3336–3343.

[384] J. Xu, R.L. Birke, J.R. Lombardi, Surface-enhanced Raman spectroscopy from flavins adsorbed on a silver electrode: Observation of the unstable semiquinone intermediate, Journal of the American Chemical Society. 109 (1987) 5645–5649.

[385] C. Shi, W. Zhang, R.L. Birke, J.R. Lombardi, Detection of short-lived intermediates in electrochemical reactions using time-resolved surface-enhanced Raman spectroscopy, Journal of Physical Chemistry. 94 (1990) 4766–4769.

[386] C. Shi, W. Zhang, R.L. Birke, J.R. Lombardi, SERS investigation of the adsorption and electroreduction of 4-cyanopyridine on a silver electrode, Journal of Electroanalytical Chemistry. 423 (1997) 67–81.

[387] R.L. Birke, C. Shi, W. Zhang, J.R. Lombardi, A time-resolved SERS study of the adsorption and electrochemical reduction of 4-pyridinecarboxaldehyde and 4-(hydroxymethyl)pyridine, Journal of Physical Chemistry B. 102 (1998) 7983–7996.

[388] M. Wang, T. Spataru, J.R. Lombardi, R.L. Birke, Time resolved surface enhanced Raman scattering studies of 3-hydroxyflavone on a Ag electrode, Journal of Physical Chemistry C. 111 (2007) 3044–3052.

[389] M.J. Weaver, Surface-enhanced Raman spectroscopy as a versatile in situ probe of chemisorption in catalytic electrochemical and gaseous environments, Journal of Raman Spectroscopy. 33 (2002) 309–317.

[390] S. Zou, C.T. Williams, E.K.-Y. Chen, M.J. Weaver, Surface-enhanced Raman scattering as a ubiquitous vibrational probe of transition-metal interfaces: Benzene and related chemisorbates on palladium and rhodium in aqueous solution, Journal of Physical Chemistry B. 102 (1998) 9039–9049.

[391] S. Farquharson, P.A. Lay, M.J. Weaver, Surface-enhanced Raman spectroscopy of pentaammineosmium (III)/(II) and pentaammineruthenium (II) containing pyridine, pyrazine or 4,4′-bipyridine ligands at silver electrodes: vibrational assignments, Spectrochimica Acta Part A: Molecular Spectroscopy. 40 (1984) 907–921.

[392] M.F. Mrozek, H. Luo, M.J. Weaver, Formic acid electrooxidation on platinum-group metals: Is adsorbed carbon monoxide solely a catalytic poison?, Langmuir. 16 (2000) 8463–8469.

[393] J.L. Yao, B. Ren, Z.F. Huang, P.G. Cao, R.A. Gu, Z.-Q. Tian, Extending surface Raman spectroscopy to transition metals for practical applications IV. A study on corrosion inhibition of benzotriazole on bare Fe electrodes, Electrochimica Acta. 48 (2003) 1263–1271.

[394] D.-Y. Wu, B. Ren, X. Xu, G.-K. Liu, Z.-L. Yang, Z.-Q. Tian, Periodic trends in the bonding and vibrational coupling: Pyridine interacting with transition metals and noble metals studied by surface-enhanced Raman spectroscopy and density-functional theory, Journal of Chemical Physics. 119 (2003) 1701–1709.

[395] Y. Zhao, X. Yang, J. Tian, Electrocatalytic oxidation of methanol at 2-aminophenoxazin-3-one-functionalized multiwalled carbon nanotubes supported PtRu nanoparticles, Electrochimica Acta. 54 (2009) 7114–7120.

[396] L. Cui, D.-Y. Wu, A. Wang, B. Ren, Z.-Q. Tian, Charge-Transfer Enhancement Involved in the SERS of Adenine on Rh and Pd Demonstrated by Ultraviolet to Visible Laser Excitation, Journal of Physical Chemistry C. 114 (2010) 16588–16595.

[397] T. Itoh, R.L. McCreery, In situ Raman spectroelectrochemistry of electron transfer between glassy carbon and a chemisorbed nitroazobenzene monolayer, Journal of the American Chemical Society. 124 (2002) 10894–10902.

[398] T. Itoh, R.L. McCreery, In situ Raman spectroelectrochemistry of azobenzene monolayers on glassy carbon, Analytical and Bioanalytical Chemistry. 388 (2007) 131–134.

[399] R.T. Packard, R.L. McCreery, Raman monitoring of reactive electrogenerated species: Kinetics of halide addition to o-quinones, Journal of Physical Chemistry. 92 (1988) 6345–6351.

[400] F.J. Vidal-Iglesias, J. Solla-Gullón, J.M. Pérez, A. Aldaz, Evidence by SERS of azide anion participation in ammonia electrooxidation in alkaline medium on nanostructured Pt electrodes, Electrochemistry Communications. 8 (2006) 102–106.

[401] J. Solla-Gullón, F.J. Vidal-Iglesias, J.M. Pérez, A. Aldaz, Alkylidynes-modified Pt nanoparticles: A spectroelectrochemical (SERS) and electrocatalytic study, Electrochimica Acta. 54 (2009) 6971–6977.

[402] L. Kavan, L. Dunsch, Ionic liquid for in situ Vis/NIR and Raman spectroelectrochemistry: Doping of carbon nanostructures., Chemphyschem : A European Journal of Chemical Physics and Physical Chemistry. 4 (2003) 944–950.

[403] L. Kavan, M. Kalbac, M. Zukalova, L. Dunsch, Optical and Raman spectroelectrochemistry of carbon nanostructures, in: Physics, Chemistry and Application of Nanostructures - Reviews and Short Notes to NANOMEETING 2005, 2005: pp. 55–61.

[404] M. Kalbáč, L. Kavan, L. Dunsch, Selective etching of thin single-walled carbon nanotubes, Journal of the American Chemical Society. 131 (2009) 4529–4534.

[405] L. Kavan, M. Kalbáč, M. Zukalová, M. Krause, L. Dunsch, Electrochemical doping of double-walled carbon nanotubes: An in situ Raman spectroelectrochemical study, ChemPhysChem. 5 (2004) 274–277.

[406] L. Kavan, L. Dunsch, Diameter-selective electrochemical doping of HiPco single-walled carbon nanotubes, Nano Letters. 3 (2003) 969–972.

[407] M. Kalbac, L. Kavan, L. Dunsch, M.S. Dresselhaus, Development of the Tangential Mode in the Raman Spectra of SWCNT Bundles during Electrochemical Charging, Nano Letters. 8 (2008) 1257–1264.

[408] M. Kalbáč, L. Kavan, M. Zukalová, L. Dunsch, An in situ Raman spectroelectrochemical study of the controlled doping of single walled carbon nanotubes in a conducting polymer matrix, Carbon. 45 (2007) 1463–1470.

[409] L. Kavan, M. Kalbáč, M. Zukalová, L. Dunsch, Electrochemical and chemical redox doping of fullerene (C60) peapods, Carbon. 44 (2006) 99–106.

[410] M. Kalbac, H. Farhat, J. Kong, P. Janda, L. Kavan, M.S. Dresselhaus, Raman spectroscopy and in situ Raman spectroelectrochemistry of bilayer 12C/13C graphene., Nano Letters. 11 (2011) 1957–1963.

[411] M. Bousa, O. Frank, L. Kavan, Progressive in situ reduction of graphene oxide studied by Raman spectroelectrochemistry: Implications for a spontaneous activation of $LiFePO_4$ (Olivine), Electroanalysis. 26 (2014) 57–61.

[412] R. Mažeikiene, A. Statino, Z. Kuodis, G. Niaura, A. Malinauskas, In situ Raman spectroelectrochemical study of self-doped polyaniline degradation kinetics, Electrochemistry Communications. 8 (2006) 1082–1086.

[413] A. Malinauskas, R. Holze, Deposition and characterisation of self-doped sulphoalkylated polyanilines, Electrochimica Acta. 43 (1998) 521–531.

[414] A. Malinauskas, M. Bron, R. Holze, Electrochemical and Raman spectroscopic studies of electrosynthesized copolymers and bilayer structures of polyaniline and poly(o-phenylenediamine), Synthetic Metals. 92 (1998) 127–137.

[415] R. Mažeikiene, G. Niaura, A. Malinauskas, In situ Raman spectroelectrochemical study of redox processes at poly(Toluidine blue) modified electrode, Electrochimica Acta. 53 (2008) 7736–7743.

[416] R. Mažeikiene, G. Niaura, A. Malinauskas, Raman spectroelectrochemical study of electrochemical decomposition of poly(neutral red) at a gold electrode, Journal of Colloid and Interface Science. 336 (2009) 195–199.

[417] A. Pron, G. Louarn, M. Lapkowski, M. Zagorska, J. Glowczyk-Zubek, S. Lefrant, "In situ" Raman spectroelectrochemical studies of poly(3,3′-dibutoxy-2,2′-bithiophene), Macromolecules. 28 (1995) 4644–4649.

[418] M. Trznadel, M. Zagórska, M. Lapkowski, G. Louarn, S. Lefrant, A. Pron, UV-VIS-NIR and Raman spectroelectrochemistry of regioregular poly(3-octylthiophene): Comparison

with its non-regioregular analogue, Journal of the Chemical Society - Faraday Transactions. 92 (1996) 1387–1393.

[419] C. Fernandez-Blanco, D. Ibañez, A. Colina, V. Ruiz, A. Heras, Spectroelectrochemical study of the electrosynthesis of Pt nanoparticles/poly(3,4-(ethylenedioxythiophene) composite, Electrochimica Acta. 145 (2014) 139–147.

[420] T. Kuwana, R.K. Darlington, D.W. Leedy, Electrochemical Studies Using Conducting Glass Indicator Electrodes., Analytical Chemistry. 36 (1964) 2023–2025.

[421] R.L. McCreery, Lasers for Raman Spectroscopy, in: Raman Spectroscopy for Chemical Analysis, John Wiley & Sons, Inc., 2000: pp. 127–148.

[422] J. Garoz-Ruiz, S. Palmero, D. Ibañez, A. Heras, A. Colina, Press-transfer optically transparent electrodes fabricated from commercial single-walled carbon nanotubes, Electrochemistry Communications. 25 (2012) 1–4.

[423] V. Marecek, Z. Samec, Electrolysis at the Interface Between Two Immiscible Electrolyte Solutions: Determination of Acetylcholine by Differential Pulse Stripping Voltammetry, Analytical Letters. 14 (1981) 1241–1253.

[424] D. Izquierdo, A. Martinez, A. Heras, J. Lopez-Palacios, V. Ruiz, R.A.W. Dryfe, A. Colina, Spatial scanning spectroelectrochemistry. Study of the electrodeposition of Pd nanoparticles at the liquid/liquid interface., Analytical Chemistry. 84 (2012) 5723–5730.

[425] H. Nagatani, R.A. Iglesias, D.J. Fermin, P.R Brevet, H.H. Girault, P.-F. Brevet, Adsorption behavior of charged zinc porphyrins at the water/1,2-dichloroethane interface studied by potential modulated fluorescence spectroscopy, Journal of Physical Chemistry B. 104 (2000) 6869–6876.

[426] Z. Ding, R.G. Wellington, P.F. Brevet, H.H. Girault, Spectroelectrochemical Studies of $Ru(bpy)_3^{2+}$ at the Water/1,2-Dichloroethane Interface, Journal of Physical Chemistry. 100 (1996) 10658–10663.

[427] H. Tanida, H. Nagatani, M. Harada, Development of the total-reflection XAFS method for the liquid-liquid interface, Journal of Physics: Conference Series. 83 (2007) 012019.

[428] R.D. Webster, R.A.W. Dryfe, B.A. Coles, R.G. Compton, In Situ Electrochemical EPR Studies of Charge Transfer across the Liquid/Liquid Interface, Analytical Chemistry. 70 (1998) 792–800.

[429] R.A.W. Dryfe, R.D. Webster, B.A. Coles, R.G. Compton, In situ EPR studies of electron transfer across a polarised liquid/liquid interface, Chemical Communications. (1997) 779–780.

[430] N. Rozlosnik, New directions in medical biosensors employing poly(3,4-ethylenedioxy thiophene) derivative-based electrodes, Analytical and Bioanalytical Chemistry. 395 (2009) 637–645.

[431] D. Hohnholz, H. Okuzaki, A.G. MacDiarmid, Plastic electronic devices through line patterning of conducting polymers, Advanced Functional Materials. 15 (2005) 51–56.

[432] A. Laforgue, All-textile flexible supercapacitors using electrospun poly(3,4-ethylenedioxythiophene) nanofibers, Journal of Power Sources. 196 (2011) 559–564.

[433] R. Liu, J. Duay, S.B. Lee, Redox exchange induced MnO_2 nanoparticle enrichment in poly(3,4-ethylenedioxythiophene) nanowires for electrochemical energy storage, ACS Nano. 4 (2010) 4299–4307.

[434] K.K. Tintula, A.K. Sahu, A. Shahid, S. Pitchumani, P. Sridhar, A.K. Shukla, Mesoporous carbon and poly(3,4-ethylenedioxythiophene) composite as catalyst support for polymer electrolyte fuel cells, Journal of the Electrochemical Society. 157 (2010) B1679–B1685.

[435] W. Feng, Y. Li, J. Wu, H. Noda, A. Fujii, M. Ozaki, K. Yoshino, Improved electrical and optical properties of Poly(3,4- ethylenedioxythiophene) via ordered microstructure, Journal of Physics Condensed Matter. 19 (2007) 186220.

[436] M. Lefebvre, Z. Qi, D. Rana, P.G. Pickup, Chemical synthesis, characterization, and electrochemical studies of poly(3,4-ethylenedioxythiophene)/ Poly(styrene-4-sulfonate) composites, Chemistry of Materials. 11 (1999) 262–268.

[437] L. Groenendaal, G. Zotti, P.-H. Aubert, S.M. Waybright, J.R. Reynolds, Electrochemistry of poly(3,4-alkylenedioxythiophene) derivatives, Advanced Materials. 15 (2003) 855–879.

[438] L. Pigani, A. Heras, A. Colina, R. Seeber, J. López-Palacios, Electropolymerisation of 3,4-ethylenedioxythiophene in aqueous solutions, Electrochemistry Communications. 6 (2004) 1192–1198.

[439] E. Ventosa, A. Colina, A. Heras, A. Martínez, O. Orcajo, V. Ruiz, J. Lopez-Palacios, Electrochemical, spectroscopic and electrogravimetric detection of oligomers occluded in electrochemically synthesized poly(3,4-ethylenedioxythiophene) films, Electrochimica Acta. 53 (2008) 4219–4227.

[440] Z.-Q. Feng, J. Wu, W. Cho, M.K. Leach, E.W. Franz, Y.I. Naim, Z.-Z. Gu, J.M. Corey, D.C. Martin, Highly aligned poly(3,4-ethylene dioxythiophene) (PEDOT) nano- and microscale fibers and tubes, Polymer (United Kingdom). 54 (2013) 702–708.

[441] S. Garreau, G. Louarn, G. Froyer, M. Lapkowski, O. Chauvet, Spectroelectrochemical studies of the C14-alkyl derivative of poly(3,4-ethylenedioxythiophene) (PEDT), Electrochimica Acta. 46 (2001) 1207–1214.

[442] M. Lapkowski, A. Proń, Electrochemical oxidation of poly(3,4-ethylenedioxythiophene) - `in situ' conductivity and spectroscopic investigations, Synthetic Metals. 110 (2000) 79–83.

[443] F. Tran-Van, S. Garreau, G. Louarn, G. Froyer, C. Chevrot, Fully undoped and soluble oligo(3,4-ethylenedioxythiophene)s: Spectroscopic study and electrochemical characterization, Journal of Materials Chemistry. 11 (2001) 1378–1382.

[444] S. Garreau, G. Louarn, J.P. Buisson, G. Froyer, S. Lefrant, In situ spectroelectrochemical Raman studies of poly(3,4-ethylenedioxythiophene) (PEDT), Macromolecules. 32 (1999) 6807–6812.

[445] T. Amemiya, K. Hashimoto, A. Fujishima, K. Itoh, Analyses of spectroelectrochemical behavior of polypyrrole films using the Nernst equation. “Monomer unit model” and polaron/bipolaron model, Journal of the Electrochemical Society. 138 (1991) 2845–2850.

[446] P. Marque, J. Roncali, Structural effect on the redox thermodynamics of poly(thiophenes), Journal of Physical Chemistry. 94 (1990) 8614–8617.

[447] S. Majumdar, K. Kargupta, S. Ganguly, Mathematical modeling for the ionic inclusion process inside conducting polymer-based thin-films, Polymer Engineering and Science. 48 (2008) 2229–2237.

[448] S. Servagent, E. Vieil, In-situ quartz microbalance study of the electrosynthesis of poly(3-methylthiophene), Journal of Electroanalytical Chemistry. 280 (1990) 227–232.

[449] C.K. Baker, J.R. Reynolds, A quartz microbalance study of the electrosynthesis of polypyrrole, Journal of Electroanalytical Chemistry. 251 (1988) 307–322.

[450] I. Efimov, S. Winkels, J.W. Schultze, EQCM study of electropolymerization and redox cycling of 3,4-polyethylenedioxythiophene, Journal of Electroanalytical Chemistry. 499 (2001) 169–175.

[451] C. Nützenadel, Electrochemical Storage of Hydrogen in Nanotube Materials, Electrochemical and Solid-State Letters. 2 (1999) 30–32.

[452] R.H. Baughman, A.A. Zakhidov, W.A. de Heer, Carbon nanotubes-the route toward applications., Science. 297 (2002) 787–792.

[453] E. Katz, I. Willner, Biomolecule-functionalized carbon nanotubes: applications in nanobioelectronics., ChemPhysChem. 5 (2004) 1084–1104.

[454] F. Picó, J.M. Rojo, M.L. Sanjuán, A. Ansón, A.M. Benito, M.A. Callejas, W. K. Maser, M.T. Martínez, Single-Walled Carbon Nanotubes as Electrodes in Supercapacitors, Journal of The Electrochemical Society. 151 (2004) A831–A837.

[455] S. Ghosh, A.K. Sood, N. Kumar, Carbon nanotube flow sensors., Science. 299 (2003) 1042–1044.

[456] A. Bachtold, P. Hadley, T. Nakanishi, C. Dekker, Logic circuits with carbon nanotube transistors., Science. 294 (2001) 1317–1320.

[457] S.J. Tans, A.R.M. Verschueren, C. Dekker, Room-temperature transistor based on a single carbon nanotube, Nature. 672 (1998) 669–672.

[458] A. Star, E. Tu, J. Niemann, J.-C.P. Gabriel, C.S. Joiner, C. Valcke, Label-free detection of DNA hybridization using carbon nanotube network field-effect transistors., Proceedings of the National Academy of Sciences of the United States of America. 103 (2006) 921–926.

[459] S. Gupta, M. Hughes, A.H. Windle, J. Robertson, In situ Raman spectro-electrochemistry study of single-wall carbon nanotube mat, Diamond and Related Materials. 13 (2004) 1314–1321.

[460] A. Das, A. Sood, A. Govindaraj, A. Saitta, M. Lazzeri, F. Mauri, C. Rao, Doping in Carbon Nanotubes Probed by Raman and Transport Measurements, Physical Review Letters. 99 (2007) 1–4.

[461] M. Kalbac, L. Kavan, Evaluation of defect concentration in doped SWCNT, Physica Status Solidi (B) Basic Research. 247 (2010) 2797–2800.

[462] J. Chen, Solution Properties of Single-Walled Carbon Nanotubes, Science. 282 (1998) 95–98.

[463] L. Zhang, V. Liao, Z. Yu, Raman spectroelectrochemistry of a single-wall carbon nanotube bundle, Carbon. 48 (2010) 2582–2589.

[464] M. Kalbac, H. Farhat, L. Kavan, J. Kong, K.-I.K. Sasaki, R. Saito, M.S. Dresselhaus, Electrochemical charging of individual single-walled carbon nanotubes, ACS Nano. 3 (2009) 2320–2328.

[465] M. Kalbac, L. Kavan, J. Heyrovsky, L. Dunsch, Effect of bundling on the tangential displacement mode in the Raman spectra of semiconducting single-walled carbon nanotubes during electrochemical charging, Journal of Physical Chemistry C. 113 (2009) 16408–16413.

[466] L. Kavan, L. Dunsch, Electrochemistry of Carbon Nanotubes, Topics in Applied Physics. 111 (2008) 567–603.

[467] L. Kavan, P. Rapta, L. Dunsch, M.J. Bronikowski, P. Willis, R.E. Smalley, Electrochemical Tuning of Electronic Structure of Single-Walled Carbon Nanotubes: In-situ Raman and Vis-NIR Study, Journal of Physical Chemistry B. 105 (2001) 10764–10771.

[468] L. Jia, Y. Zhang, J. Li, C. You, E. Xie, Aligned single-walled carbon nanotubes by Langmuir–Blodgett technique, Journal of Applied Physics. 104 (2008) 0743181–0743186.

[469] X. Li, L. Zhang, X. Wang, I. Shimoyama, X. Sun, W.-S. Seo, H. Dai, Langmuir-Blodgett assembly of densely aligned single-walled carbon nanotubes from bulk materials., Journal of the American Chemical Society. 129 (2007) 4890–4891.

[470] G. Giancane, S. Bettini, L. Valli, State of art in the preparation, characterisation and applications of Langmuir–Blodgett films of carbon nanotubes, Colloids and Surfaces A: Physicochemical and Engineering Aspects. 354 (2010) 81–90.

[471] C. Venet, C. Pearson, A.S. Jombert, M.F. Mabrook, D.A. Zeze, M.C. Petty, The morphology and electrical conductivity of single-wall carbon nanotube thin films prepared by the Langmuir–Blodgett technique, Colloids and Surfaces A: Physicochemical and Engineering Aspects. 354 (2010) 113–117.

[472] N.P. Armitage, Quasi-Langmuir–Blodgett thin film deposition of carbon nanotubes, Journal of Applied Physics. 95 (2004) 3228–3230.

[473] Y. Guo, N. Minami, S. Kazaoui, J. Peng, M. Yoshida, T. Miyashita, Multi-layer LB films of single-wall carbon nanotubes, Physica B: Condensed Matter. 323 (2002) 235–236.

[474] S.-W. Choi, W.-S. Kang, J.-H. Lee, C.K. Najeeb, H.-S. Chun, J.-H. Kim, Patterning of hierarchically aligned single-walled carbon nanotube Langmuir-Blodgett films by microcontact printing, Langmuir: The ACS Journal of Surfaces and Colloids. 26 (2010) 15680–15685.

[475] M. Sano, A. Kamino, J. Okamura, S. Shinkai, Self-Organization of PEO-graft-Single-Walled Carbon Nanotubes in Solutions and Langmuir−Blodgett Films, Langmuir. 17 (2001) 5125–5128.

[476] Y. Kim, N. Minami, W. Zhu, S. Kazaoui, R. Azumi, M. Matsumoto, Langmuir–Blodgett Films of Single-Wall Carbon Nanotubes: Layer-by-layer Deposition and In-plane Orientation of Tubes, Japanese Journal of Applied Physics. 42 (2003) 7629–7634.

[477] J.L. Hernandez-López, E.R. Alvizo-Paez, S.E. Moya, J. Ruiz-García, Trapping, pattern formation, and ordering of polyelectrolyte/single-wall carbon nanotube complexes at the air/water and air/solid interfaces., Journal of Physical Chemistry. B. 110 (2006) 23179–23191.

[478] L. Kavan, P. Rapta, L. Dunsch, In situ Raman and Vis-NIR spectroelectrochemistry at single-walled carbon nanotubes, Chemical Physics Letters. 328 (2000) 363–368.

[479] C. Burda, X. Chen, R. Narayanan, M.A. El-Sayed, Chemistry and properties of nanocrystals of different shapes., Chemical Reviews. 105 (2005) 1025–1102.

[480] J. Wang, O. Rincón, R. Polsky, E. Dominguez, Electrochemical detection of DNA hybridization based on DNA-templated assembly of silver cluster, Electrochemistry Communications. 5 (2003) 83–86.

[481] Y. Lu, Y. Mei, M. Drechsler, M. Ballauff, Thermosensitive core-shell particles as carriers for ag nanoparticles: modulating the catalytic activity by a phase transition in networks., Angewandte Chemie - International Edition. 45 (2006) 813–816.

[482] M. Rai, A. Yadav, A. Gade, Silver nanoparticles as a new generation of antimicrobials., Biotechnology Advances. 27 (2009) 76–83.

[483] K.L. Kelly, E. Coronado, L.L. Zhao, G.C. Schatz, The optical properties of metal nanoparticles: the influence of size, shape and dielectric enviroment, Journal of Physical Chemistry B. 107 (2003) 668–677.

[484] W. Xie, P. Qiu, C. Mao, Bio-imaging, detection and analysis by using nanostructures as SERS substrates., Journal of Materials Chemistry. 21 (2011) 5190–5202.

[485] K.C. Bantz, A.F. Meyer, N.J. Wittenberg, H. Im, O. Kurtuluş, S.H. Lee, N.C. Lindquist, S.-H. Oh, C.L Haynes, Recent progress in SERS biosensing., Physical Chemistry Chemical Physics. 13 (2011) 11551–11567.

[486] R.A. Álvarez-Puebla, L.M. Liz-Marzán, Environmental applications of plasmon assisted Raman scattering, Energy & Environmental Science. 3 (2010) 1011–1017.

[487] J.N. Anker, W.P. Hall, O. Lyandres, N.C. Shah, J. Zhao, R.P. Van Duyne, Biosensing with plasmonic nanosensors., Nature Materials. 7 (2008) 442–453.

[488] H. Kim, K.M. Kosuda, R.P. Van Duyne, P.C. Stair, Resonance Raman and surface- and tip-enhanced Raman spectroscopy methods to study solid catalysts and heterogeneous catalytic reactions., Chemical Society Reviews. 39 (2010) 4820–4844.

[489] M.R. Langille, M.L. Personick, C. a Mirkin, Plasmon-mediated syntheses of metallic nanostructures., Angewandte Chemie - International Edition . 52 (2013) 13910–13940.

[490] Y.J. Choi, U. Huh, T.M. Luo, Spontaneous formation of silver nanoparticles in aminosilica, Journal of Sol-Gel Science and Technology. 51 (2009) 124–132.

[491] G.S. Metraux, C.A. Mirkin, Rapid Thermal Synthesis of Silver Nanoprisms with Chemically Tailorable Thickness, Advanced Materials. 17 (2005) 412–415.

[492] O.L.A. Monti, J.T. Fourkas, D.J. Nesbitt, Diffraction-Limited Photogeneration and Characterization of Silver Nanoparticles, Journal of Physical Chemistry B. 108 (2004) 1604–1612.

[493] A. Wang, H. Yin, C. Ge, M. Ren, Y. Liu, T. Jiang, Synthesis of hollow silver spheres using poly-(styrene-methyl acrylic acid) as templates in the presence of sodium polyacrylate, Applied Surface Science. 256 (2010) 2611–2615.

[494] L. Rodríguez-Sánchez, M.C. Blanco, M.A. López-Quintela, Electrochemical Synthesis of Silver Nanoparticles, Journal of Physical Chemistry B. 104 (2000) 9683–9688.

[495] S. Chen, D.L. Carroll, Silver Nanoplates: Size Control in Two Dimensions and Formation Mechanisms, Journal of Physical Chemistry B. 108 (2004) 5500–5506.

[496] S.J. Oldenburg, S.L. Westcott, R.D. Averitt, N.J. Halas, Surface enhanced Raman scattering in the near infrared using metal nanoshell substrates, Journal of Chemical Physics. 111 (1999) 4729–4735.

[497] G.V.P. Kumar, J. Irudayaraj, SERS in salt wells., ChemPhysChem. 10 (2009) 2670–2673.

[498] L. Baia, M. Baia, J. Popp, S. Astilean, Gold films deposited over regular arrays of polystyrene nanospheres as highly effective SERS substrates from visible to NIR., Journal of Physical Chemistry B. 110 (2006) 23982–23986.

[499] R. Wen, Y. Fang, An investigation of the surface-enhanced Raman scattering (SERS) effect from a new substrate of silver-modified silver electrode., Journal of Colloid and Interface Science. 292 (2005) 469–475.

[500] J. Lee, S. Shim, B. Kim, H.S. Shin, Surface-enhanced Raman scattering of single- and few-layer graphene by the deposition of gold nanoparticles., Chemistry - A European Journal. 17 (2011) 2381–2387.

[501] N. Félidj, J. Aubard, G. Lévi, J. Krenn, G. Schider, A. Leitner, F. Aussenegg, Enhanced substrate-induced coupling in two-dimensional gold nanoparticle arrays, Physical Review B. 66 (2002) 1–7.

[502] N. Félidj, J. Aubard, G. Lévi, J.R. Krenn, A. Hohenau, G. Schider, A. Leitner, F.R. Aussenegg, Optimized surface-enhanced Raman scattering on gold nanoparticle arrays, Applied Physics Letters. 82 (2003) 3095–3097.

[503] X.M. Lin, Y. Cui, Y.H. Xu, B. Ren, Z.Q. Tian, Surface-enhanced Raman spectroscopy: substrate-related issues., Analytical and Bioanalytical Chemistry. 394 (2009) 1729–1745.

[504] J. Cejkova, V. Prokopec, S. Brazdova, A. Kokaislova, P. Matejka, F. Stepanek, Characterization of copper SERS-active substrates prepared by electrochemical deposition, Applied Surface Science. 255 (2009) 7864–7870.

[505] H. Chen, Y. Wang, S. Dong, E. Wang, An approach for fabricating self-assembled monolayer of Ag nanoparticles on gold as the SERS-active substrate., Spectrochimica Acta Part A: Molecular and Biomolecular Spectroscopy. 64 (2006) 343–348.

[506] M. Fleischmann, Z.Q. Tian, An SERS study of silver electrodeposition from thiourea and cyanide containing solutions, Electrochimica Acta. 31 (1985) 907–916.

[507] F. Schaaf, G. Laufer, J.T. Huneke, Surface enhanced Raman spectroscopy of cyanide complexes on silver surfaces, Chemical Physics Letters. 82 (1981) 571–577.

[508] M. Tsuji, S. Gomi, Y. Maeda, M. Matsunaga, S. Hikino, K. Uto, T. Tsuji, H. Kawazumi, Rapid transformation from spherical nanoparticles, nanorods, cubes, or bipyramids to triangular prisms of silver with PVP, citrate, and H_2O_2., Langmuir. 28 (2012) 8845–8861.

[509] B. Tang, S. Xu, J. An, B. Zhao, J.R. Lombardi, Kinetic effects of halide ions on the morphological evolution of silver nanoplates, Physical Chemistry Chemical Physics. 11 (2009) 10286–10292.

[510] C.M. Tsai, M.S. Hsu, J.C. Chen, C.L. Huang, Mechanistic Study of Shape Evolution of Silver Nanoprisms in The Presence of KSCN, Journal of Physical Chemistry C. 116 (2012) 461–467.

[511] R. Jin, Y. Cao, C.A. Mirkin, K.L. Kelly, G.C. Schatz, J.G. Zheng, Photoinduced conversion of silver nanospheres to nanoprisms, Science. 294 (2001) 1901–1903.

[512] S. Chen, Z. Fan, D.L. Carroll, Silver nanodisks: synthesis, characterization, and self-assembly, Journal of Physical Chemistry B. 106 (2002) 10777–10781.

[513] S.K. Ghosh, S. Kundu, T. Pal, Evolution, dissolution and reversible generation of gold and silver nanoclusters in micelle by UV-activation, Bulletin of Materials Science. 25 (2002) 581–582.

[514] F. Fathi, M. Schlitt, D.B. Pedersen, H.-B. Kraatz, Chemical behavior of electrochemically generated nanostructured silver surfaces., Langmuir. 27 (2011) 12098–12105.

[515] B.H. Lee, M.S. Hsu, Y.C. Hsu, C.W. Lo, C.L. Huang, A Facile Method To Obtain Highly Stable Silver Nanoplate Colloids with Desired Surface Plasmon Resonance Wavelengths, Journal of Physical Chemistry C. 114 (2010) 6222–6227.

[516] T. Tan, C. Tian, Z. Ren, J. Yang, Y. Chen, L. Sun, Z. Li, A. Wu, J. Yin, H. Fu, LSPR-dependent SERS performance of silver nanoplates with highly stable and broad tunable LSPRs prepared through an improved seed-mediated strategy., Physical Chemistry Chemical Physics. 15 (2013) 21034–21042.

[517] Y. Liu, K. Yang, T. Hsu, Improved Surface-Enhanced Raman Scattering Performances on Silver - Silica, Journal of Physical Chemistry C. 113 (2009) 8162–8168.

[518] E.J. Baran, C.C. Wagner, M.H. Torre, Synthesis and characterization of EDTA complexes useful for trace elements supplementation, Journal of the Brazilian Chemical Society. 13 (2002) 576–582.

[519] J. Koryta, P. Vanýsek, M. Březina, Electrolysis with electrolyte dropping electrode II. basic properties of the system, Journal of Electroanalytical Chemistry. 75 (1977) 211–228.

[520] Z. Samec, Charge transfer between two immiscible electrolyte solutions. Part III. Stationary curve of current vs. potential of electron transfer across interface, Journal of Electroanalytical Chemistry. 103 (1980) 1–9.

[521] V. Mareček, Z. Samec, J. Koryta, Charge transfer across the interface of two immiscible electrolyte solutions, Advances in Colloid and Interface Science. 29 (1988) 1–78.

[522] Z. Samec, Dynamic electrochemistry at the interface between two immiscible electrolytes, Electrochimica Acta. 84 (2012) 21–28.

[523] M. Platt, R.A.W. Dryfe, Structural and electrochemical characterisation of Pt and Pd nanoparticles electrodeposited at the liquid/liquid interface: part 2., Physical Chemistry Chemical Physics. 7 (2005) 1807–1814.

[524] Y. Gründer, M.D. Fabian, S.G. Booth, D. Plana, D.J. Fermín, P.I. Hill, R.A.W. Dryfe, Solids at the liquid–liquid interface: Electrocatalysis with pre-formed nanoparticles, Electrochimica Acta. 110 (2013) 809–815.

[525] R.A.W. Dryfe, The electrified liquid-liquid interface, Advances in Chemical Physics. 141 (2009) 153–215.

[526] M. Platt, R.A.W. Dryfe, Electrodeposition at the liquid/liquid interface: The chronoamperometric response as a function of applied potential difference, Journal of Electroanalytical Chemistry. 599 (2007) 323–332.

[527] David J. Fermín, Linear and Non-linear Spectroscopy at the Electrified Liquid/Liquid Interface, in: R.C. Alkire, D.M. Kolb, J. Lipkowski, P.N. Ross (Eds.), Advances in Electrochemical Science and Engineering, WILEY-VCH Verlag GmbH & Co. KGaA, Weinheim, 2006: pp. 127–162.

[528] Z. Ding, D.J. Fermin, P.-F. Brevet, H.H. Girault, Spectroelectrochemical approaches to heterogeneous electron transfer reactions at the polarised water/1,2-dichloroethane interfaces, Journal of Electroanalytical Chemistry. 458 (1998) 139–148.

[529] H. Nagatani, H. Watarai, Direct Spectrophotometric Measurement of Demetalation Kinetics of 5,10,15,20-Tetraphenylporphyrinatozinc(II) at the Liquid-Liquid Interface by a Centrifugal Liquid Membrane Method, Analytical Chemistry. 70 (1998) 2860–2865.

[530] D.A. Higgins, R.M. Corn, Second harmonic generation studies of adsorption at a liquid-liquid electrochemical interface, Journal of Physical Chemistry. 97 (1993) 489–493.

[531] K.B. Eisenthal, Liquid Interfaces Probed by Second-Harmonic and Sum-Frequency Spectroscopy, Chemical Reviews. 96 (1996) 1343–1360.

[532] G.L. Richmond, Molecular bonding and interactions at aqueous surfaces as probed by vibrational sum frequency spectroscopy, Chemical Reviews. 102 (2002) 2693–2724.

[533] A. Ohashi, H. Watarai, Azo-imine resonance in palladium(II)-pyridylazo complex adsorbed at liquid-liquid interfaces studied by centrifugal liquid membrane-resonance Raman microprobe spectroscopy, Langmuir. 18 (2002) 10292–10297.

[534] S. Yamamoto, H. Watarai, Surface-Enhanced Raman Spectroscopy of Dodecanethiol-Bound Silver Nanoparticles at the Liquid/Liquid Interface, Langmuir. 22 (2006) 6562–6569.

[535] L. Poltorak, M. Dossot, G. Herzog, A. Walcarius, Interfacial processes studied by coupling electrochemistry at the polarised liquid-liquid interface with in situ confocal Raman spectroscopy, Physical Chemistry Chemical Physics. 16 (2014) 26955–26962.

[536] V. Mareček, M. Gratzl, A. Pungor, J. Janata, Fluctuation analysis of liquid/liquid and gel/liquid interfaces, Journal of Electroanalytical Chemistry. 266 (1989) 239–252.

[537] V. Mareček, M.P. Colombini, Charge transfer across a polymer gel/liquid interface: the polyvinyl chloride + nitrobenzene gel/water interface, Journal of Electroanalytical Chemistry. 241 (1988) 133–141.

[538] V. Mareček, H. Jänchenová, M.P. Colombini, P. Papoff, Charge transfer across a polymer gel/liquid interface. A voltammetric detector for a flow system, Journal of Electroanalytical Chemistry. 217 (1987) 213–219.

[539] E. Wang, Z. Sun, Development of electroanalytical chemistry at the liquid-liquid interface, Trends in Analytical Chemistry. 7 (1988) 99–106.

[540] D.J. Fermin, H.D. Duong, Z. Ding, Ó. Brevet, H.H. Girault, Photoinduced electron transfer at liquid/liquid interfaces. Part II., Physical Chemistry Chemical Physics. 1 (1999) 1461–1467.

[541] H.J. Lee, D.J. Fermín, R.M. Corn, H.H. Girault, Marangoni flow in micro-channels, Electrochemistry Communications. 1 (1999) 190–193.

[542] M. Muniz-Miranda, Surface enhanced Raman scattering and normal coordinate analysis of 1,10-phenanthroline adsorbed on silver sols, Journal of Physical Chemistry A. 104 (2000) 7803–7810.

[543] R. Mažeikiene, G. Niaura, A. Malinauskas, Electrochemical redox processes at cobalt hexacyanoferrate modified electrodes: An in situ Raman spectroelectrochemical study, Journal of Electroanalytical Chemistry. 719 (2014) 60–71.

[544] A. Moisala, A.G. Nasibulin, D.P. Brown, H. Jiang, L. Khriachtchev, E.I. Kauppinen, Single-walled carbon nanotube synthesis using ferrocene and iron pentacarbonyl in a laminar flow reactor, Chemical Engineering Science. 61 (2006) 4393–4402.

[545] M.G. Albrecht, J.A. Creighton, Anomalously intense Raman spectra of pyridine at a silver electrode, Journal of American Chemical Society. 99 (1976) 5215–5217.

[546] I. Chourpa, F.H. Lei, P. Dubois, M. Manfait, G.D. Sockalingum, Intracellular applications of analytical SERS spectroscopy and multispectral imaging., Chemical Society Reviews. 37 (2008) 993–1000.

[547] Z.Q. Tian, B. Ren, Adsorption and reaction at electrochemical interfaces as probed by surface-enhanced Raman spectroscopy., Annual Review of Physical Chemistry. 55 (2004) 197–229.

[548] M. Muniz-Miranda, B. Pergolese, A. Bigotto, A. Giusti, Stable and efficient silver substrates for SERS spectroscopy., Journal of Colloid and Interface Science. 314 (2007) 540–544.

[549] H. Guo, L. Ding, Y. Mo, Adsorption of 4-mercaptopyridine onto laser-ablated gold, silver and copper oxide films: A comparative surface-enhanced Raman scattering investigation, Journal of Molecular Structure. 991 (2011) 103–107.

[550] P. Gao, D. Gosztola, L.-W.H. Leung, M.J. Weaver, Surface-enhanced Raman scattering at gold electrodes: dependence on electrochemical pretreatment conditions and comparisons with silver, Journal of Electroanalytical Chemistry. 233 (1987) 211–222.

[551] X. Zhu, H. Yang, N. Wang, R. Zhang, W. Song, Y. Sun, G. Duan, W. Ding, Z. Zhang, A facile method for preparation of gold nanoparticles with high SERS efficiency in the presence of inositol hexaphosphate., Journal of Colloid and Interface Science. 342 (2010) 571–574.

[552] A. Hyvärinen, E. Oja, Independent component analysis: algorithms and applications, Neural Networks. 13 (2000) 411–430.

[553] M.T. Reetz, W. Helbig, Size-Selective Synthesis of Nanostructured Transition Metal Clusters, Journal of the American Chemical Society. 116 (1994) 7401–7402.

[554] F.M. El-Cheick, F.A. Rashwan, H.A. Mahmoud, M. El-Rouby, Gold nanoparticle-modified glassy carbon electrode for electrochemical investigation of aliphatic di-carboxylic acids in aqueous media, Journal of Solid State Electrochemistry. 14 (2009) 1425–1443.

[555] S. Huang, H. Ma, X. Zhang, F. Yong, X. Feng, W. Pan, X. Wang, Y. Wang, S. Chen, Electrochemical synthesis of gold nanocrystals and their 1D and 2D organization., Journal of Physical Chemistry. B. 109 (2005) 19823–19830.

[556] R.M. Penner, Mesoscopic Metal Particles and Wires by Electrodeposition, Journal of Physical Chemistry B. 106 (2002) 3339–3353.

[557] H. Liu, F. Favier, K. Ng, M. Zach, R. Penner, Size-selective electrodeposition of meso-scale metal particles: a general method, Electrochimica Acta. 47 (2001) 671–677.

[558] L. Wang, S. Guo, X. Hu, S. Dong, Facile electrochemical approach to fabricate hierarchical flowerlike gold microstructures: Electrodeposited superhydrophobic surface, Electrochemistry Communications. 10 (2008) 95–99.

[559] C. Huang, J. Jiang, M. Lu, L. Sun, E.I. Meletis, Y. Hao, Capturing electrochemically evolved nanobubbles by electroless deposition. A facile route to the synthesis of hollow nanoparticles., Nano Letters. 9 (2009) 4297–4301.

[560] J.S. Suh, M. Moskovits, Surface-Enhanced Raman Spectroscopy of Amino Acids and Nucleotide Bases Adsorbed on Silver, Journal of American Chemical Society. 108 (1986) 4711–4718.

[561] T. Yamada, K. Shirasaka, A. Takano, M. Kawai, Adsorption of cytosine, thymine, guanine and adenine on Cu(110) studied by infrared reflection absorption spectroscopy, Surface Science. 561 (2004) 233–247.

[562] T. Watanabe, O. Kawanami, H. Katoh, K. Honda, Y. Nishimura, M. Tsuboi, SERS study of molecular adsorption: some nucleic acid bases on Ag electrodes, Surface Science. 158 (1985) 341–351.

[563] M. Ostblom, B. Liedberg, L.M. Demers, C.A. Mirkin, On the structure and desorption dynamics of DNA bases adsorbed on gold: a temperature-programmed study, Journal of Physical Chemistry. B. 109 (2005) 15150–15160.

[564] R. Huang, H.-T. Yang, L. Cui, D.-Y. Wu, B. Ren, Z.-Q. Tian, Structural and Charge Sensitivity of Surface-Enhanced Raman Spectroscopy of Adenine on Silver Surface: A Quantum Chemical Study, Journal of Physical Chemistry C. 117 (2013) 23730–23737.

[565] B. Giese, D. McNaughton, Surface-Enhanced Raman Spectroscopic and Density Functional Theory Study of Adenine Adsorption to Silver Surfaces, Journal of Physical Chemistry B. 106 (2002) 101–112.

[566] R.P. Lopes, R. Valero, J. Tomkinson, M.P.M. Marques, L.A.E. Batista de Carvalho, Applying vibrational spectroscopy to the study of nucleobases – adenine as a case-study, New Journal of Chemistry. 37 (2013) 2691–2699.

[567] M. Castro, R. Santamaria, E. Charro, A. Zacarias, Vibrational Spectra of Nucleic Acid Bases and Their Watson-Crick, Journal of Computational Chemistry. 20 (1999) 511–530.

[568] D. Li, D.-W. Li, J.S. Fossey, Y.-T. Long, Portable surface-enhanced Raman scattering sensor for rapid detection of aniline and phenol derivatives by on-site electrostatic preconcentration, Analytical Chemistry. 82 (2010) 9299–9305.

[569] P. Neelakantan, The Raman Spectrum of Cyclohexanol, Proceedings of the Indian Academy of Sciences - Section A. 57 (1963) 94–102.

[570] N.A. Marley, C.K. Mann, T.J. Vickers, Determination of Phenols in Water Using Raman Spectroscopy., Applied Spectroscopy. 38 (1984) 540–543.

[571] N.H. Jang, The Coordination Chemistry of DNA Nucleosides on Gold Nanoparticles as a Probe by SERS, Bulletin of the Korean Chemical Society. 23 (2002) 1790–1800.

8. Apendix

Acronyms and definitions

Acronyms	Definition
A	Adenine
2-oxoA	2-oxoadenine
2,8-dioxoA	2,8-dioxoadenine
BTPPATPBF$_{20}$	Bis(triphenylphosphoranylidene) ammonium tetrakis(pentafluoro) phenylborate
Bend	Bending
CE	Counter electrode
CN^-	Cyanide
CNT	Carbon nanotubes
SWCNT	Single-walled carbon nanotubes
DWCNT	Double-walled carbon nanotubes
MWCNT	Multi-walled carbon nanotubes
D	Dimensional
0-D	Zero-dimensional
1-D	One-dimensional
2-D	Two-dimensional
3-D	Three-dimensional
DCB	1,2-dichlorobenzene
DCE	1,2-dichloroethane
Def	Deformation
DMFc	Dimethylferrocene
DNA	Deoxyribonucleic acid
DOS	Density of states
ECPs	Extrinsic conducting polymers
EDOT	3,4-ethylenedioxythiophene
EDTA	Ethylenediaminetetraacetic acid

G	Guanine
8-oxoG	8-oxoguanine
8-oxoG^{ox}	8-oxoguanine oxidized
GC	Glassy carbon
ICA	Independent Components Analysis
ICPs	Intrinsic conducting polymers
ITIES	Interface between two immiscible electrolyte solutions
L/L	Liquid/Liquid
NPs	Nanoparticles
AuNPs	Gold nanoparticles
AgNPs	Silver nanoparticles
PEDOT	Poly(3,4-ethylenedioxythiophene)
PET	Polyethyleneterphtalate
PMMA	Polymethyl methacrylate
PTFE	Polytetrafluoroethylene
PVC	Polyvinylchloride
RBM	Radial breathing mode
RE	Reference electrode
Rock	Rocking
Sciss	Scissoring
SEM	Scanning Electron Microscope
SERS	Surface-enhanced Raman scattering
Sqz	Squeezing
Str	Stretching
UV/Vis	Ultraviolet/Visible
Wag	Wagging
WE	Working electrode

Magnitudes and Units

Magnitude		Unit	
A	Absorbance	**a.u**	Arbitrary units
$\Delta\phi$	Potential difference	**V**	Volts
E	Potential	**V**	Volts
I	Intensity	**A**	Amperes
I_{Raman}	Raman intensity	**a.u**	Arbitrary units
λ	Wavelength	**nm**	Nanometers
Q	Charge	**C**	Coulombs
t	Time	**s**	Seconds